ABSTRACT

SMITH, GLEN. Bond Characteristics and Qualifications of Adhesives for Marine Applications and Steel Pipe Repair. (Under the direction of Dr. Sami Rizkalla.)

Performance of adhesives significantly affects the overall behavior of structural elements, especially in the process of developing innovative designs using new materials. Adhesives that bond metals, plastics, FRP and other materials have been used in transportation, industrial and marine applications. Fundamental understanding of the bond behavior and load transfer mechanisms of different adhesives is essential prior to their use in civil infrastructure applications.

This thesis presents the results of an extensive research program conducted to determine the engineering properties of different structural adhesives under normal and severe environmental conditions. The bond characteristics between composite-to-composite and composite-to-steel materials are investigated. The performances of two different structural adhesives are evaluated by testing 105 single-lap shear specimens. The research includes the effect of severe environmental conditions using the classical direct lap-shear tests. The factor considered is time-to-failure in which the specimens are submerged in de-ionized water with different pH values and subjected to different temperatures at different stresses. The program includes also examining the cleavage peel and short term creep properties. Adhesive behaviors, as well as the failure modes for each adhesive, are presented. The influence of preparation procedures of the substrate on the shear strength of the adhesives is also studied.

Test results show a significant impact of the pH level and temperature on the shear strength and bond characteristics of the two structural adhesives considered in this investigation. Test results were used to determine the most appropriate adhesive for marine application and repair of steel pipeline.

BOND CHARACTERISTICS AND QUALIFICATIONS OF ADHESIVES FOR MARINE APPLICATIONS AND STEEL PIPE REPAIR

By
Glen E. Smith

A thesis submitted to the Graduate Faculty of
North Carolina State University in partial fulfillment of
the requirements of the Degree of Master of Science

**Department of Civil, Construction,
and Environmental Engineering**

Raleigh

2005

APPROVED BY:

_____
Chair of Advisory Committee

_____ _____
Member of Advisory Committee Member of Advisory Committee

BIOGRAPHY

Glen Eugene Smith was born on November 16, 1980, in Goldsboro, North Carolina, to Ralph and Teresa Smith. He attended Wayne County public schools and graduated from Eastern Wayne High School in May 1999. The following fall, he began attending North Carolina State University as a Class of 2003 Park Scholar.

Glen was involved in student organizations and service projects throughout his time at NC State University. In January 2001, he began studying Civil Engineering and in the summer of 2002 interned with R.N. Rouse Construction in Goldsboro, NC. Glen graduated Magna Cum Laude with a Bachelor of Science in Civil Engineering in May 2003.

Immediately following graduation, Glen worked as a Laboratory Assistant at the Constructed Facilities Laboratory on the Centennial Campus of North Carolina State University. In the fall of 2003, he began pursuing his Master's of Science in Civil Engineering with a concentration in Structures at NC State University and focused his research on structural adhesives. During his graduate studies, Glen also acted as a Research and Teaching Assistant.

Glen is currently living in Missouri City, Texas, and working for a structural engineering firm in Houston designing buildings.

ACKNOWLEDGMENTS

I would like to acknowledge the support of the NSF (Award No. EEC-0225055) Industry/University Collaborative Research Center on the use of FRP for the Repair of Bridges and Buildings with Composites (RB^2C). I wish to also acknowledge the National Science and Engineering Research Council of Canada. Additionally, I thank the industry partners whom I have had the opportunity to work with during this project, and who provided the composite and adhesive materials.

I would like to thank Dr. Sami Rizkalla for giving me the opportunity to work with him and for all the guidance that he has given me with this project. I also thank Dr. Jim Nau and Dr. Emmett Sumner, whom I have thoroughly enjoyed interacting with as both a student and teaching assistant. These three men are all incredible teachers, and I greatly respect and admire each of them. I also acknowledge and thank all of the other professors in the Department of Civil, Construction, and Environmental Engineering at North Carolina State University who have taught me so much during the last six years that I have spent as an undergraduate and graduate student in that department, as well as Barbara and Renee who have taken care of so much for me in the past two years.

Additional thanks and acknowledgement is due to Dr. Tarek Hassan for his part in organizing, executing, analyzing, and writing the first two phases of this project. I never truly understood the vast amount of help he provided until he left. Also, I thank Engin Reis for beginning the work to this project before my arrival as a graduate student at NC

State, and his continued guidance after I began to take the project as my own. In addition, I would like to thank Josh Sutton who was a tremendous help with executing the Environmental Exposure phase.

I also thank Jerry Atkinson for his constant help at every stage of my research. Not only could I have not done it without him, I would not have even known where to start. Thanks also to Matt Vorys for help with the beginning stages of the project, especially with the construction of the Environmental Exposure test setup. Also, Bill Dunleavy's patient guidance with the computer and electrical related portions of the project was extremely helpful, and I cannot begin to thank him, Dr. Roy Borden, and all of the other brothers enough for their spiritual guidance outside of the laboratory. I also thank Lee Nelson, who was always available to answer my questions, even before becoming Lab Manager. Thanks should also go to Pat and Amy, the former and present CFL secretaries who have provided me with the necessary sugar to get through the long days, as well as all the Sharpies and purchase orders I could talk them out of. Additionally, I would like to acknowledge and thank Birgit Andersen of the Department of Textile Engineering for performing the FTIR tests on the adhesives for this research project.

As for my CFL friends, I would have never gotten through it all without you. I will not list names, but you know who you are. I have made some of the closest friends of my life while working on this project, and I cannot begin to write what you all mean to me. You have studied with me, brainstormed with me, and helped me to understand concepts and ideas more thoroughly than I would have ever been able to on my own. Even more, you

have gone to the gym with me when I needed to release some tension, you have laughed with me when I was stressing out, and you have prayed with me when I needed that more than anything else.

I must also thank my family for their consistent support, concern, and prayers. I have been blessed with incredible parents, grandparents, a sister, brothers, parents-in-law, grandparents-in-law, and brothers and sisters-in-law who have all contributed to this research through their continued love and support. As for my wife, Gillian, I have made it through many long, hard days this past year from knowing that when they finally came to an end, I would be going home to you. Thank you for taking care of me and putting up with me while I focused my time on this project.

Lastly, I give thanks to the Lord for all His blessings, and for allowing me to be a part of His great work on this earth.

TABLE OF CONTENTS

List of Tables

List of Figures

1.0 Introduction

1.1 Background

As adhesives are used more frequently in structural applications, research to understand their behavior and properties has been undertaken by many researchers worldwide. Recently, the use of adhesives in conjunction with newly popular fiber composite materials has been considered by industry for special applications such as marine structures and in the repair of steel pipelines. The research described in this thesis focuses on evaluation of the properties of a newly developed adhesive designated as adhesive S, which is intended to be used for these two application fields. The behavior is compared to an established adhesive designated adhesive M, which is currently commonly used by the industry.

Both of the adhesives studied in this program are patented compositions based on two-component polymerizable methacrylate technology. Each consists of an adhesive liquid comprising of elastomeric or thermoplastic polymers dissolved in methyl methacrylate monomer (MMA), along with an amine promoter for the polymerization reaction. Each adhesive is supplied with a polymerization catalyst or initiator containing benzoyl peroxide. An amount of initiator sufficient to provide the desired working time and cure time for the given environmental conditions of application is added just before application of the adhesives. A working time of 30 to 45 minutes allows sufficient application time for large assemblies. Functional cure (20 to 30 percent) should occur within 1 to 3 hours, depending on the application conditions, and 90 to 95 percent

of full properties are generally obtained in 8 to 24 hours, which is highly dependant on the environmental conditions at the time of application.

No attempt was made to fully analyze the proprietary formulations to determine compositional differences that might contribute to the differences in the performance of the two adhesives. However, FTIR spectra were conducted on polymer films provided by evaporating the MMA from the uncatalyzed liquid adhesive on a silver chloride plate to ascertain any fundamental differences in the composition of the polymeric component. Both films showed absorption bands characteristic of unsaturated vinyl polymers and some methacrylate content. The latter may have been present from dissolved polymer content or unevaporated MMA monomer.

One of primary differences noted during the investigation is the presence of absorption peaks in the S adhesive, which is characteristic of a carbon-nitrogen triple bond (nitrile group) and carbon-chlorine bonds. These bands were not present in the M adhesive and suggest that the S adhesive contains a nitrile polymer or elastomer and a chlorinated polymer. The spectra of the M adhesive residue suggest some combination of methacrylate polymers and unsaturated polymers. No further chemical analysis was performed on the adhesives.

1.2 Objective

The main goal of this research is to determine the properties of the two adhesives that are pertinent to their use for marine applications and the repair of steel pipelines. The specific objectives can be summarized as follows:

- Investigate the engineering properties, bond characteristics, and qualifications of the adhesives for marine and steel pipeline repair applications
- Evaluate the effect of severe environmental conditions on the performance and the fundamental characteristics of the two adhesives
- Study the cleavage and peeling behavior, which is normally used to compare two types of adhesive tested under the same conditions
- Examine the short term creep behavior of the two adhesives over a limited time of 48 hours

1.3 Scope

The research program consists of four phases, which are in line with the four specific objectives. The first phase explores the behavior using lap shear specimens. Specimens were tested to failure under no environmental conditioning, in order to evaluate the shear stress-strain behavior of the adhesives and to determine the effect of preparation techniques. The second phase investigates the effect of selected severe environmental conditions, including temperature and pH level, on the performance and the fundamental characteristics of the adhesives. The third phase examines the cleavage peel characteristics, while the fourth phase investigates the short-term creep properties within 48 hours.

This thesis consists of five chapters; the first chapter is the introduction.

Chapter 2 discusses the use of adhesives for civil and structural engineering applications. The chapter reviews current knowledge and work conducted by others, as well the need for future research.

Chapter 3 thoroughly details the testing program considered in this study. Fabrication procedures of specimens, as well as test setups and methods, are presented.

Chapter 4 presents all of the pertinent test results and modes of failure for each of the four phases. For each phase, detailed analysis and the significance of the results are discussed.

Chapter 5 presents the summary and conclusions of the completed research work.

Appendices A, B, and C are included to present some additional detailed data not included elsewhere.

2.0 Literature Review

2.1 Introduction

Fiber-reinforced polymer materials (FRP's) are gaining more acceptance in civil engineering applications. The use of FRP for structural applications has been promoted due to their excellent mechanical properties including high strength to weight ratio and non corrosive characteristics (Malvar et al. 2003). As with any material being newly introduced in the structural realm, there are obstacles to overcome, such as lack of ductility, sensitivity to the environment, and higher initial costs. Architectural benefits, such as translucency of load-bearing elements, luminosity of glass fibers, and the possibility of dyed matrices, along with structural benefits, such as low thermal conductivity and lower life-cycle costs, can, however, justify these initial obstacles (Keller et al. 2004).

One recent example of successful use of structural FRP is the Pontresina pedestrian bridge. This bridge is located over the Flaz Creek in Switzerland, and was constructed of FRP in the winter of 1997. The high-strength yet light-weight properties of the FRP allow for the bridge to be removed each spring, which is necessary as snow begins to melt because of the bridge's location in the Flaz's floodplain (Keller et al. 1999).

One of the very promising uses of FRP is for marine applications. Currently, FRP is more commonly being used in the structural field for repair than for new construction, and already it has been put to use in the retrofit of marine structures (Malvar et al. 2003).

Another popular use of FRP is repair of steel pipelines. In particular, Clock Spring Company LP has developed the Clock Spring® repair system for corrosion, mechanical damage or other defects on high-pressure pipelines. This repair system consists of reducing the stresses in the pipe wall by reinforcing the damaged section of the pipeline by wrapping the pipes with an FRP sleeve to resist the hoop stresses, as shown in Figure 2.1 (Porter et al. 2001). As with the other mentioned uses of FRP, this use also provides an excellent solution in comparison to traditional alternatives. By implementing the use of FRP, a permanent repair which restores the original pressure capabilities and provides resistance to further structural deterioration can be made to a high-pressure pipeline typically in less than 25 minutes and without having to even reduce the pressure within the pipe (Porter et al. 2001).

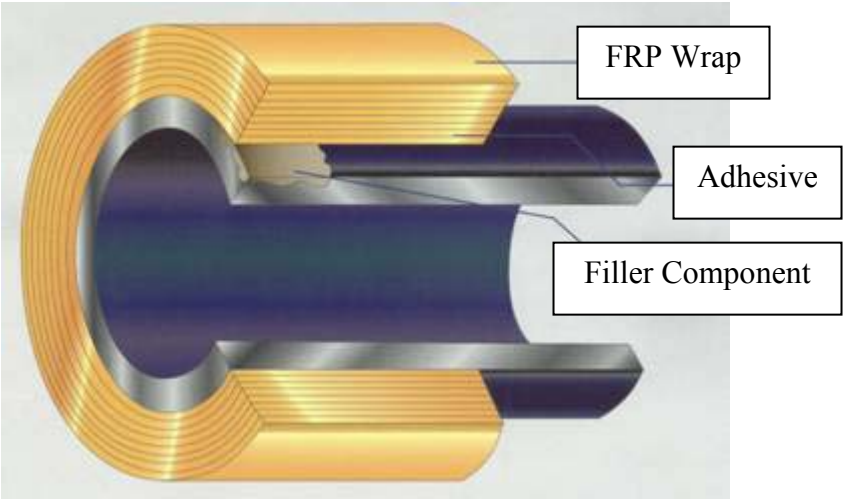

Figure 2.1 – Clock Spring® Steel Pipeline Repair System

2.2 Importance of Adhesive

In addition to cost, other issues related to the use of these new materials must be dealt with in order to use the materials efficiently. One of these challenges deals with the bonding of the FRP to itself and the base steel materials. Unlike with steel or concrete, bolted connections have substantial economic and durability disadvantages for FRP material due to its anisotropic and brittle characteristics, which are significantly weaker in the direction transverse to the fibers. Much research has been done in the field of bolted connections, but adhesive bonding seems to be a more material-adapted connection technique (Keller et al. 2004).

The aforementioned Pontresina pedestrian bridge shown in Figure 2.2 has explored the use of bolts versus adhesive connection for FRP materials. The bridge consists of two spans; one span was constructed using bolted connections while the other span used adhesive connections. When the bridge was removed each spring, engineers examined each span, with emphasis being put on further testing the adhesive span (Keller et al. 1999). For the bolted connection span, the shapes of the truss chords were controlled by the bolted joints. Therefore, to reduce bolt node forces, crossed truss members were included in the lattice girder, which resulted in a configuration that uses only 30 percent of the composite element's carrying capacity between joints. In the adhesively connected span the transmission of forces occurs more evenly over wide areas between adjoining chords and the adhesive and synthetic resin matrix work well together due to their similar characteristics. This more efficient connection technique resulted in section sizes that could have been reduced from the sizes used in the bolted span, but were not in order to

allow for a more accurate comparison of the behavior of the two spans (Keller et al. 1999). In general, using traditional bolted connections did not take full advantage of the properties of the FRP, while using adhesive connections achieved full utilization of the member cross sections. In reference to the structural use of FRP, Keller et al. conclude that "developing the best connection techniques will be the essential requirement for the full exploitation of the properties of the material and for the broad breakthrough of such materials in the civil engineering sector" (1999).

Figure 2.2 – Pontresina Pedestrian Bridge in Switzerland

Others have also noted the importance of adhesive research to the use of FRP in structural applications. In research dealing with shear peel behavior, Damatty et al. found that for relatively thick bonded laminates, failure occurred in the adhesive that was used to bond the steel and the plastic sections. Thus the successful use of adhesively bonded FRP for civil engineering applications relies on the behavior of the adhesives, and therefore, requires more understanding of their behavior (2003).

The two part adhesive used in the Clock Spring® pipe repair system is one of the three structural components, with the other two being a high compressive strength compound and a unidirectional composite structure made up of glass fibers and a polymer base. In general, composite repairs can be applied by either the full-cure or wet wrap method. The full-cure method uses a composite sleeve which is completely cured in the manufacturing facility and installed using filler and adhesive in the field. The full-cure installation procedure is more desirable because it allows the glass direction, mechanical properties and composition to be fully controlled, and there are no issues with the variability of wrap tension, glass alignment, resin saturation, and composite length such as arise with the wet-wrap procedure (Porter et al. 2001). In order to take advantage of the full-cure procedure, the installation of the Clock Spring® system consists of filling the defect and other voids under the repair with the high compressive strength compound and securing the sleeve, which is wrapped around the pipe typically eight times, with adhesive between each layer. Then the unit is tightened onto the pipe, and the adhesive cures after approximately two hours (Chavez et al. 2003). Because the adhesive must transfer all of the stresses from the pipe into the FRP, it is an essential part of the system. However, in addition to the strength requirements, the adhesive must also meet certain workability and durability requirements. The main requirements of a good adhesive can be summarized as follows:

- Easy to mix and to apply in field conditions.
- Retain its workability for a minimum of forty-five minutes at field application temperatures.

- Cure within two to four hours over the range of thirty to one hundred degrees Fahrenheit.
- Should achieve a lap shear strength of at least 600 psi for both composite and steel bonds.
- Compatible with cathodic protection systems.
- Resistant to wet soils for extended periods.
- Have a shelf life of at least six months.
- Operate over a wide range of temperatures.
- Capable of twenty years durability under worst-case conditions.

(Chavez et al. 2003). In order to meet these requirements it was decided to use a methacrylate type adhesive, which can be made to have excellent lap shear strength on both composite-to-composite and composite-to-steel bonds, have an adjustable working time dependant on the activator to adhesive ratio without any serious degradation in performance, and have excellent durability under severe environmental conditions (Chavez et al. 2003).

2.3 Lap Shear

In general, the major stress formed in the adhesive layer of FRP structures is shear. As was mentioned above, for the use of FRP as a repair system it is required for the FRP to share the hoop stresses in the pressurized pipe. Therefore load transfer from the pipe to the sleeve is an integral part of the repair (Porter et al. 2001). Because of the wrapping of the FRP sleeve, the major stresses induced in the adhesive are shear stresses caused by

the mechanism where the two layers of FRP tend to separate from each other. This is why a specified shear strength is required for many companies working in this field.

ASTM *Standard Test Method for Determining Strength of Adhesively Bonded Rigid Plastic Lap-Shear Joints in Shear by Tension Loading*, designated D 3163 – 01, describes a lap shear test recommended to determine the bonding characteristics of adhesives for joining FRP to FRP base surfaces and to metal base surfaces. The test method is useful for generating comparative apparent shear strength data to compare different adhesives, including effects of surface treatments of the base material and FRP materials.

2.4 Environmental Exposure

One of the primary advantages of some FRP materials is their superior durability under extreme environmental conditions. Also, one of the primary disadvantages of using bolted connections with FRP, especially in extreme environmental conditions, is their tendency to rust and deteriorate. It is therefore essential that in order to efficiently put FRP to use in extreme environmental conditions, structural adhesives must show similar durability properties.

Previous research has shown concern that factors such as ambient temperature, relative humidity, substrate moisture, and substrate surface contamination could cause significant property changes in structural adhesives. High temperature and humidity have been of particular concern, as heat can accelerate curing or degrade the components of a two-part adhesive, and moisture can cause problems with the reaction of the two components and

reduce the strength of the adhesive, which is why regulations are in place that deal with the moisture conditions during the mixing of most adhesives (Malvar et al. 2003). Test results show that bond strength decreases so dramatically at high temperatures and humidity that in some cases the resulting strength is insufficient to meet requirements proposed by ACI and the U.S. Navy (Malvar et al. 2003).

In the FRP repair system proposed in this thesis, adhesive durability is the prime research focus. Several of the adhesive requirements deal with durability in extreme environmental conditions, including that the adhesive must exhibit resistance to wet soils for extended periods, operate over a wide range of temperatures, and be capable of twenty years durability under worst-case conditions. These durability and environmental properties are extremely important for any repair system to ensure permanency. The rate of degradation of a pipeline repair application is somewhat dependent on environmental factors such as moisture, temperature, and soil properties, but the structural adhesive must not degrade at a rate that causes the repair to not be deemed permanent (Porter et al. 2001). There are many different situations in which pipe repairs are subjected to these typical conditions. For example, pipelines hanging from highway or pedestrian bridges are exposed to severe conditions from road debris, road and deicing salt, and pollution (Chavez et al. 2003).

Furthermore, the splash zones of off-shore risers are especially prone to corrosion and other degradation, and the FRP repair system has recently been used to repair of one of these risers, with a repair area extending from fourteen feet above the waterline to

fourteen feet below (Banton et al. 2005). Underwater repair was not possible using the typical commercially available adhesives. However, some adhesives were being used for FRP repairs above the waterline and were becoming more common and accepted, and this type of repair was needed to be performed also at and below the waterline. Thus it was necessary to develop an adhesive that would meet or exceed the performance characteristics of the adhesive originally used in the FRP repair system, even when applied and cured underwater. In order to find these characteristics, short-term strength and long-term durability tests similar to the tests performed on the original adhesive were necessary for the new adhesive (Banton et al. 2005).

2.5 Cleavage Peel Testing

Although the major stress seen by the adhesive layer in most adhesively-bonded FRP systems is shear, there are also other stresses induced at the connection. Peeling stresses are especially important to note, specially due to the fact that the peel strength of an adhesive is much less than the shear strength, and because an initial adhesive crack caused by peeling stresses can propagate under a sustained load and cause failure at a relatively low stress load.

Literature on the Pontresina pedestrian bridge notes that it was necessary to account for high peeling stresses at connection edges. These stresses, in fact, required the application of supplementary bolts, which ensure a compression force on the adhesive zones and act as a backup in case of adhesive failure (Keller et al. 2004).

Additionally, the literature dealing with the FRP pipe repair system indicates that the stress in the adhesive layer is not uniformly distributed along the entire bond length, but instead is focused at the end (Banton et al. 2005). If the adhesive properties are insufficient, these high end loads could cause peeling stresses that could result in adhesive cracking that could propagate through the entire system.

Standard Test Method for Strength Properties of Adhesives in Cleavage Peel by Tension Loading (Engineering Plastics-to-Engineering Plastics), ASTM designation D 3807 – 98 (Reapproved 2004), acknowledges that peeling forces are common in bonded assemblies, and therefore provides the method by which to determine the comparative cleavage peel strengths of adhesive when tested on a standard specimen and under specific conditions.

2.6 Creep

Another important characteristic of a structural adhesive is its creep behavior. With the Pontresina pedestrian bridge, particular attention was given to study the creep behavior (Keller et al. 1999). Similarly, attention should be given to the creep behavior of any structural adhesive expected to have any significant service life. Previous research has found that, while thin adhesive layers are less affected, creep behavior of adhesively bonded joints cause particular problems in structural applications, and it is noted that in new adhesive systems, research dealing with creep must be done anew (Schonwalder et al. 2003).

3.0 Experimental Program

3.1 Introduction

The main objectives of this program are to determine the influence of environmental conditions on the properties of a newly developed adhesive and compare the results to a current commercially available adhesive used for the repair of pipe systems. The experimental program was conducted at the Constructed Facilities Laboratory at North Carolina State University. Research findings are not limited to the use of this adhesive for the repair of pipe line systems, but in general for several marine applications.

3.2 Overview

The experimental program consisted of four phases, which included: 1) Direct Lap Shear Property Study, 2) Environmental Exposure Study, 3) Cleavage Peel Tests, and 4) Creep Tests. Fourier Transform Infrared (FTIR) testing, which permits the classification of organic compounds, was performed on the new and existing adhesives to determine the fundamental chemical properties and differences in the composition of the polymeric components. This work was performed by the College of Textiles at North Carolina State University with samples of the uncatalyzed liquid adhesives from which the methyl methacrylate monomer was evaporated. These FTIR spectra are the full extent of the chemical research performed in this program.

3.3 Phase I: Direct Lap Shear Property Tests

The first phase of the experimental program focused on evaluation of the shear characteristics of the two adhesives, under normal environmental conditions. Specimens were fabricated and tested in accordance to ASTM D 3163 – 01, *Standard Test Method for Determining Strength of Adhesively Bonded Rigid Plastic Lap-Shear Joints in Shear by Tension Loading*. Bonded composite-to-composite specimens, as well as bonded steel-to-composite specimens, were tested.

3.3.1 Composite-to-Composite Lap Shear

In field applications, some factors cannot be as easily controlled as is the case for laboratory conditions. It was therefore decided to look in to the effect of the composite surface preparation. The suggested preparation of the composite includes thorough sanding until the glossy surface is removed and a rougher surface is gained. Five of the composite-to-composite specimens of each adhesive were prepared using this method. However, this preparation is often hard to achieve in the field, so the first five composite-to-composite specimens of each adhesive were prepared with light sanding.

3.3.1.1 Lightly-Sanded Specimen Configuration and Preparation

According to the ASTM standard, the lap shear specimen dimensions were 1 inch wide, 11 inches long with a 1 inch overlap. Therefore, the area of the bond surface is one square inch. Thicknesses of the GFRP material and the adhesive layer were 0.06 and 0.01 inches respectively. Additional one-inch by five-inch strips of the composite material were bonded to the specimens to achieve a center concentric location of the

applied load with respect to the adhesive shear planer. Aluminum grips were bonded to the ends of the specimens to insure that failure occurred within the adhesive layer and not at the gripping location of the base material. The configuration of the lightly-sanded composite-to-composite specimens is shown in Figure 3.1.

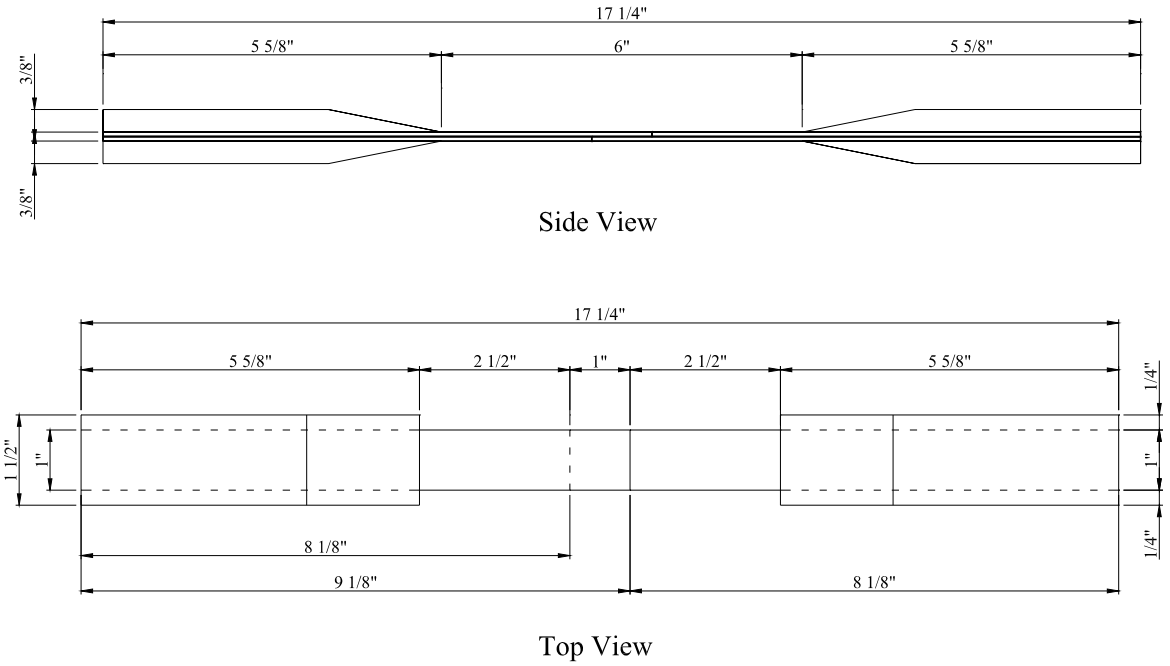

Figure 3.1 – Original Composite-to-Composite Lap Shear Specimens

The composite-to-composite lap shear specimens were prepared by cutting the composite material into 6 inch by 12 inch sheets using a wet saw. The ends of the first set of sheets were lightly-sanded. The ends of the thoroughly-sanded specimens were sanded until the glossy surface was removed and a rougher surface was obtained, as is shown in Figure 3.2. With both the lightly-sanded and thoroughly-sanded specimens, the sanded area was thoroughly cleaned with alcohol, as shown in Figure 3.3, and a line was marked at one inch from the end of the sheets to provide the correct overlap and bond area.

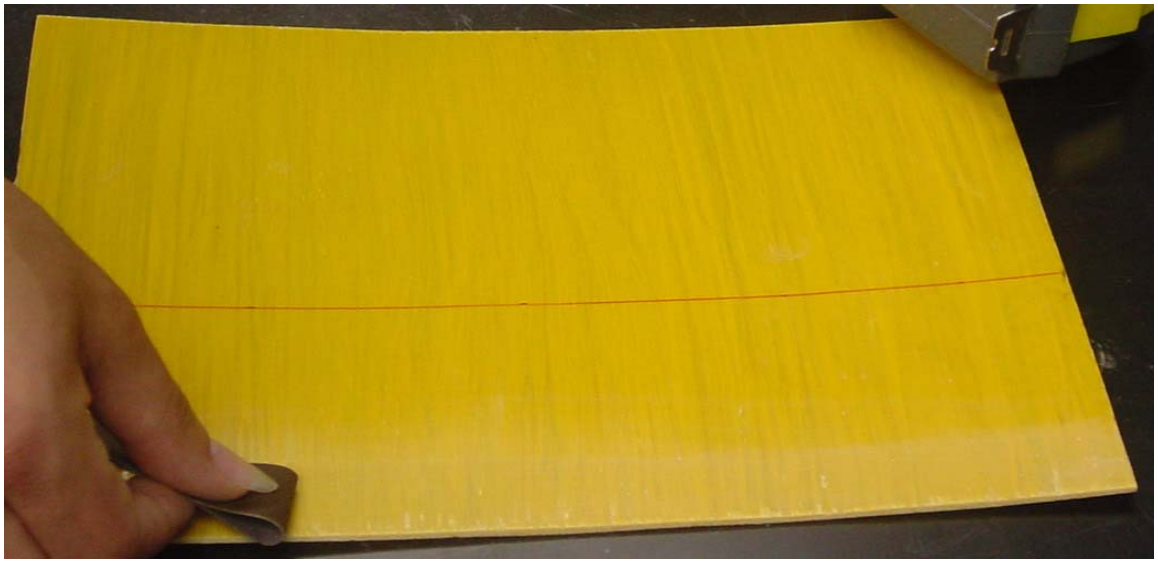

Figure 3.2 – Hand-Sanding Composite Bond Area

Figure 3.3 – Cleaning Composite Bond Area

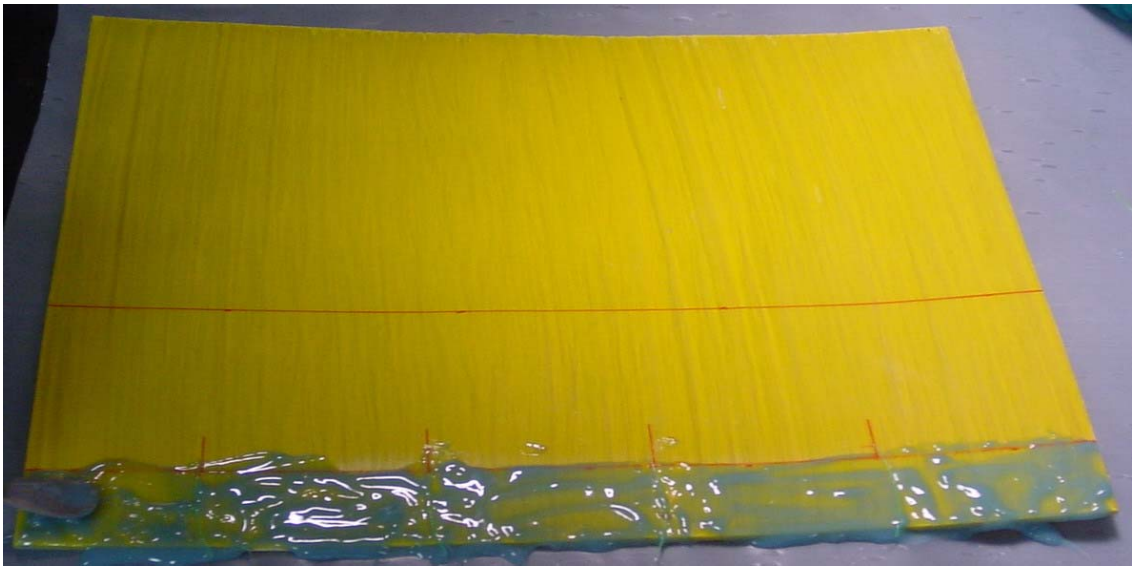

Figure 3.4 – Applying Adhesive to Composite Bond Area

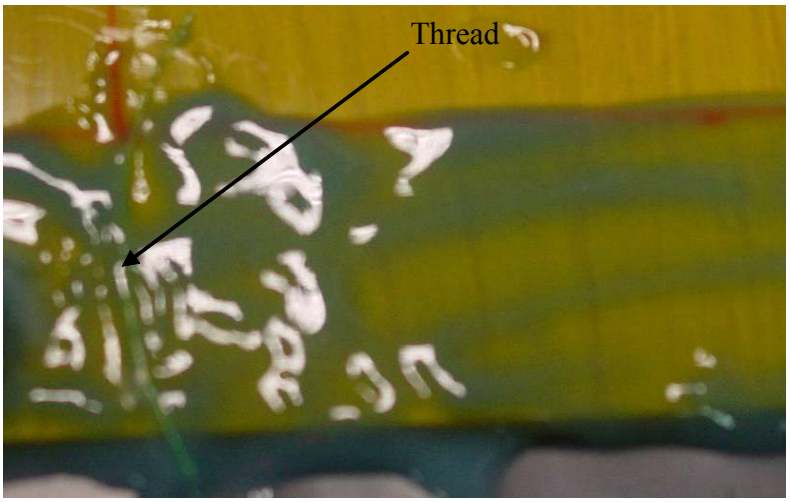

Figure 3.5 – Thread Spacer in Adhesive Layer

Figure 3.6 – Typical Finished Lightly-Sanded

Composite-to-Composite Lap Shear Specimen

After the composite material was prepared, the adhesive was mixed according to the product data specifications and applied to one composite sheet, as is shown in Figure 3.4. Two 0.01 inch diameter threads each were placed on the bond area to insure the bond thickness is uniform and is approximately 0.01 inch, as shown in Figure 3.5. The other sheet was then placed accurately on the sheet with the adhesive, to ensure an overlap length of one inch. The specimens were then covered with plastic, and 22 pound weights were applied to each sheet. After the specimens were sufficiently cured, the spacers were bonded to the ends. All specimens cured for at least one week before being tested.

After the bond area and the spacers were cured, the composite-to-composite sheets were cut into 1 inch strips using a wet saw. Nine specimens were obtained from each pair of composite-to-composite sheets. Once the strips were cut, the aluminum tabs were bonded to the ends. A typical finished lightly-sanded composite-to-composite specimen is shown in Figure 3.6.

3.3.1.2 Test Method

The composite-to-composite lap shear specimens were tested using an MTS closed loop testing machine. The test load was applied using a displacement controlled option with a rate of 0.05 inches per minute. Displacements were measured using an MTS extensometer with a gauge length of 2 inches, which was centered along the bond area, therefore providing half of an inch of composite on each side of the lap. Figure 3.7 shows the testing of a composite-to-composite lap shear specimen.

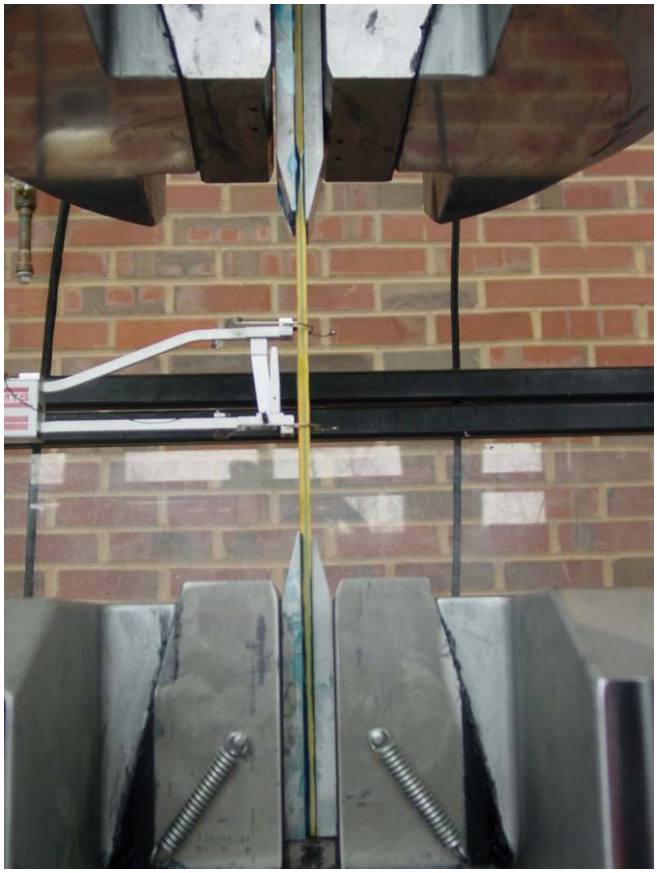

Figure 3.7 – Lightly-Sanded Composite-to-Composite Lap Shear Test

3.3.1.3 Thoroughly-Sanded Specimen Configuration

During fabrication of the lightly-sanded composite-to-composite specimens, it was observed that the composite spacers that spanned the entire length of the specimen increased the difficulty of ensuring the absence of end effects that may contribute to the apparent bond strength. Therefore, the spacers for the thoroughly-sanded composite-to-composite specimens, and all subsequent specimens, were modified. Rather than being 5 inches long and reaching from the end of the specimen to the lap, the new spacers were only 3 inches long and reached from the end of the specimen to the end of the grip. A

typical thoroughly-sanded composite-to-composite specimen test setup with the modified spacer is shown in Figure 3.8.

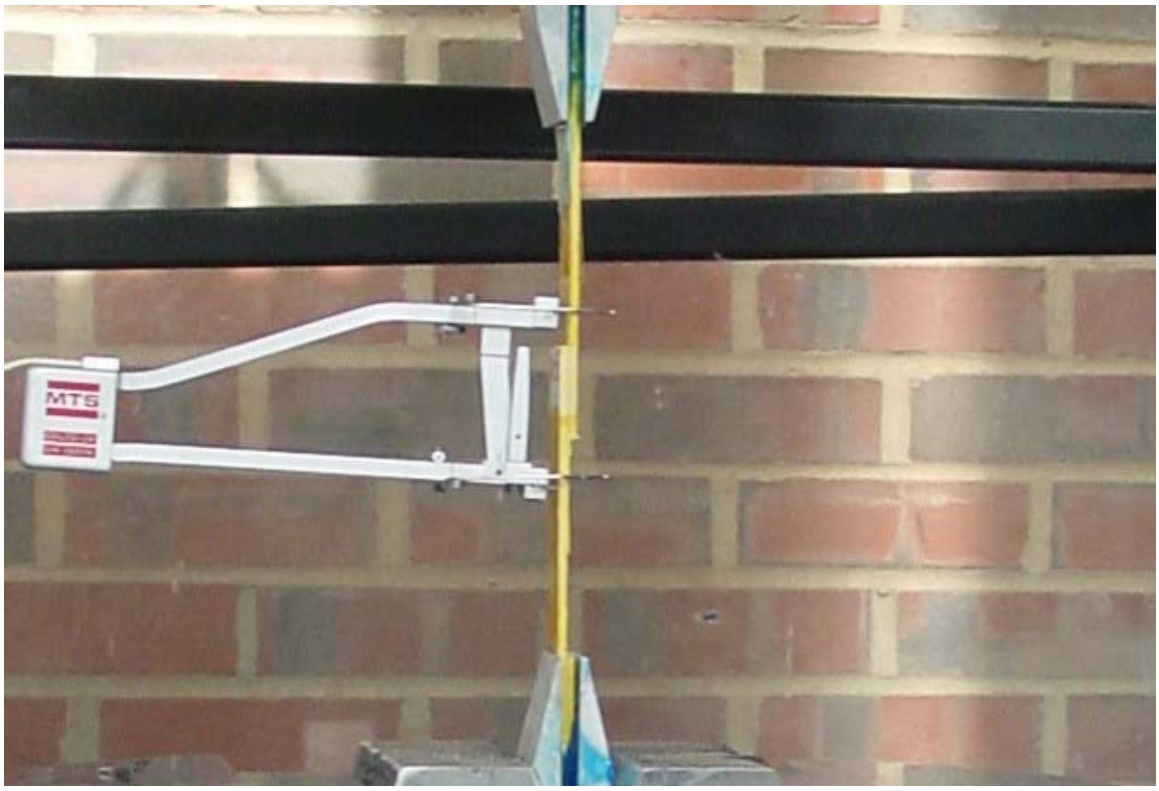

Figure 3.8 – Testing of a Modified Composite-to-Composite Lap Shear Specimen

3.3.2 Steel-to-Composite Lap Shear

Steel-to-composite lap shear specimens were made in a similar fashion to the composite-to-composite lap shear specimens. The dimensions of the specimens were the same, except that the thickness of the steel used was approximately 0.08 inches and smaller steel tabs were used instead of the aluminum ones used on the composite-to-composite specimens. The configuration of the steel-to-composite specimens is shown in Figure 3.9.

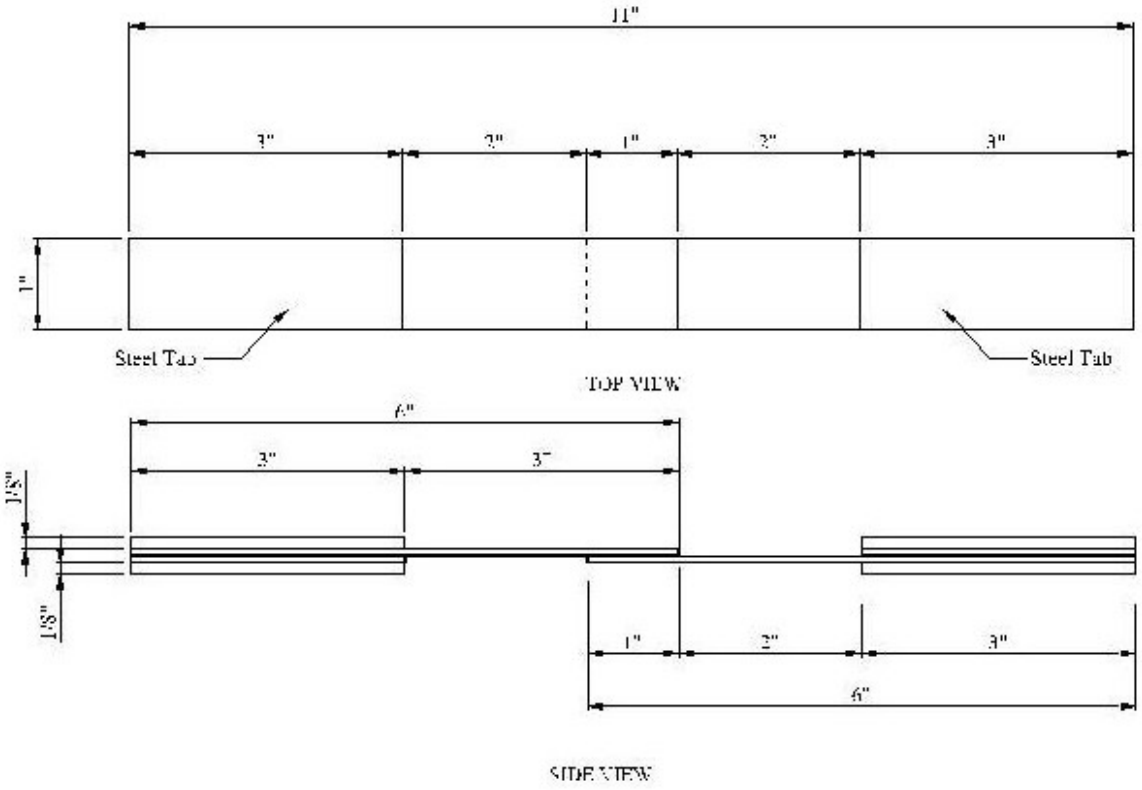

Figure 3.9 – Steel-to-Composite Lap Shear Specimen Configuration

One main difference with the preparation of steel-to-composite specimens in comparison to composite-to-composite specimens is that they cannot follow the fabrication process of being bonded in sheets and then cut in strips with a wet saw. Instead, the steel was ordered pre-cut into strips, and the composite material was then cut into strips and each specimen was bonded individually. Bonding individually caused concern with use of spacer threads to insure adhesive thickness. Using two threads in each one square inch bond area would cause too significant of a bond area loss. Therefore it was decided to not use spacers at all, so as to preserve all of the bond area. After curing, the adhesive layer thickness was measured to insure that the appropriate thickness was achieved, and it

was found that all specimens attained suitable thickness. A completed steel-to-composite specimen is shown in Figure 3.10.

Figure 3.10 – Steel-to-Composite Lap Shear Specimen

Before testing the lap shear specimens, a notch was cut into any adhesive that squeezed out during the curing process. A photograph of the notch being cut in a creep specimen is shown later in Figure 3.32. This was to insure that no tension forces were contributing to the measured strength. The steel-to-composite specimens were tested in a similar manner to the composite-to-composite.

3.3.2.1 Preparation Effects

As with the composite-to-composite specimens, the effects of key preparation factors were researched with the steel-to-composite specimens. The first factor explored was the lateral pressure that was applied to the bonded area during curing. The suggested laboratory preparation method is to apply approximately 25 pounds for every five specimens, which equals 5 pounds per square inch on each specimen, and twelve steel-to-composite lap shear specimens of each adhesive were tested using this method. In addition, five specimens of each adhesive were clamped, thus providing higher pressure, and two specimens of each adhesive were not pressured at all.

The second preparation factor is the steel surface preparation. The suggested preparation of the steel includes grinding and sandblasting. Five of the steel-to-composite specimens of each adhesive were prepared using this method. However, this preparation is often hard to achieve in the field, so fourteen of the steel-to-composite specimens were prepared with hand-sanding. All of the composite surfaces were thoroughly-sanded, and all of these specimens were tested in the manner similar to the composite-to-composite lap shear tests.

3.4 Phase II: Environmental Exposure Tests

The main objective of the second phase is to determine the effect of environmental conditions such temperature, pH level, and moisture during bonding and curing on the bond strength. In order to accomplish this objective the test matrix shown in Table 3.1 was developed. For each environmental exposure, each type of lap shear specimen was loaded by constant load and the length of time before failure occurred was recorded. Any specimen that did not fail after 1000 hours was removed from the environmental conditioning and was later tested to failure in the same manner as the Phase I specimens to see if the environmental conditioning had any permanent effects on the bond behavior. As can be seen in the test matrix, both composite-to-composite and steel-to-composite specimens were tested, some of which were bonded and cured in air and others in water. The temperature was examined using three temperature levels including room temperature (approximately 72 degrees Fahrenheit), 120 degrees Fahrenheit, and 140 degrees Fahrenheit. The effect of the pH level was examined under pH levels of 4, 7, and 9.5, and the applied loads were 200 pounds, 600 pounds, and 800 pounds. Because the

specimens were made with a one square inch bond area, these loads translate to 200, 600, and 800 pounds per square inch of shear stress.

Environmental Exposure Test Matrix						
Material	**Bond Conditions**	**Temp(F)**	**pH**	**Load(lb)**	**# Repeat**	**Speciman ID**
		72	7	800	2	C-RM-7-800-S
				200	3	C-120-7-200-S
		120	7	600	3	C-120-7-600-S
				800	3	C-120-7-800-S
			4	200	3	C-140-4-200-S
	Air Bonded			600	3	C-140-4-600-S
Composite-to-Composite				200	3	C-140-7-200-S
		140	7	600	3	C-140-7-600-S
				800	3	C-140-7-800-S
			9.5	200	3	C-140-9.5-200-S
				600	3	C-140-9.5-600-S
			4	600	2	*C-140-4-600-S
	Underwater Bonded	140	7	600	2	*C-140-7-600-S
			9.5	600	2	*C-140-9.5-600-S
		120	7	200	2	S-120-7-200-S
Steel-to-Composite	Air Bonded			600	2	S-120-7-600-S
		140	7	200	2	S-140-7-200-S
				800	2	S-140-7-800-S
				200	3	C-120-7-200-M
		120	7	600	3	C-120-7-600-M
				800	3	C-120-7-800-M
			4	200	3	C-140-4-200-M
	Air Bonded			600	3	C-140-4-600-M
				200	3	C-140-7-200-M
Composite-to-Composite		140	7	600	3	C-140-7-600-M
				800	3	C-140-7-800-M
			9.5	200	3	C-140-9.5-200-M
				600	3	C-140-9.5-600-M
			4	600	2	*C-140-4-600-M
	Underwater Bonded	140	7	600	2	*C-140-7-600-M
			9.5	600	2	*C-140-9.5-600-M
		120	7	200	2	S-120-7-200-M
Steel-to-Composite	Air Bonded			600	2	S-120-7-600-M
		140	7	200	2	S-140-7-200-M
				800	2	S-140-7-800-M

Table 3.1 – Environmental Exposure Test Matrix

The lap shear specimens were configured in the same manner as the Phase I specimens, except that both composite-to-composite and steel-to-composite specimens used the smaller steel tabs and holes were drilled into the ends of the tabs and the specimens so that they could be secured to hooks for loading purposes, as is shown in Figure 3.11. Figure 3.12 shows holes being drilled into the ends of the specimens. All specimens used the modified spacer design, all steel specimens were grinded and sandblasted, and all specimens were weighted during the curing process.

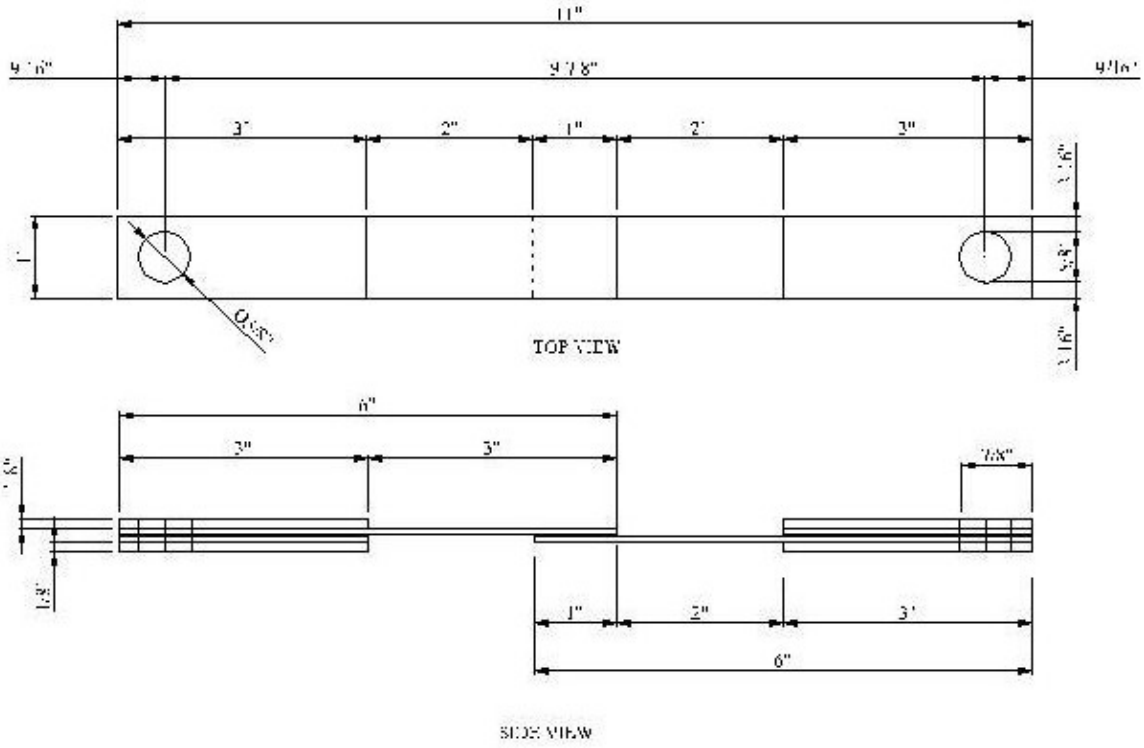

Figure 3.11 – Environmental Exposure Lap Shear Specimen Configuration

Figure 3.12 – Anchorage Holes Being Drilled into Specimen

3.4.1 Test Setup

In order to execute the Environmental Program test matrix, the load was applied to the test specimens using a specially designed test set up. To study the environmental conditions, the set up allowed for locating each specimen in a CPVC cylindrical container with water, a heater, and a thermostat. These containers were fabricated by securing and sealing J-bolts through a CPVP cap. As these bolts would be submersed in water they were all painted with a zinc-rich primer. Photographs of the spray-painting process and of inserting the J-bolts are shown in Figures 3.13 and 3.14, respectively. The bolts and caps were then secured to wooden boards located on the floor of the lab, as shown in

Figure 3.15. CPVC tubes were sealed to the anchored caps, as shown in Figure 3.16. Immersion heaters wired into thermostats were used to control the temperature of the water, and plastic tops with holes cut out to allow the specimens to slide through were used to hold the heaters and thermostats in place and to prevent excessive evaporation of the water. The heaters and thermostats are shown in Figure 3.17. These heaters were later replaced by better insulated ones, as the high moisture environment began damaging the electrical wires and causing heater failures. A newer heater in a plastic top is shown in Figure 3.18. A total of 19 environmental test setups were constructed.

Figure 3.13 – Spray Painting J-Bolts for Environmental Exposure Setup

Figure 3.14 – Inserting J-Bolts into Caps

Figure 3.15 – Bolts and Caps Secured

Figure 3.16 – Tubes Sealed onto Caps

Figure 3.17 – Heater and Thermostat

Figure 3.18 – Heater, Thermostat and Specimen in Plastic Top

The loading mechanism utilizes a lever system to apply different levels of sustained tensile load to the lap shear specimens. Posts were placed between the ceiling and the wooden boards, to hold the horizontal wood member in place. One end of each specimen was hooked onto the J-bolt in one of the CPVC tubes. The other end of the specimen was hooked onto another J-bolt that was secured to a 63 inch long, 52 pound HSS member. At 6.2 inches from the J-bolt, the HSS member was supported by a roller which was welded to the member and allowed it to pivot. The roller fit into a notched plate that was secured onto a wooden support frame. Initially, the plate was not notched, and the roller was not welded onto the HSS member. However, this setup caused preliminary failure in

some specimens due to the instability of the roller. At the other end of the HSS member, another J-bolt was secured, and 22 pound steel plates could be hung from that bolt to add weight to the system. Using the weight of the HSS members and the steel plates, the 6.2 inch distance was calculated to provide 200 pounds of tension force when no plates were hung at the end and an additional 200 pounds for every plate that was hung at the end. Another support was also built up at the weighted end to catch the HSS and steel plates after failure. The complete environmental exposure test setup is shown in Figure 3.19, along with details of a tube and specimen shown in Figure 3.20.

Figure 3.19 – Environmental Exposure Test Setup

Figure 3.20 – Side and Top Views of Detail A of the Loading Systems

In addition to the environmental and loading systems, a method of capturing the time up to failure was also developed. The system uses a computer web camera that was mounted from the ceiling to provide a bird's-eye view of the entire test setup, as is shown in Figure 3.21. The camera was connected to a personal computer, and, using basic camera software, was programmed to take and store a picture of the setup ever 6 minutes, or 0.1 hours. Each photograph also included a time stamp, so the date and exact time of each picture was known. Therefore, after a failure occurred, the time up to failure could be determined to an accuracy of 0.1 hours by reviewing the pictures taken by the camera. An example of two photographs taken by the camera, seen in Figure 3.22, shows how the failure time was obtainable by reviewing the web camera pictures.

Figure 3.21 – Web Camera Mounted from Ceiling

Figure 3.22 – Web Camera Pictures Showing Failure in Closest Specimen

3.4.2 Test Method

Each environmental exposure test began by emptying the water from the tube from the previous test. The lap shear specimen was then placed into the tube, and secured on the hook. The tube was then refilled with water, the heater, thermostat, and plastic top were put in place, and the thermostat was set to the appropriate temperature. Two to three hours later the temperature of the water was checked with a thermometer and any necessary adjustments to the thermostat were made. After the temperature was settled at the appropriate level, the pH level of the water was measured using pH strips and adjusted as necessary. The pH level was lowered using a diluted solution of hydrochloric acid, and the pH level was raised using a diluted solution of sodium hydroxide.

Once the appropriate environmental conditions were achieved, the specimen was ready to be loaded. The load was applied by supporting the weighted end of the HSS member so that that end was only slightly lower than the end at which the specimen would be connected. The J-bolt was then hooked through the specimen, and run through the end of the HSS member. The J-bolt was then held in place as a nut tightened it to the HSS member. By holding the J-bolt in place, torque forces were prevented from forming in the specimen. As the nut was tightened on the J-bolt, tension forces slowly developed in the lap shear specimen and the far end of the HSS member slowly began to rise. When the free end of the HSS member had completely risen off of its support, the temporary support blocks were removed and the full load was in the lap shear specimen. The tightening of the bolt took approximately one minute to complete, thus preventing any

impact loads from occurring in the specimen. As soon as the specimen was loaded, the starting time was recorded.

All specimens were observed for at least the first 12 minutes of testing, in order to get a more accurate failure time in case that time was unusually short. For those specimens that lasted prolonged amounts of time, the temperature and pH level of the environment were monitored on a semi-daily basis. When failure occurred, the web camera pictures were reviewed to determine the failure time, the specimen was removed, and the tube and loading mechanism was prepared for another test. A maximum testing time of 1000 hours was set for all environmental exposure specimens. Those specimens that did not fail after 1000 hours were tested in direct lap shear in a manner identical to the Phase I specimens in order to determine if the severe environmental conditions had any permanent effects on the behavior of the bond.

3.5 Phase III: Cleavage Peel Tests

3.5.1 Specimen Preparation

The third phase of testing followed the guidelines given in ASTM D 3807 – 98 (04) for determining the strength properties of adhesives bonding FRP to FRP in cleavage peel by tension loading. As is stated in the standard, the specimens were 1 inch wide by 7 inches long, with the first 3 inches of the specimen bonded with adhesive, and the load applied at 1 inch from the other end. Figure 3.23 shows the cleavage peel specimen diagram as specified by the ASTM standard.

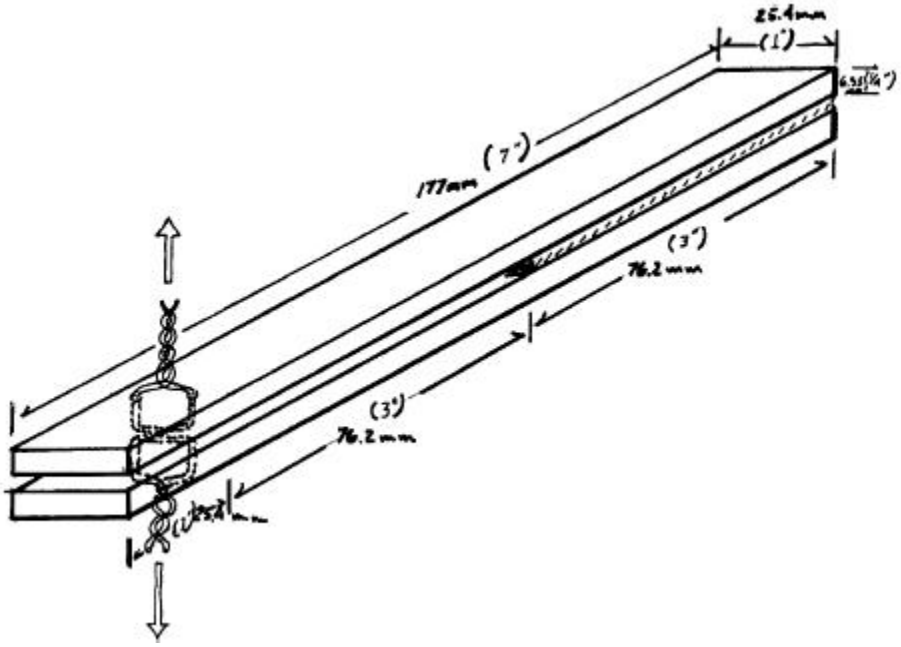

Figure 3.23 – Cleavage Peel Specimen from ASTM D 3807 – 98

These specimens were created by first cutting 12-inch wide sheets of the FRP to 7 inches in length, using a wet saw. The bond area of each sheet was thoroughly-sanded and cleaned in the same manner as the lap shear specimens. The 3 inch bond area was marked on the sheets, and plastic was wrapped around the remaining 4 inches to prevent bonding from occurring on those areas. Adhesive was then applied to the bond area, and the bonded area was weighted with approximately 22 pounds, and was allowed to cure. Figure 3.24 shows a set of bonded sheets with the plastic wrap.

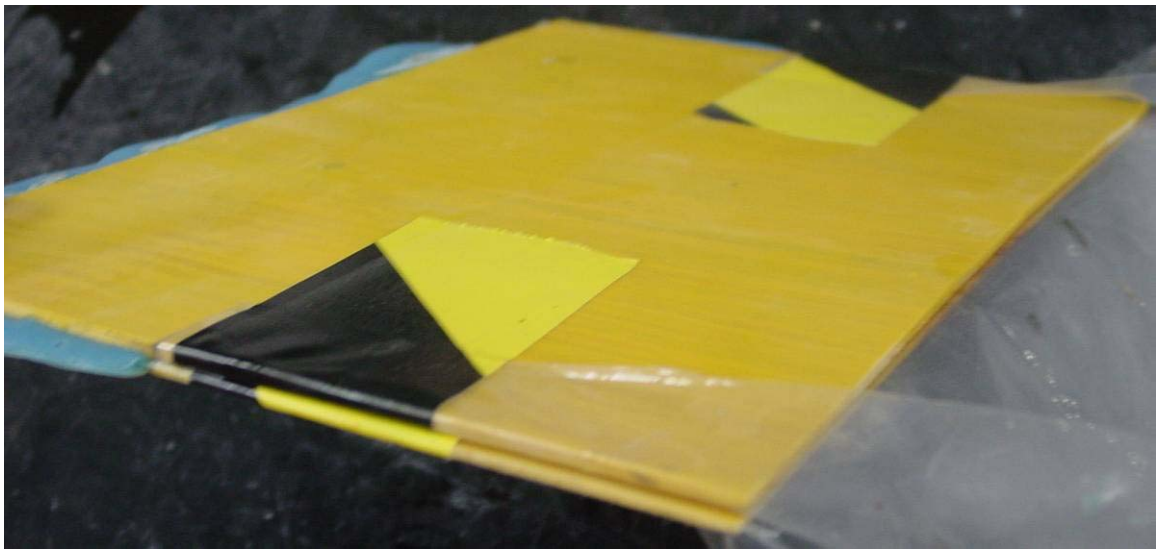

Figure 3.24 – Cured Cleavage Peel Sheets with Plastic Wrap

After the bonded sheets were cured, the plastic wrap was removed, and the sheets were cut into one inch strips using a wet saw. The distance to the point of loading was then measured using calipers, and notches were cut into the specimens at this point using a hack saw, to insure that the wire loading mechanism did not slip. An un-notched specimen is shown in Figure 3.25, and measuring and cutting of the notch is shown in Figure 3.26 and Figure 3.27, respectively.

3.5.2 Test Setup

The applied load was transferred to the cleavage peel specimen through 16 gage piano wire. This piano wire was bent to fit in the notches cut into the specimens, and was therefore capable of pulling the cleavage peel specimen apart without slipping. The load was applied using the MTS QTest machine. Special grips were manufactured to fit into the QTest machine and also house a bolt system to which the piano wire could be secured.

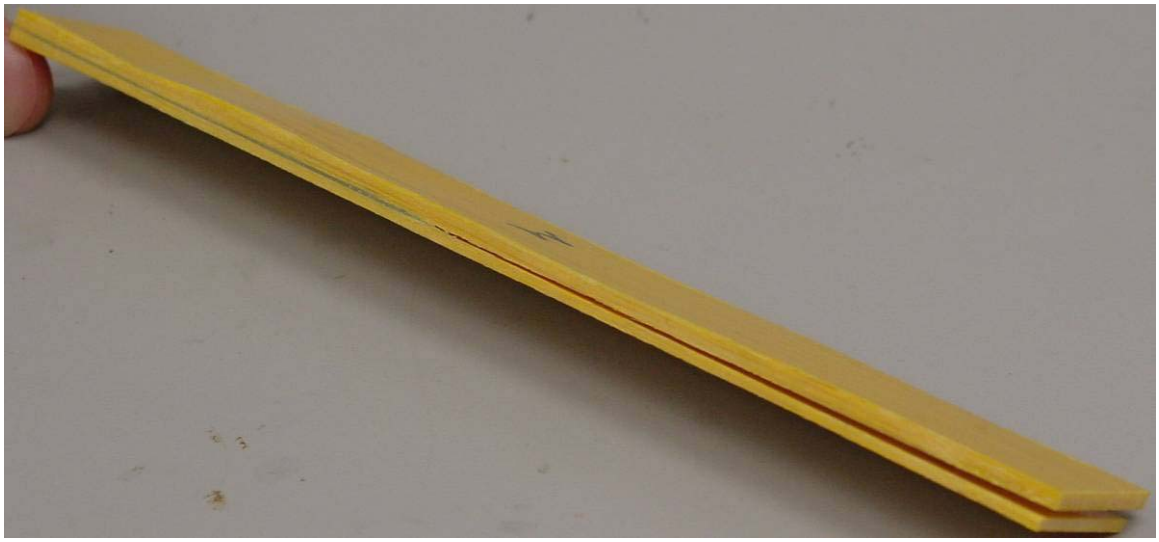

Figure 3.25 – Cleavage Peel Specimen

Figure 3.26 – Measuring for Point of Loading

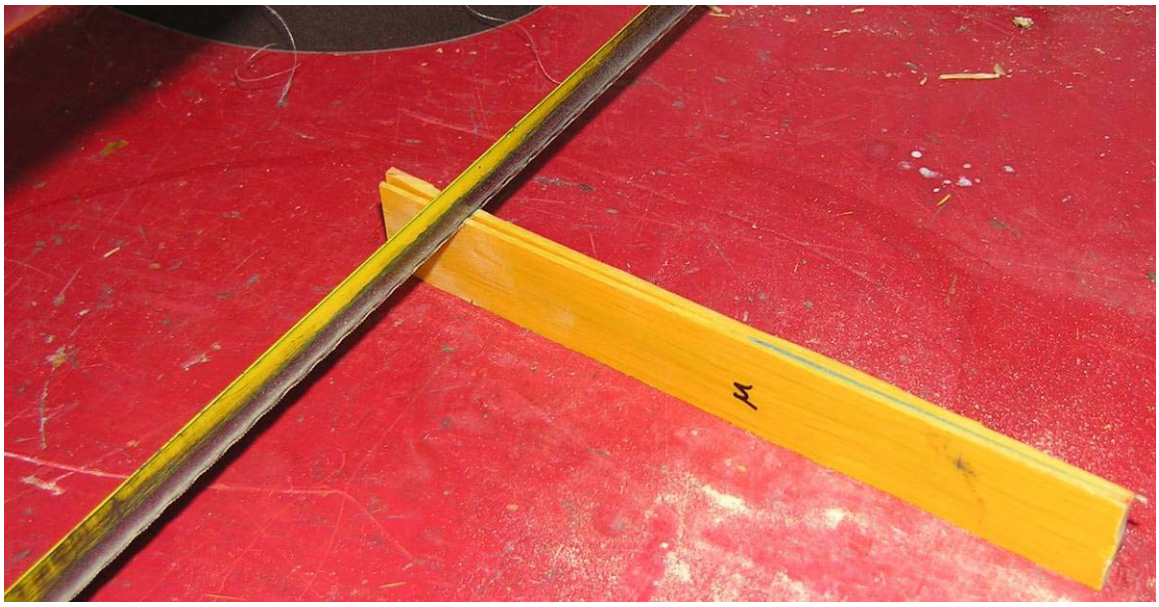

Figure 3.27 – Cutting Notch for Loading

The bottom of the specimen was held in place by a length of piano wire of only about one inch that was secured to the stationary grip at the bottom of the testing machine, as shown in Figure 3.28. The top of the specimen was secured to another length of piano wire of about one foot. This length was secured to a grip which was fastened to a 1000 pound load cell and the moving frame of the QTest machine. The complete loading mechanism is shown in Figure 3.29. Because of the stretching of the long length of piano wire, the crosshead movement of the QTest machine could not be used as the displacement of the specimen. Also, the center point of the specimen at the point of loading was inaccessible because of the piano wire. Therefore, deflections were instead measured on each side of the specimen at the point of loading, and these measurements were then averaged to determine the deflection at the center point. To measure the deflection accurately to the sides of the point of loading, two 6 inch metal tabs were bolted tightly together around the piano wire just above the specimen. String potentiometers, 15 inches long, were then

placed vertically below each end of the tabs and were secured between the tabs. This system allowed the specimen to rotate freely as it opened, and also allowed the string potentiometers to be used vertically to measure the opening deflection. The system used to measure deflection is shown in Figure 3.30.

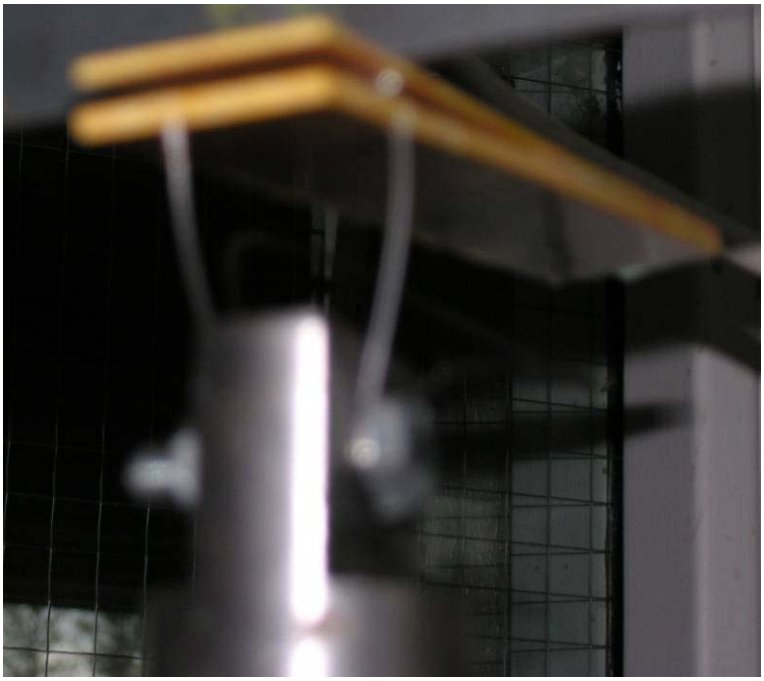

Figure 3.28 – Bottom of Specimen Secured with Short Piano Wire

The cleavage peel specimens were tested using the displacement control option of the QTest machine, with a rate of 0.5 inches per minute. A separate data acquisition system was used to collect readings from the load cell and string potentiometers. Eight specimens of each of the two adhesive were tested to failure. A typical specimen during different stages of testing is shown in Figure 3.31.

Figure 3.39 – Cleavage Peel Test Setup

Figure 3.30 – System for Measurement of Cleavage Peel Deflection

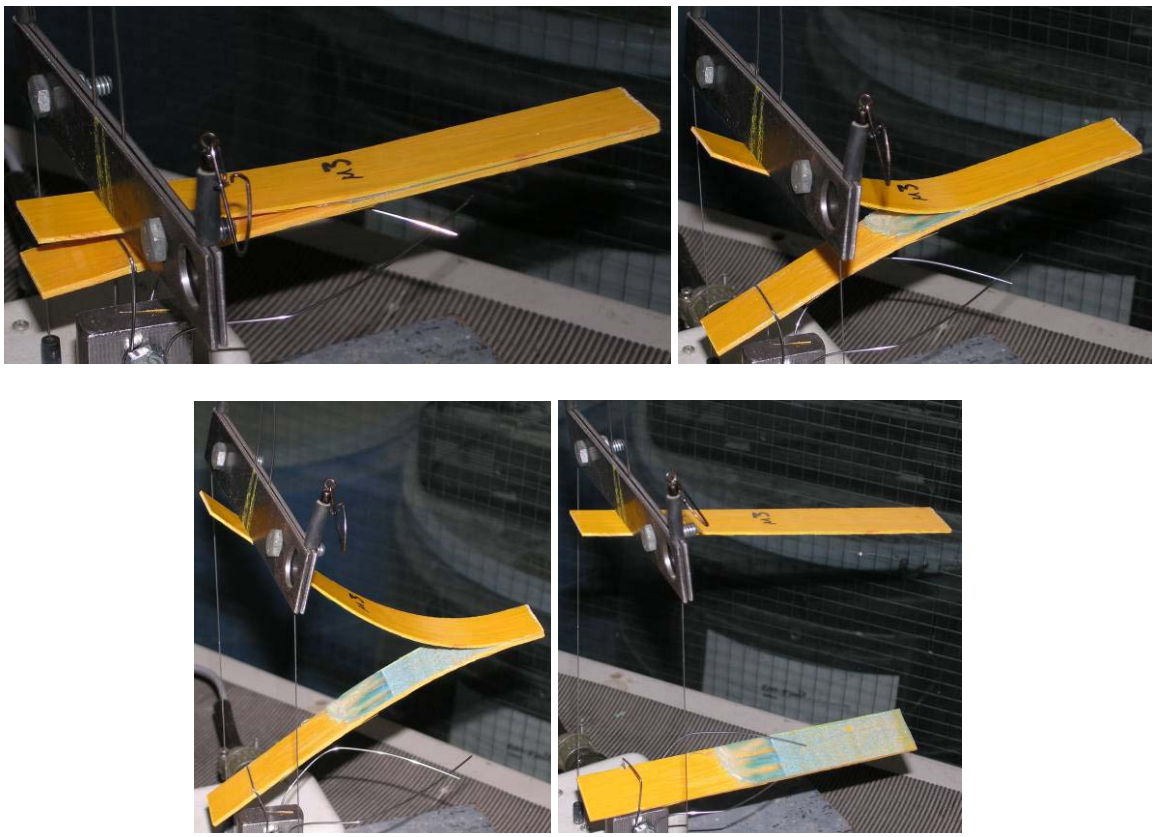

Figure 3.31 – Various Stages of Cleavage Peel Test

3.6 Creep Tests

The purpose of this phase of this project was to examine the displacement behavior of each of the two adhesives for 48 hours of constant loading. Both composite-to-composite and steel-to-composite specimens were tested at sustained loads of 400 pounds, 600 pounds, 800 pounds, and 1000 pounds. The specimens used were identical to the specimens used in the environmental exposure tests; lap shear specimens with one square inch of bond area. Therefore, the shear stresses present in the bond area under the different loads were 400, 600, 800, and 1000 pounds per square inch. Three specimens of each combination of adhesive, substrate bonded, and load were tested to provide

repeatability of the test results, which resulted in a total of 48 specimens tested. The specimens were prepared in the exact same manner as the lap shear specimens in Phase I. Notching the excess adhesive in order to insure no tension end effects is shown in Figure 3.32.

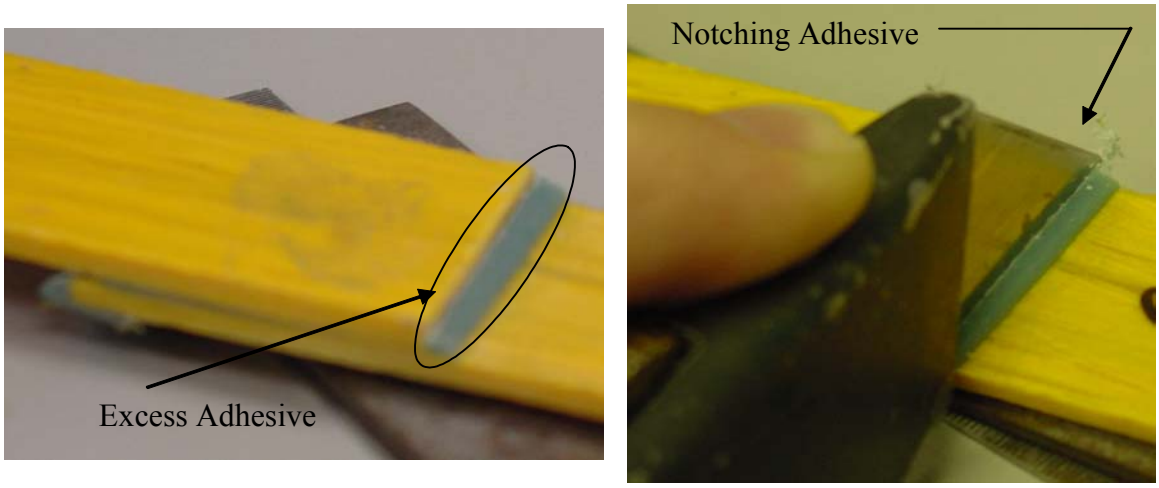

Figure 3.32 – Notching Excess Adhesive to Avoid Tension End Effects

The loading mechanism from the environmental exposure tests was also used to apply the sustained load for the creep tests, with the environmental tubes being emptied of all liquid. The displacement was monitored using a special method. Because the displacements expected after the initial displacements were so small, displacement measuring equipment with a very good resolution was necessary. Therefore, four 0.1 inch and three 0.2 inch Linear Variable Displacement Transducers (LVDT's) were acquired and used. These devices have a full displacement range of only 0.1 inches and 0.2 inches, respectively, and can therefore read very minute displacements within those ranges. In order to use these LVDT's to measure the displacements of the lap shear

specimens, brackets to hold the LVDT's and provide a surface for them to measure against were bonded on each side of the lap with epoxy, so that the relative displacement of the adhesively bonded materials could be monitored. Typical bonded brackets are shown in Figure 3.33. After curing of the epoxy, small bolts were used to secure the LVDT's to the brackets and to make small adjustments to the position of the LVDT's to achieve readings as close as possible to zero. Figure 3.34 shows an LVDT securely fastened to a creep specimen.

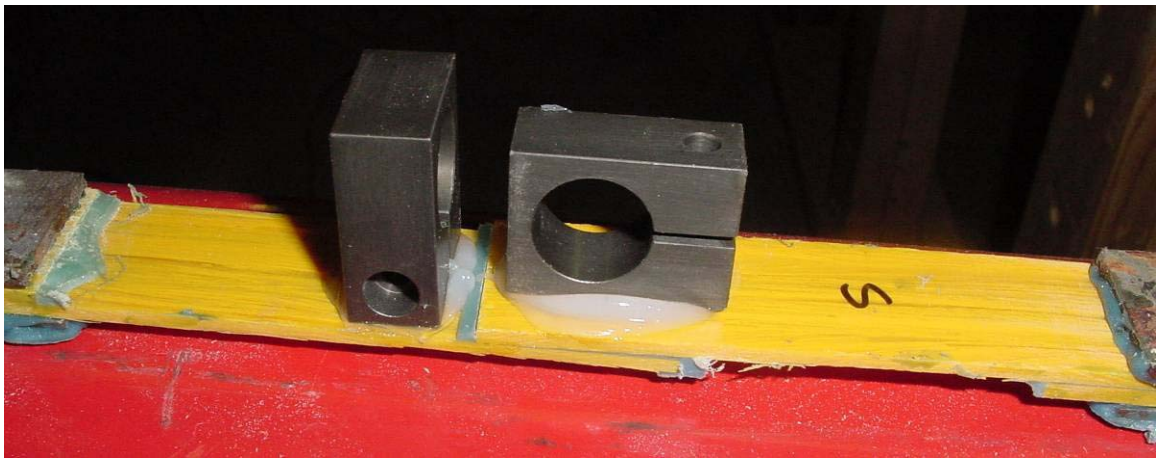

Figure 3.33 – Brackets Bonded to Creep Specimen

In the first several rounds of creep tests, LVDT's were secured to both sides of the creep specimen, to take into account any out of plane bending that may occur. However, this proved to be very problematic because of the limited space available using the loading mechanism from the environmental exposure tests which included the environmental tubes. Also, after reviewing the data from these tests, it was decided that out of plane bending was not causing any noticeable effect. This led to further tests being performed with only one LVDT mounted on each specimen. The LVDT displacement was

measured using a data acquisition system which recorded 0.01 scans per second, or one scan every 100 seconds. The loading procedure was identical to that of the environmental exposure tests.

Figure 3.34 – LVDT Secured to Creep Specimen

4.0 Results, Analysis, and Discussion

4.1 Introduction

As was discussed in Chapter 3, four investigative phases were performed and data was collected from each. The following sections will present the results of each phase, as well as an analysis and discussion of the test results.

4.2 Phase I: Lap Shear

All lap shear specimens were tested to failure using the displacement control loading condition. Load was measured using a 2,000,000 pound load cell and displacements were measured using a two inch extensometer secured over the lap. Shear stress was calculated by assuming that the load is acting on the measured area of adhesive at the bond. The displacement of the composite and steel within the extensometer range was calculated using the moduli of the two substrates, and this displacement was deducted from the total displacement to calculate the adhesive displacement. This value was used to calculate the adhesive shear strain. All of the results of the lap shear tests are presented using the calculated shear stresses and adhesive shear strains.

4.2.1 Composite-to-Composite

Figure 4.1 shows the results of the lap shear tests of the lightly-sanded composite-to-composite specimens bonded with adhesive M. Table 4.1 summarizes the measured ultimate shear stress, adhesive shear strain at ultimate stress, shear strain at failure, and adhesive strain at failure. Figure 4.1 indicates that the initial behavior of the adhesive is

primarily linear, and the average shear modulus on the initial linear range is 133 ksi. At a higher range of loading, the behavior became nonlinear and all of the specimens exhibit a peak stress, followed by a descending behavior up to failure. This behavior is favorable since it reflects ductility of the joint before failure. It should be noted that the amount of stress carried and the amount of strain sustained after the peak was quite variable among the specimens as shown in Figure 4.1 for the five tested specimens. Test results indicate the large standard deviations of the measured shear and strain values at failure.

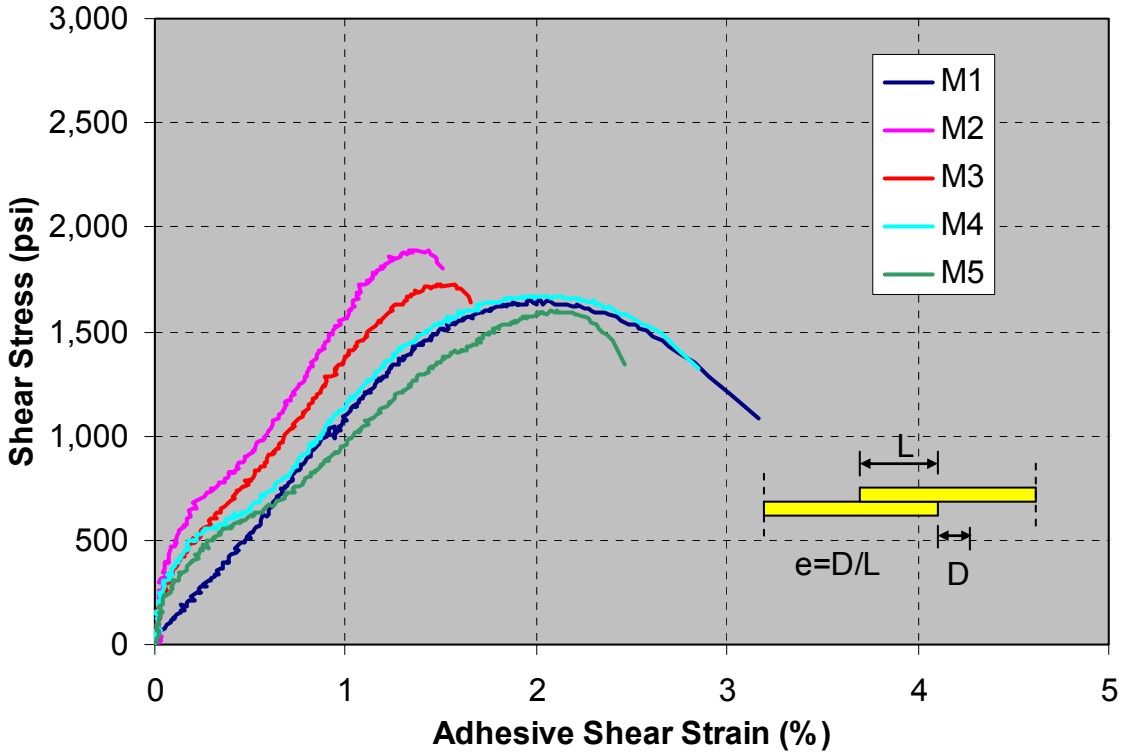

Figure 4.1 – Results of Lightly-Sanded Composite-to-Composite Tests using M Adhesive

Specimen	Ultimate Shear Strength (psi)	Adhesive Shear Strain at Ultimate Strength (%)	Shear Stress at Failure (psi)	Strain at Failure (%)
M1	1644	1.950	1083	3.163
M2	1892	1.375	1803	1.506
M3	1722	1.480	1636	1.660
M4	1672	1.937	1322	2.853
M5	1599	2.077	1343	2.461
Average	**1706**	**1.764**	**1438**	**2.329**
Std Deviation	113	0.314	284	0.727

Table 4.1 – Summary of Lightly-Sanded Composite-to-Composite Tests using M Adhesive

A typical failure mode of the lightly-sanded composite-to-composite using M adhesive lap shear specimens is shown in Figure 4.2. The failure shown is completely cohesive, which means that the failure takes place completely within the adhesive layer.

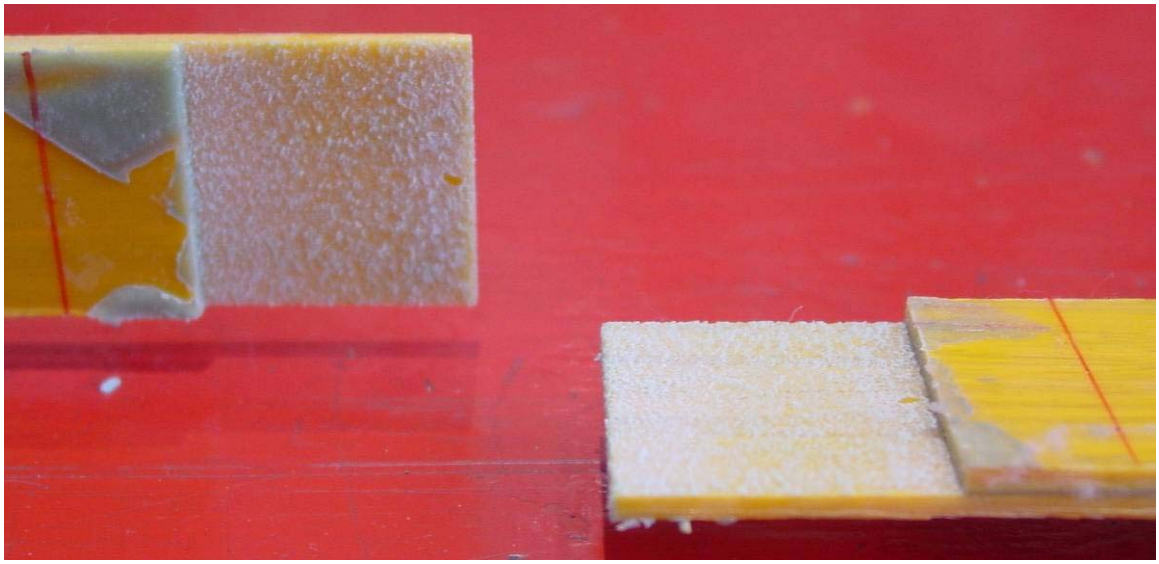

Figure 4.2 – Lightly-Sanded Composite-to-Composite Failure Mode using S Adhesive

Figure 4.3 and Table 4.2 show the results of the lightly-sanded composite-to-composite lap shear tests using the S adhesive. The behavior of the S adhesive specimens was similar to that of the M adhesive specimens. However several variances are apparent. The moduli of all of the specimens were consistent in the linear zone, and the average measured modulus of the S adhesive is 95 ksi, smaller than that of the M adhesive. The average ultimate shear strength of the S adhesive was 9.1 percent higher than that of the M adhesive. As mentioned before, the behavior after reaching the ultimate strength is also very important. Similar to the M adhesive specimens, the S adhesive specimens show a wide-ranged descending relationship before failure. Test results indicate that the average shear stress at failure of the S adhesive specimens is 25.5 percent lower than that of the M adhesive specimens. However, the average shear strain at failure is 51.4 percent higher. This shows that the S adhesive can withstand higher shear strains before failure in comparison to the M adhesive.

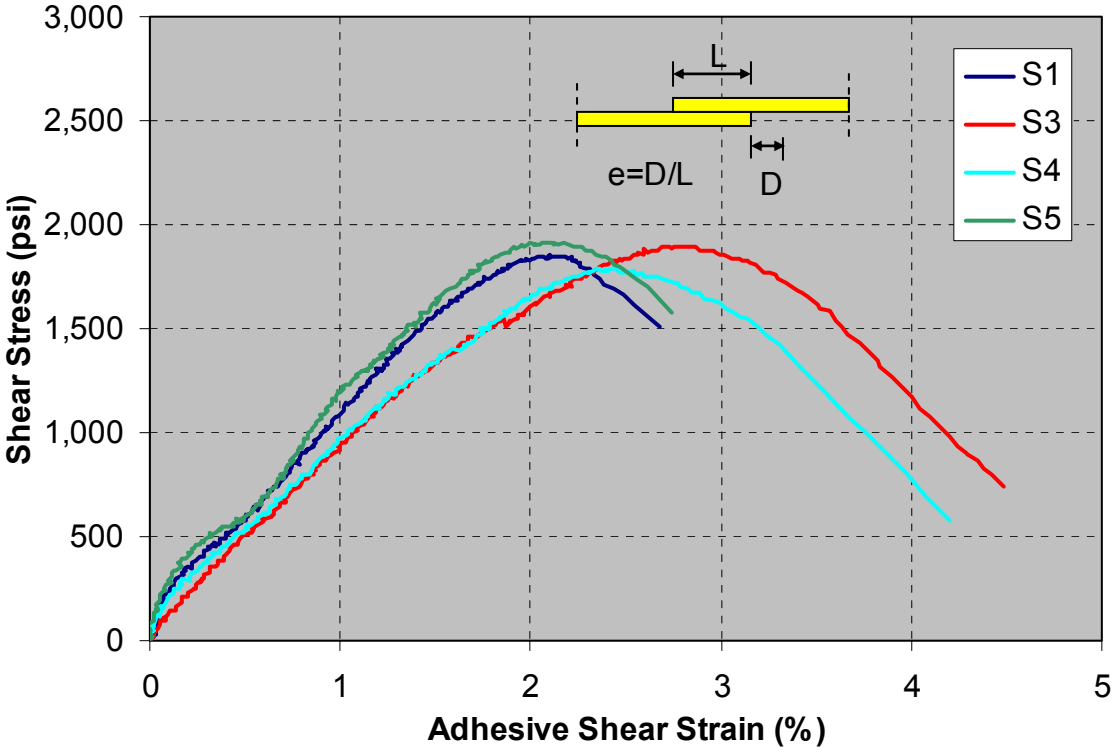

Figure 4.3 – Results of Lightly-Sanded Composite-to-Composite Tests using S Adhesive

Specimen	Ultimate Shear Stress (psi)	Adhesive Shear Strain at Ultimate Stress (%)	Shear Stress at Failure (psi)	Strain at Failure (%)
S1	1854	2.096	1506	2.677
S3	1897	2.729	739	4.484
S4	1790	2.366	575	4.199
S5	1910	2.056	1581	2.746
Average	**1862**	**2.312**	**1100**	**3.526**
Std Deviation	54	0.310	517	0.949

Table 4.2 – Summary of Lightly-Sanded Composite-to-Composite Tests using S Adhesive

Figure 4.4 shows a typical failure mode for the lightly-sanded composite-to-composite lap shear specimen using the S adhesive. Unlike the M adhesive specimens, the S adhesive specimens failed mostly in an adhesive mode, a mode in which the failure occurs between the adhesive and the substrate at the surface of the substrate. Some small portions of cohesive failure were also observed.

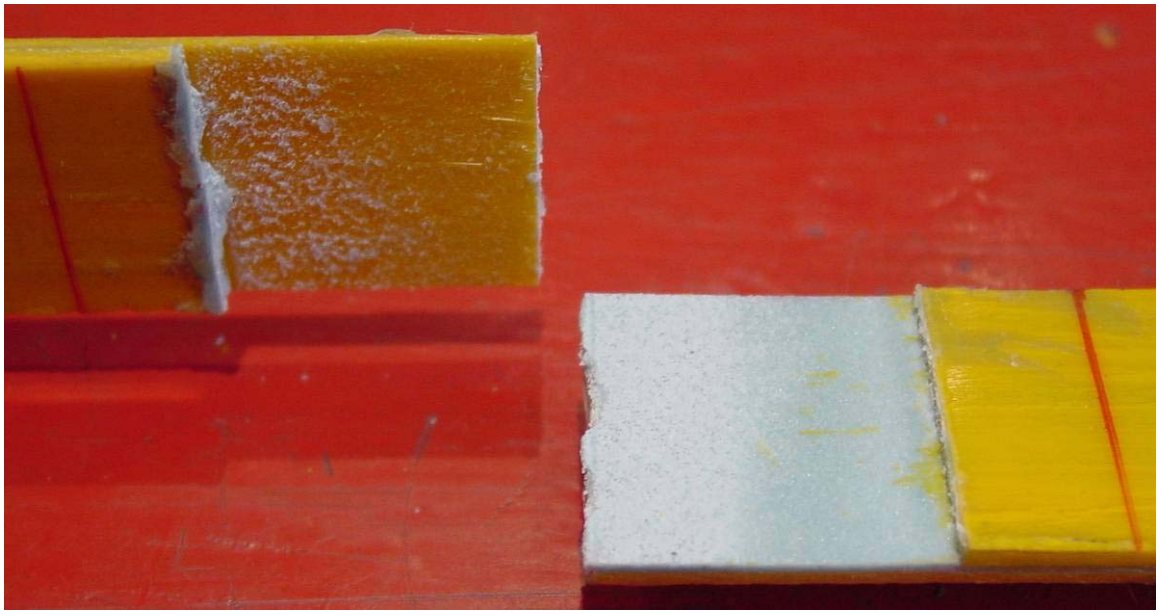

Figure 4.4 – Lightly-Sanded Composite-to-Composite Failure Mode using S Adhesive

Figure 4.5 and Table 4.3 show the results of the thoroughly-sanded composite-to-composite lap shear tests using the M adhesive. It is clear from the graph that the preparation method used with the composite substrate does affect the behavior of the adhesive M composite-to-composite lap shear specimens. The thoroughly-sanded specimens are all stiffer in the linear zone than the lightly-sanded specimens, with a modulus of approximately 200 ksi, and the behavior after the ultimate stress was

significantly different, since some of the specimens failed immediately as the applied stresses reached the ultimate strength. Most importantly, using thoroughly sanded specimens increased the average ultimate shear strength by 12.8 percent.

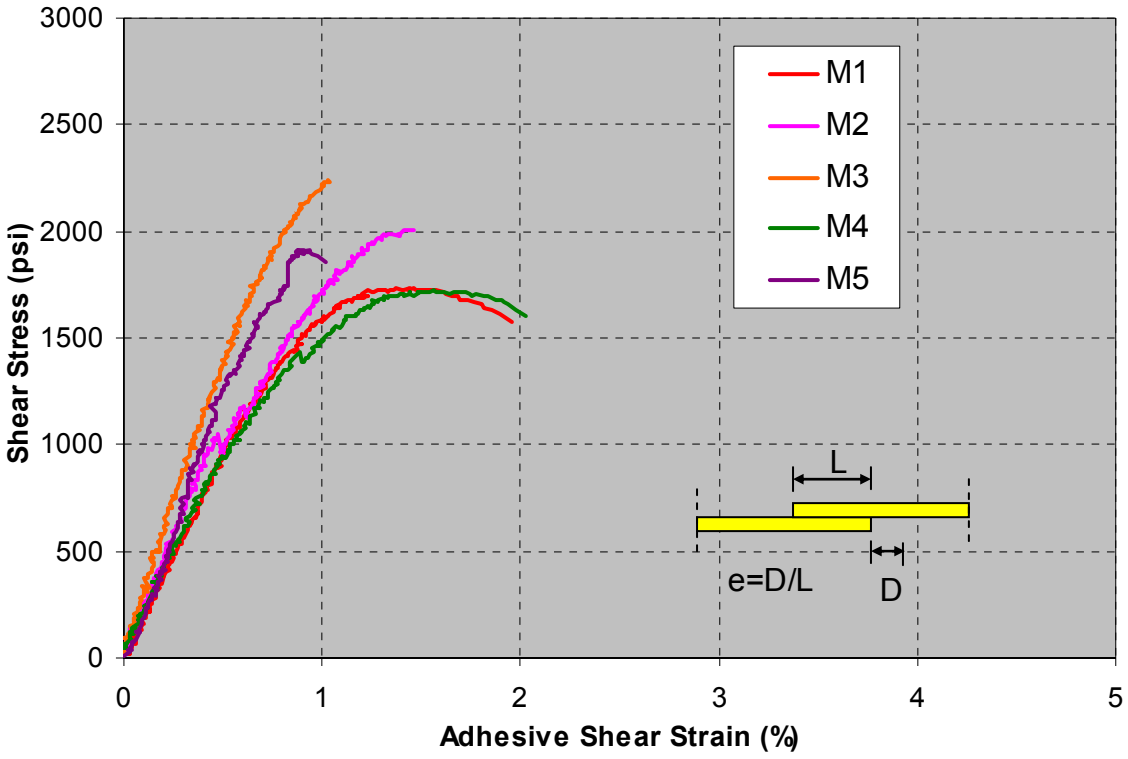

Figure 4.5 – Results of Thoroughly-Sanded Composite-to-Composite Tests using M Adhesive

Specimen	Ultimate Shear Strength (psi)	Adhesive Shear Strain at Ultimate Strength (%)	Shear Stress at Failure (psi)	Strain at Failure (%)
M1	1737	1.465	1573	1.958
M2	2005	1.464	2005	1.464
M3	2240	1.031	2240	1.031
M4	1726	1.558	1608	2.023
M5	1913	0.905	1854	1.022
Average	**1924**	**1.285**	**1856**	**1.500**
Std Deviation	213	0.295	279	0.483

Table 4.3 – Summary of Thoroughly-Sanded Composite-to-Composite Tests using M Adhesive

A typical failure mode of the adhesive M used for the thoroughly-sanded composite-to-composite lap shear specimens is shown in Figure 4.6. As with the lightly-sanded specimens, the failure mode was cohesive for all tested specimens.

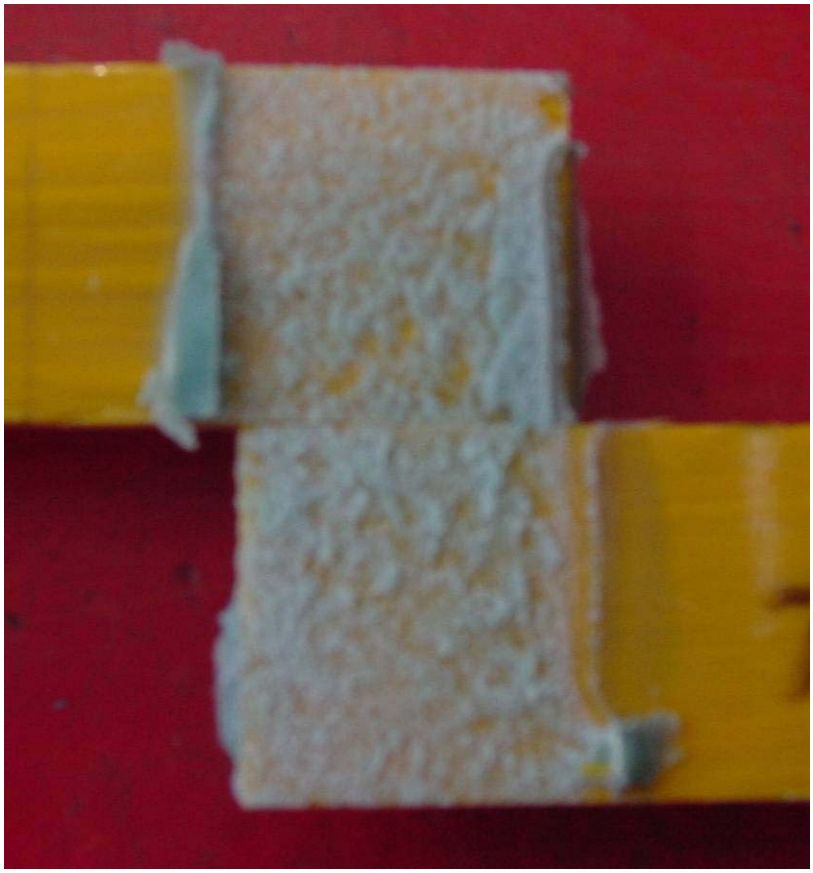

Figure 4.6 – Thoroughly-Sanded Composite-to-Composite Failure Mode using M Adhesive

Test results of the thoroughly-sanded composite-to-composite lap shear specimens using the S adhesive are shown in Figure 4.7, and the calculated values are given in Table 4.4. Similar to the behavior of adhesive M, using thoroughly-sanded specimens with adhesive S showed a higher stiffness than the lightly-sanded specimens, and the average modulus is approximately 200 ksi. Similar to the M adhesive, some of the specimens failed immediately when the applied stress reached the ultimate strength. Thoroughly sanding the composite substrate with adhesive S resulted in a 21.3 percent increase in strength.

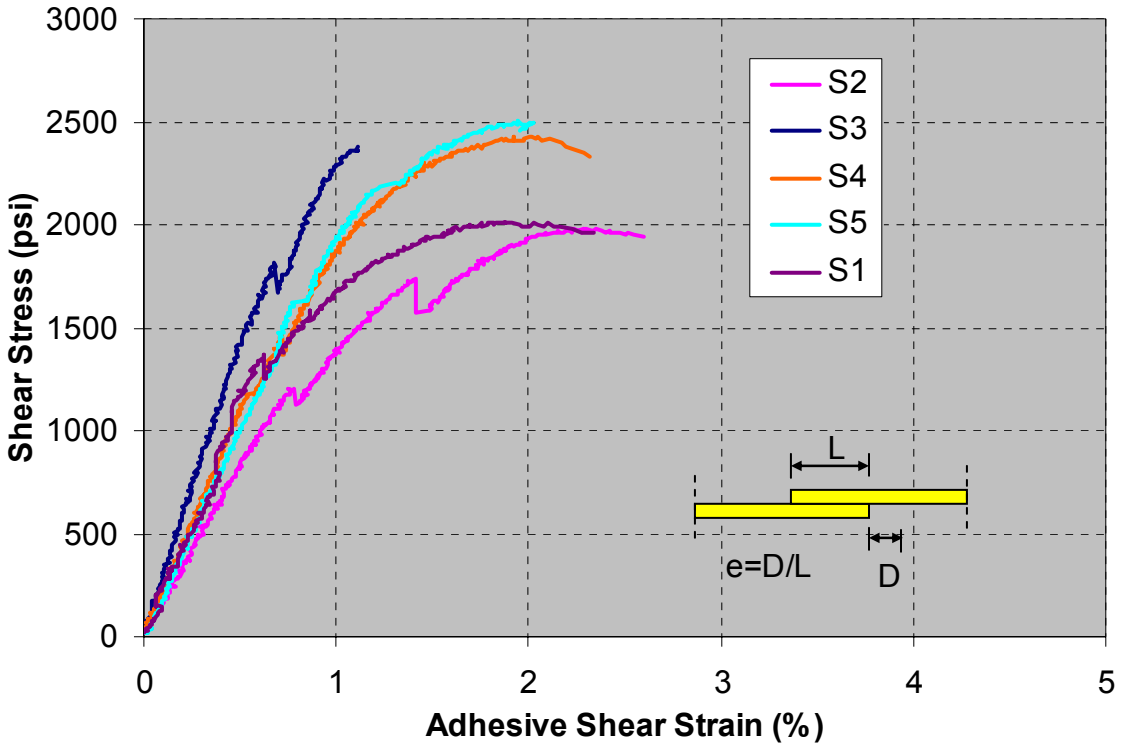

Figure 4.7 – Results of Thoroughly-Sanded Composite-to-Composite Tests using S Adhesive

Specimen	Ultimate Shear Strength (psi)	Adhesive Shear Strain at Ultimate Strength (%)	Shear Stress at Failure (psi)	Strain at Failure (%)
S1	2013	1.834	1963	2.342
S2	1977	2.232	1941	2.594
S3	2375	1.111	2375	1.111
S4	2423	2.053	2335	2.315
S5	2506	1.946	2458	1.953
Average	**2259**	**1.835**	**2214**	**2.063**
Std Deviation	246	0.431	244	0.579

Table 4.4 – Summary of Thoroughly-Sanded Composite-to-Composite Tests using S Adhesive

Figure 4.8 shows a typical failure mode of adhesive S used for a thoroughly-sanded composite-to-composite lap shear specimen. The failure is partially adhesive and cohesive, as was the case for the lightly-sanded specimens. However, a large portion of the failure was in the material of the composite substrate. This type of failure that includes adhesive, cohesive, and failure of the material of the substrate suggests that the bond strength of the adhesive to the substrate, the strength of the adhesive material, and the surface strength of the substrate material are all well balanced and all materials are being used efficiently.

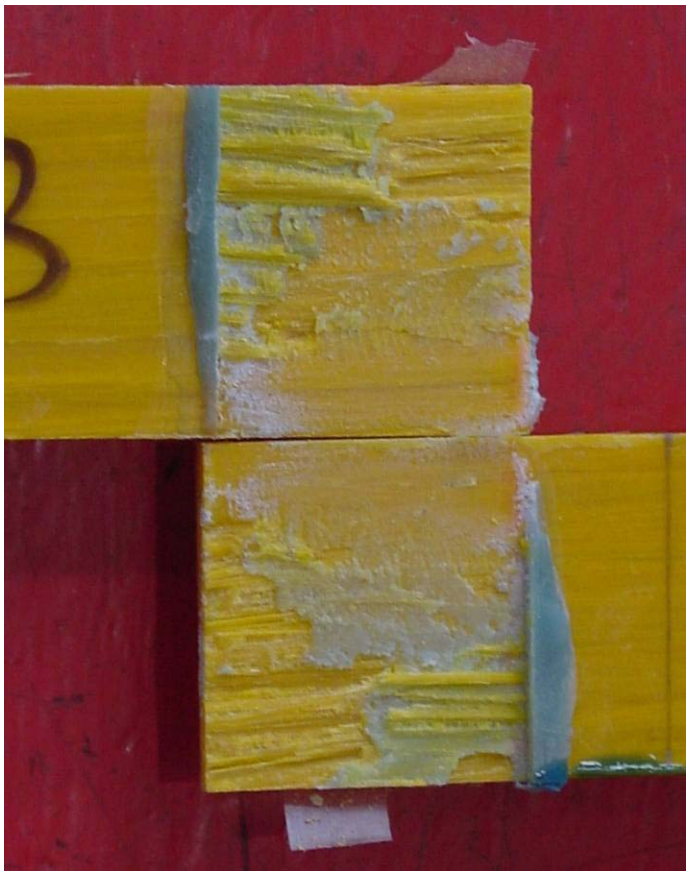

Figure 4.8 – Thoroughly-Sanded Composite-to-Composite Failure Mode using S Adhesive

Based on the test results, the thoroughly-sanded surface preparation method is highly recommended for composite-to-composite bonds for the two types of the adhesives used in this program. Test results also indicated that the ultimate shear strength of the adhesive S is about 17.4 percent higher than that of adhesive M. Additionally, adhesive S withstands more displacement after reaching the ultimate shear strength, with average stress and strain levels at failure 19.3 and 37.5 percent higher than those of adhesive M, respectively. Test results indicate that the stiffness of the two adhesive are in the same range.

4.2.2 Steel-to-Composite

For the steel-to-composite lap shear tests, attention was given to the effect of pressure during curing and the surface preparation of the steel, for the two adhesives. All of the composite substrate surfaces were thoroughly-sanded by hand. All of the steel substrate surfaces were hand-sanded when studying the effect of pressure during curing time, and when studying the effect of steel surface preparation, the pressure was applied using weights. The results of all of the tests are reported in a similar fashion to the composite-to-composite lap shear tests.

4.2.2.1 Clamped, Un-Pressured, and Weighted Specimens

Figure 4.9 and Table 4.5 provide test results of using adhesive M for the clamped steel-to-composite lap shear tests. The initial behavior was linear with an average shear modulus of 400 ksi. Failure occurred abruptly after reaching the ultimate shear strength.

The specimens show no sign of ductility before failure, which is certainly an undesirable and serious behavior. Behavior of all of the specimens was consistent.

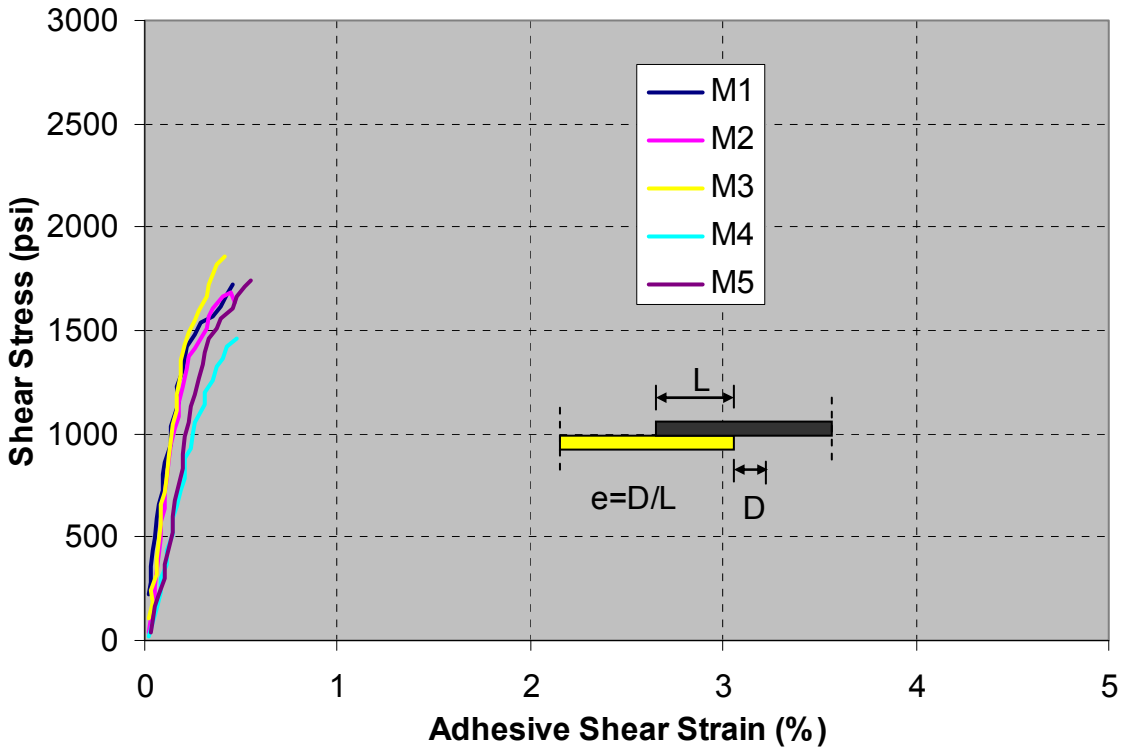

Figure 4.9 – Results of Clamped Steel-to-Composite Tests using M Adhesive

Specimen	Ultimate Shear Strength (psi)	Adhesive Shear Strain at Ultimate Strength (%)	Shear Stress at Failure (psi)	Strain at Failure (%)
M1	1722	0.455	1722	0.455
M2	1687	0.442	1635	0.468
M3	1855	0.412	1855	0.412
M4	1458	0.480	1458	0.480
M5	1741	0.554	1741	0.554
Average	**1693**	**0.469**	**1682**	**0.474**
Std Deviation	145	0.054	148	0.052

Table 4.5 – Summary of Clamped Steel-to-Composite Tests using M Adhesive

Figure 4.10 shows the typical failure mode observed for the adhesive M used for clamped steel-to-composite lap shear specimens. It should be noted that the thickness of the adhesive layer is very thin, and that the failure mode is mostly adhesive failure from the steel substrate. The thin thickness of the adhesive layer was most likely a result of the high applied pressure caused by clamping, and may have contributed to the high measured shear stiffness for this type of lap shear specimen.

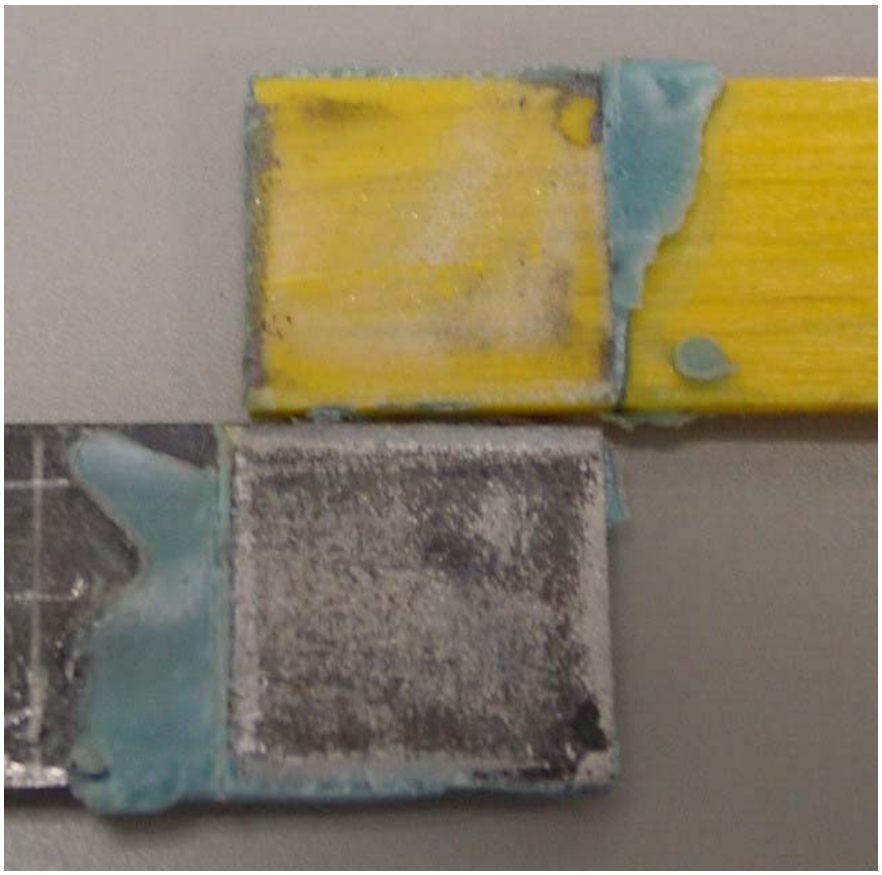

Figure 4.10 – Clamped Steel-to-Composite Failure Mode using M Adhesive

Figure 4.11 and Table 4.6 show test results of the adhesive S used for the clamped steel-to-composite lap shear tests. These specimens behaved in a very similar manner to the clamped specimens using the M adhesive. The stress-strain behavior for these specimens was mainly linear up to the ultimate strength, at which point failure occurred, also abruptly. However, the average ultimate shear strength of the adhesive S specimens was 20.3 percent less that that of the adhesive M specimens.

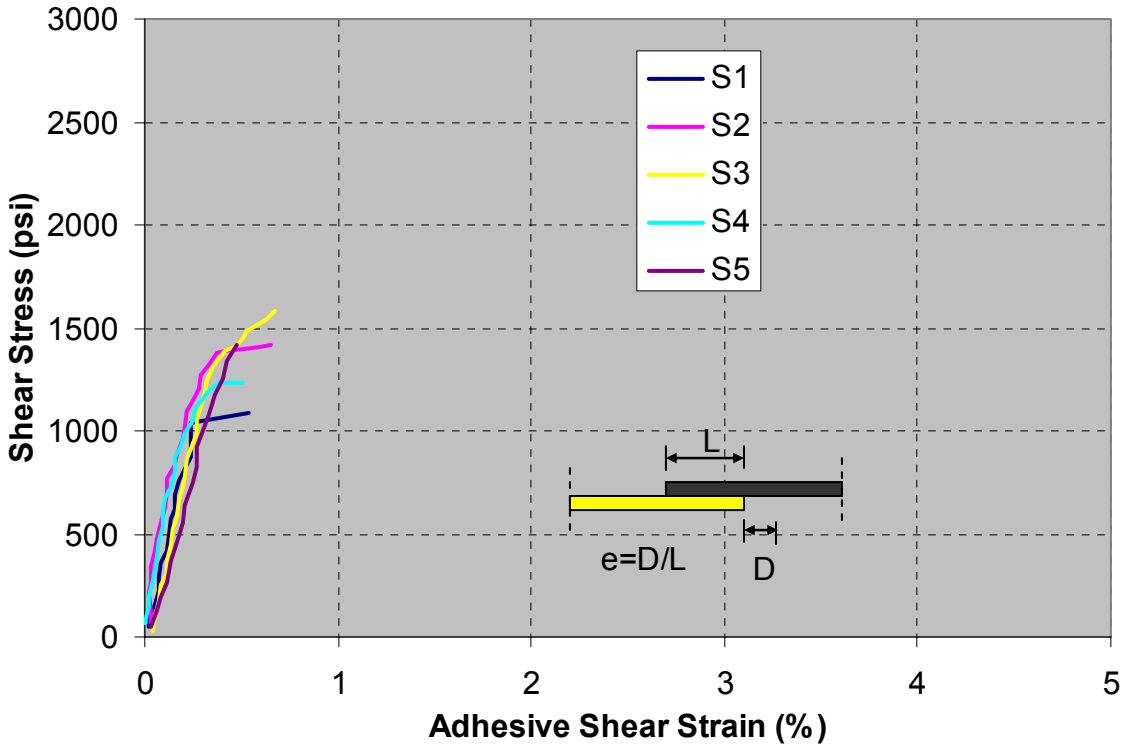

Figure 4.11 – Results of Clamped Steel-to-Composite Tests using S Adhesive

Specimen	Ultimate Shear Strength (psi)	Adhesive Shear Strain at Ultimate Strength (%)	Shear Stress at Failure (psi)	Strain at Failure (%)
S1	1092	0.538	1092	0.538
S2	1418	0.656	1418	0.656
S3	1578	0.668	1578	0.668
S4	1237	0.512	1237	0.512
S5	1420	0.479	1420	0.479
Average	**1349**	**0.571**	**1349**	**0.571**
Std Deviation	188	0.086	188	0.086

Table 4.6 – Summary of Clamped Steel-to-Composite Tests using S Adhesive

Figure 4.12 shows the typical failure mode observed for the adhesive S used for the clamped steel-to-composite lap shear specimens. The failure was very similar to that of the adhesive M specimens. Again the adhesive layer was very thin, and the failure mode was adhesive failure from the steel substrate.

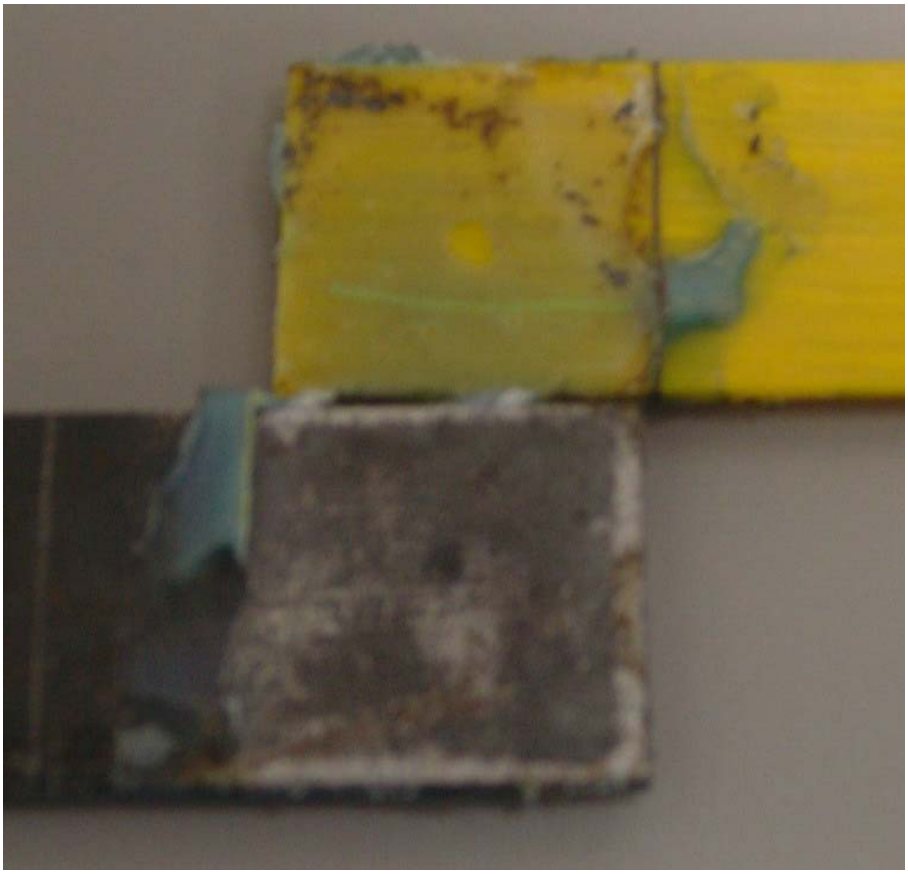

Figure 4.12 – Clamped Steel-to-Composite Failure Mode using S Adhesive

Figure 4.13 and Table 4.7 show the results of the adhesive M used for steel-to-composite lap shear tests without any pressure applied during the curing process. The behavior of these specimens was dramatically different than that of the clamped specimens. The initial behavior exhibits less stiffness with an average shear modulus of 333 ksi. However, the behavior was highly nonlinear up to failure. The nonlinear behavior started before reaching the ultimate strength, and the specimens continued to carry load over a large range of displacements after reaching ultimate strength. Test results indicate that the average ultimate shear strength decreased by 18.0 percent.

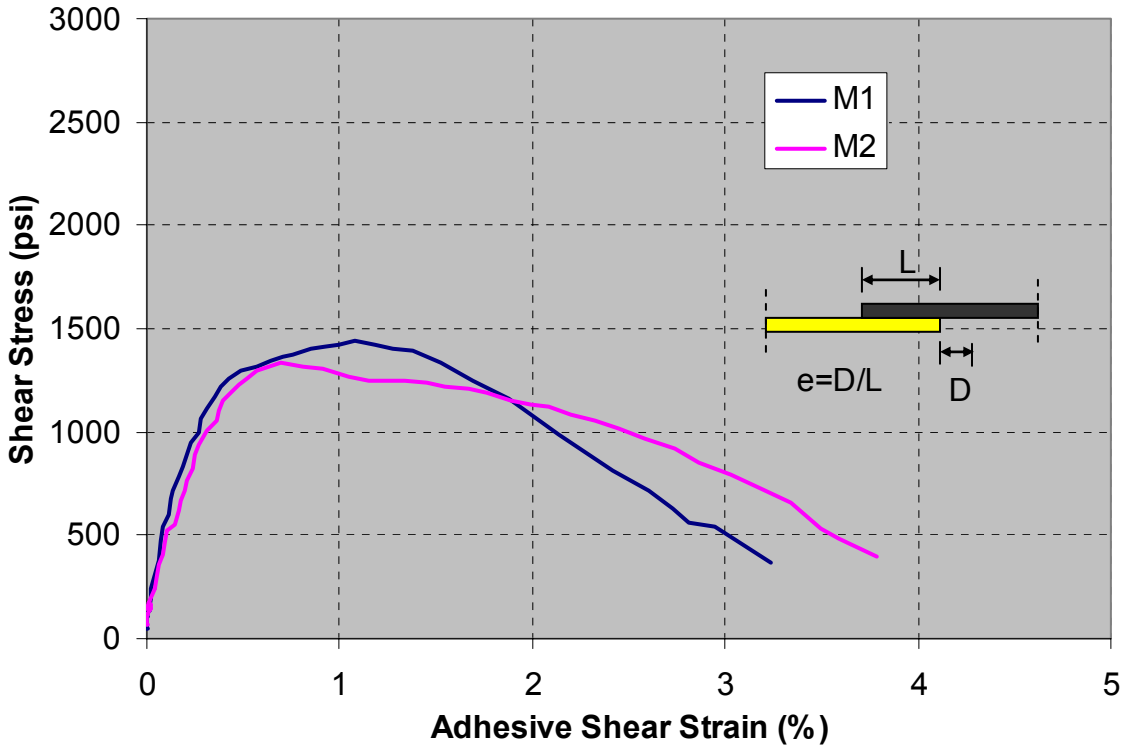

Figure 4.13 – Results of Un-Pressured Steel-to-Composite Tests using M Adhesive

Specimen	Ultimate Shear Strength (psi)	Adhesive Shear Strain at Ultimate Strength (%)	Shear Stress at Failure (psi)	Strain at Failure (%)
M1	1444	1.077	369	3.238
M2	1331	0.699	400	3.791
Average	**1388**	**0.888**	**384**	**3.514**
Std Deviation	80	0.268	22	0.391

Table 4.7 – Summary of Un-Pressured Steel-to-Composite Tests using M Adhesive

Figure 4.14 shows the failure modes of the adhesive M used for un-pressured steel-to-composite lap shear specimens. Without any pressure during bonding, the adhesive

thickness was very thick, which could account for the measured reduction of the stiffness. The observed failure was mixed cohesive and adhesive from both substrates.

Figure 4.14 – Un-Pressured Steel-to-Composite Failure Modes using M Adhesive

Figure 4.15 and Table 4.8 provides test results of the adhesive S used for the un-pressured steel-to-composite test. This specimen performed in a similar manner to the clamped specimens. Unlike the adhesive M used for the un-pressured specimens, the adhesive S displayed approximately the same stiffness as the clamped specimens and failed immediately after reaching its ultimate shear strength. The ultimate strength was also very similar to the one measured for the clamped specimen with an average increase of 3.3 percent.

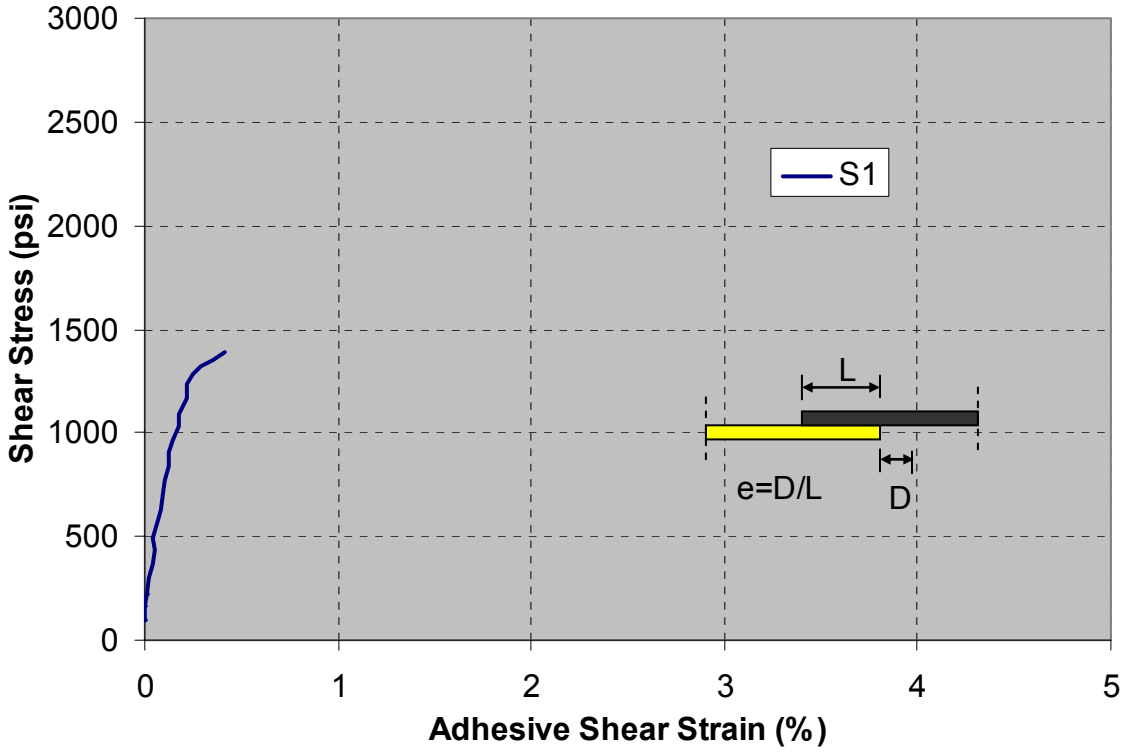

Figure 4.15 – Results of Un-Pressured Steel-to-Composite Test using S Adhesive

Specimen	Ultimate Shear Strength (psi)	Adhesive Shear Strain at Ultimate Strength (%)	Shear Stress at Failure (psi)	Strain at Failure (%)
S	1394	0.415	1394	0.415

Table 4.8 – Summary of Un-Pressured Steel-to-Composite Test using S Adhesive

Figure 4.16 shows the failure mode of the adhesive S used for the un-pressured steel-to-composite lap shear specimen. The failure mode looks very similar to that of the clamped specimens. The adhesive layer was relatively thin, and the failure type was

adhesive from the steel substrate. The similarity of the failure modes of both the clamped and un-pressured adhesive S specimens coincides with the similarity of the behavior of the specimens constructed using the two curing methods. Viscosity of the adhesive S is believed to cause the similarity of the failure modes of the clamped and un-pressured specimens. Regardless of the pressure applied during the curing process, flow of the adhesive will allow a thinner adhesive thickness in comparison to the adhesive M, which is less fluid.

Figure 4.16 – Un-Pressured Steel-to-Composite Failure Mode using S Adhesive

Figure 4.17 and Table 4.9 show the results of the adhesive M used for weighted steel-to-composite lap shear specimens. As was expected, the behavior of the weighted adhesive M specimens was something in between to that of the clamped and un-pressured specimens. However, failure did not occur immediately after reaching the ultimate strength. There was little measurable strain after reaching the ultimate strength, unlike for the un-pressured specimens, but failure was much more desirable than that of the clamped specimens. Additionally, the average ultimate strength was 42.7 and 17.0

percent higher than that of the clamped and un-pressured specimens, respectively. It is clear from these results that the most desirable behavior from adhesive M can be achieved using sufficient pressure on the bond during the curing process which can be obtained by using weights.

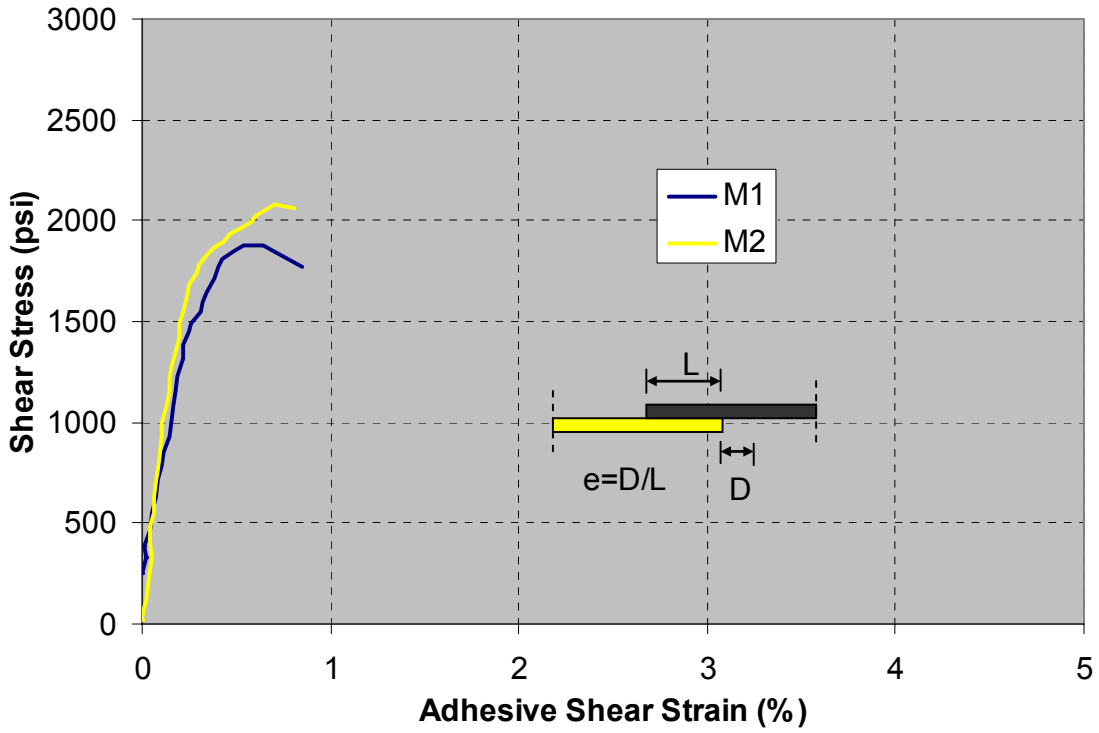

Figure 4.17 – Results of Weighted Steel-to-Composite Tests using M Adhesive

Specimen	Ultimate Shear Strength (psi)	Adhesive Shear Strain at Ultimate Strength (%)	Shear Stress at Failure (psi)	Strain at Failure (%)
M1	1881	0.540	1775	0.851
M2	2081	0.706	2063	0.807
Average	**1981**	**0.623**	**1919**	**0.829**
Std Deviation	141	0.117	203	0.031

Table 4.9 – Summary of Weighted Steel-to-Composite Tests using M Adhesive

Figure 4.18 shows the failure modes of the adhesive M used for the weighted steel-to-composite specimens. Failure mode for all tested specimens was cohesive. This mode suggests that the pressure caused by the weights is enough to provide a strong bond between the adhesive and the substrate, and is not high enough to squeeze the adhesive out of the contact area.

Figure 4.18 – Weighted Steel-to-Composite Failure Modes using M Adhesive

Figure 4.19 and Table 4.10 show test results of the adhesive S used for the weighted steel-to-composite lap shear tests. The behavior of these specimens was similar to that of

the clamped and un-pressured steel-to-composite specimens that used adhesive S. However, the behavior of the weighted specimens was slightly stiffer and more ductile before failure. The average ultimate shear strength was 58.2 and 63.5 percent higher than that of the un-pressured and clamped specimens, respectively. This suggests that while the pressure during bonding does not significantly affect the shape of the shear stress-strain relationship of the adhesive S specimens, it does greatly influence the ultimate shear strength of the bond.

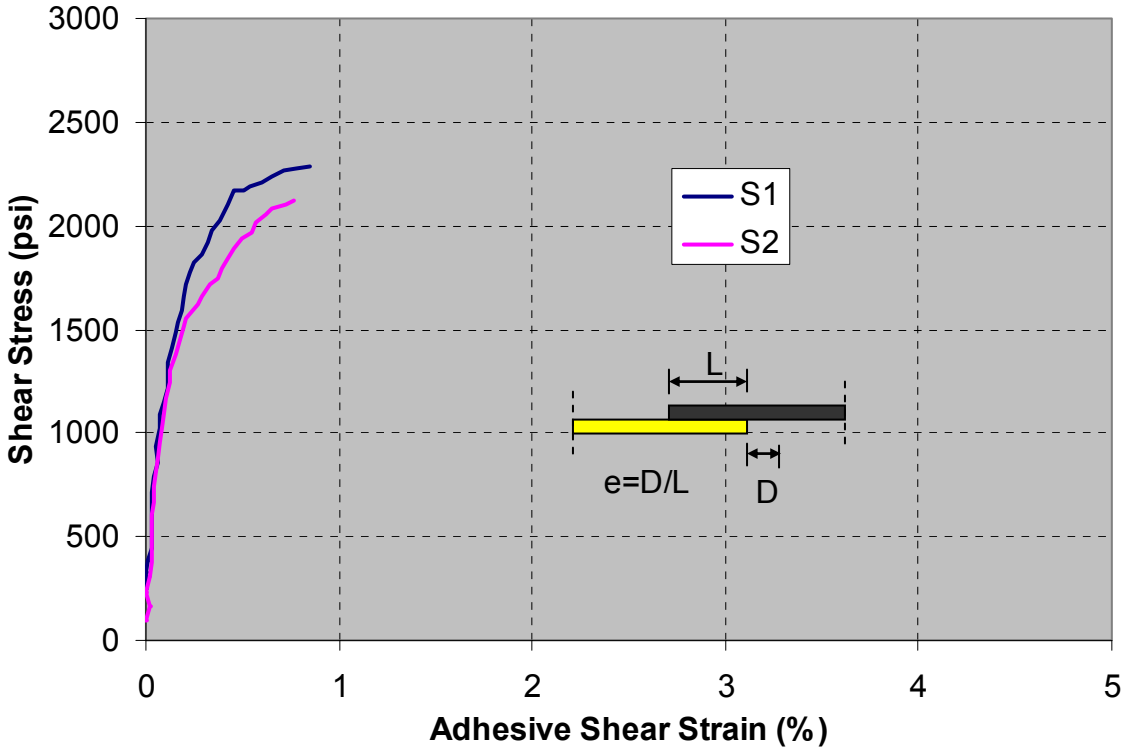

Figure 4.19 – Results of Weighted Steel-to-Composite Tests using S Adhesive

Specimen	Ultimate Shear Strength (psi)	Adhesive Shear Strain at Ultimate Strength (%)	Shear Stress at Failure (psi)	Strain at Failure (%)
S1	2288	0.844	2288	0.844
S2	2125	0.765	2125	0.765
Average	**2206**	**0.805**	**2206**	**0.805**
Std Deviation	115	0.056	115	0.056

Table 4.10 – Summary of Weighted Steel-to-Composite Tests using S Adhesive

Figure 4.20 shows the failure modes of the adhesive S used for the weighted steel-to-composite lap shear specimens. Failure mode of all specimens was adhesive from the steel substrate. The thickness of the S adhesive was thinner than was found for the M adhesive. However, while the failure mode does not appear different, it is clear from the results that the bond between the adhesive and steel substrate was definitely influenced by the amount of pressure present during curing.

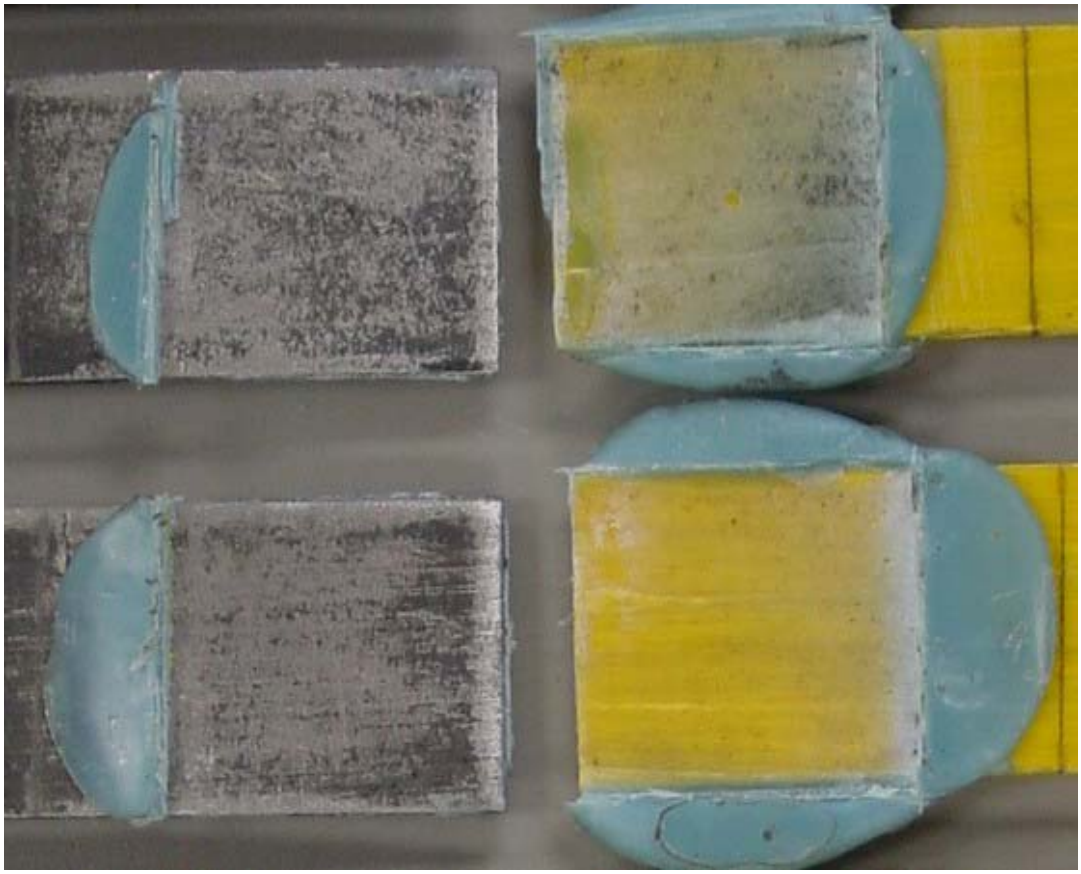

Figure 4.20 – Weighted Steel-to-Composite Failure Modes using S Adhesive

4.2.2.2 Hand-Sanded and Grinded and Sand-Blasted Specimens

Figure 4.21 and Table 4.11 provide the results of the adhesive M used for the hand-sanded steel-to-composite lap shear tests. The behavior was initially linear, with the shear modulus approximately 200 ksi. The behavior became non-linear before reaching the ultimate shear strength and continued with a descending stress-strain relationship after the ultimate until failure. This behavior is desirable because it provides sufficient warning before failure, and the failure is not sudden upon reaching the ultimate strength.

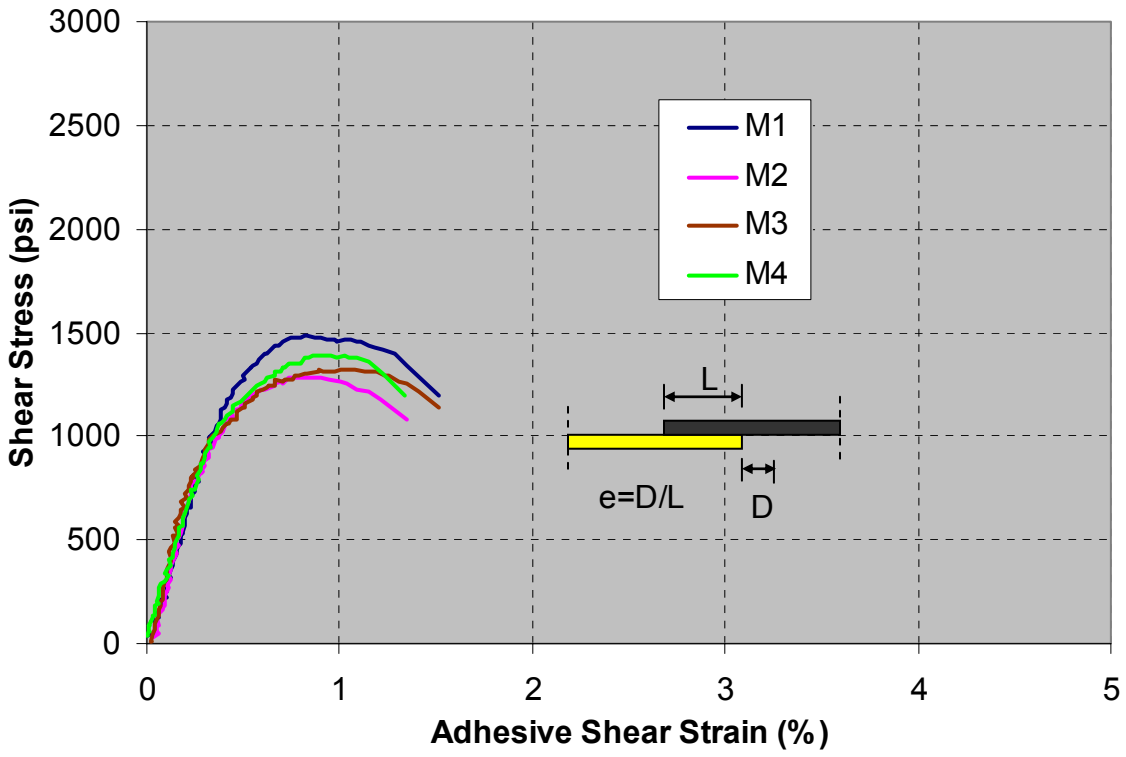

Figure 4.21 – Results of Hand-Sanded Steel-to-Composite Tests using M Adhesive

Specimen	Ultimate Shear Strength (psi)	Adhesive Shear Strain at Ultimate Strength (%)	Shear Stress at Failure (psi)	Strain at Failure (%)
M1	1490	0.818	1197	1.515
M2	1279	0.900	1079	1.343
M3	1320	1.075	1135	1.516
M4	1393	0.958	1200	1.333
Average	**1370**	**0.938**	**1153**	**1.427**
Std Deviation	93	0.108	57	0.103

Table 4.11 – Summary of Hand-Sanded Steel-to-Composite Tests using M Adhesive

Figure 4.22 shows the failure modes of the adhesive M used for the hand-sanded steel-to-composite lap shear specimens. The observed failure mode for all tested specimens was mostly cohesive, with small portions of adhesive failure at the steel substrate surface.

Figure 4.22 – Hand-Sanded Steel-to-Composite Failure Modes using M Adhesive

Figure 4.23 and Table 4.12 show the results of the adhesive S used for the hand-sanded steel-to-composite lap shear tests. The shape of the shear stress versus shear strain relationship of adhesive S is not as ductile as that observed for adhesive M. The shape is mostly linear and the failure occurred abruptly when the applied stress reached the

ultimate shear stress. The average ultimate shear strength of the adhesive S was 19.3 percent higher than that of adhesive M.

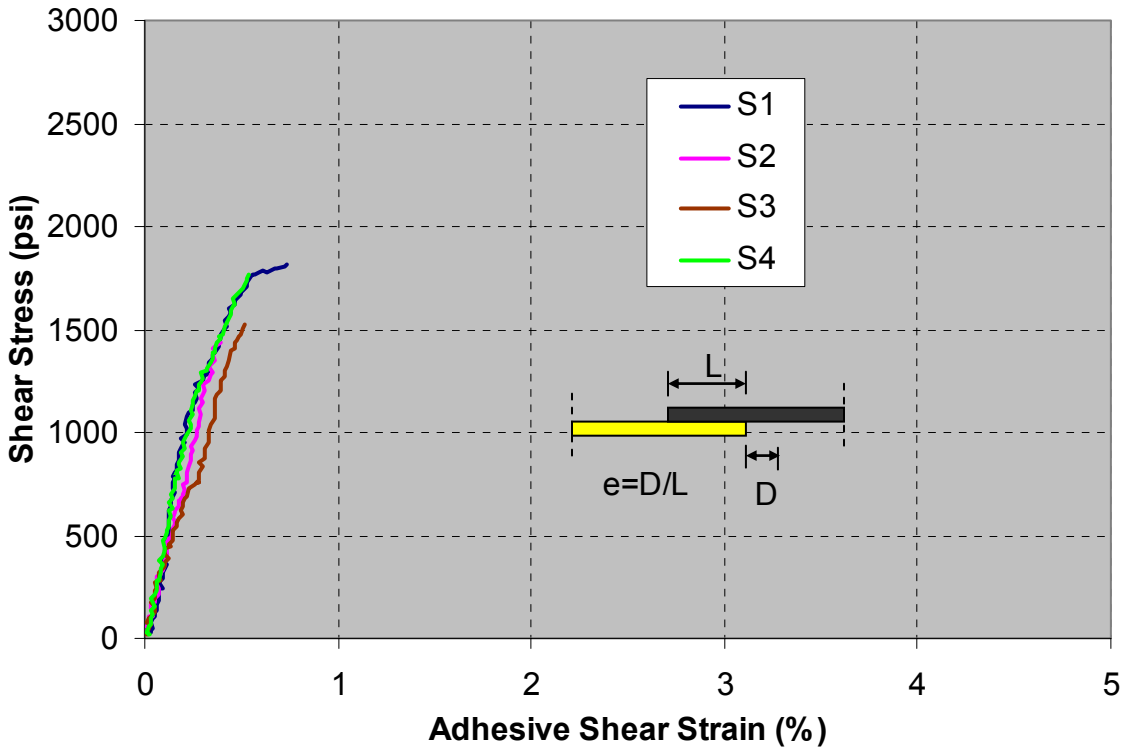

Figure 4.23 – Results of Hand-Sanded Steel-to-Composite Tests using S Adhesive

Specimen	Ultimate Shear Strength (psi)	Adhesive Shear Strain at Ultimate Strength (%)	Shear Stress at Failure (psi)	Strain at Failure (%)
S1	1811	0.737	1811	0.737
S2	1440	0.392	1440	0.392
S3	1525	0.517	1525	0.517
S4	1765	0.541	1765	0.541
Average	**1635**	**0.547**	**1635**	**0.547**
Std Deviation	181	0.143	181	0.143

Table 4.12 – Summary of Hand-Sanded Steel-to-Composite Tests using S Adhesive

Figure 4.24 shows observed failure modes of the adhesive S used for hand-sanded steel-to-composite lap shear specimens. Failure of all specimens was adhesive at the steel substrate surface. It was observed also that some mill scale of the steel peeled off from the substrate and stuck to the adhesive layer in many cases. Failure caused by mill scale peeling off of the steel substrate caused the type of abrupt failures as observed by the shape of the stress-strain relationship shown in figure 4.23.

Figure 4.24 – Hand-Sanded Steel-to-Composite Failure Modes using S Adhesive

Figure 4.25 and Table 4.13 show the results of the adhesive M used for the grinded and sandblasted steel-to-composite lap shear tests. The adhesive shows an acceptable shear stress-strain relationship with a shear modulus approximately 400 ksi. The behavior indicates that there is more variation in the measured data, and the strain at failure was less than with the hand-sanded specimens. However, there was a significant 62.0 percent increase in ultimate shear strength, which greatly compensates for the slightly less desirable curve shape.

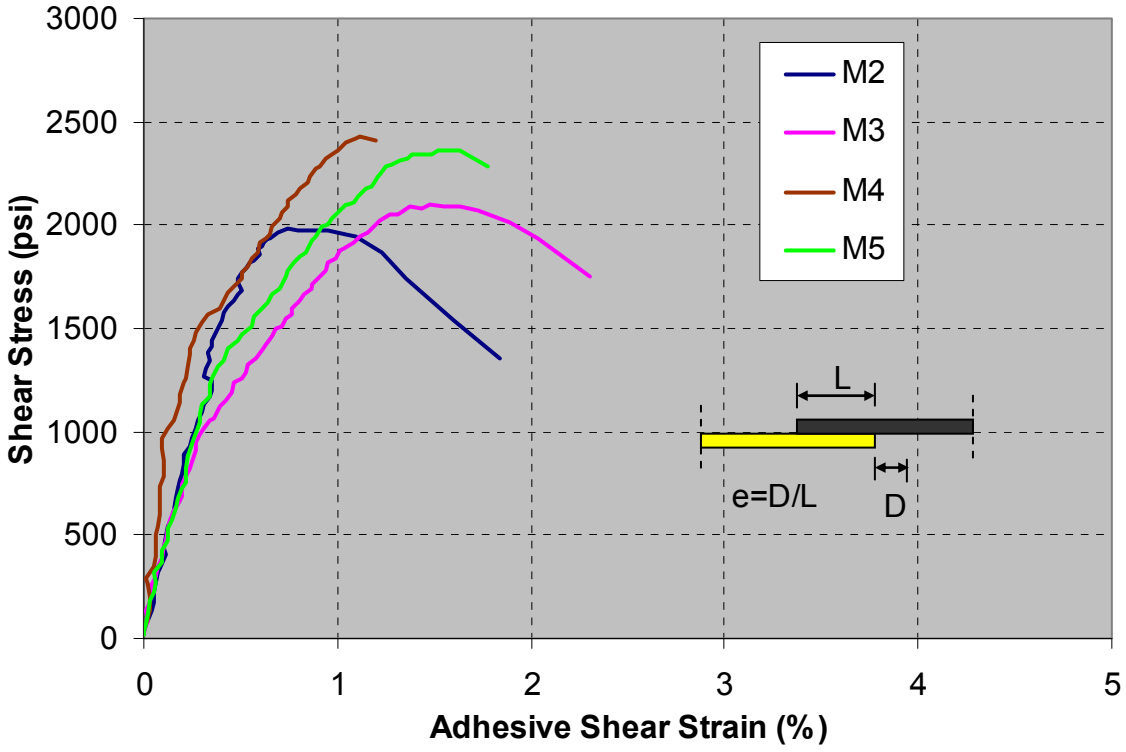

Figure 4.25 – Results of Grinded & Sandblasted Steel-to-Composite Tests using M Adhesive

Specimen	Ultimate Shear Strength (psi)	Adhesive Shear Strain at Ultimate Strength (%)	Shear Stress at Failure (psi)	Strain at Failure (%)
M2	1983	0.749	1353	1.840
M3	2099	1.478	1754	2.301
M4	2431	1.116	1754	2.301
M5	2365	1.518	2285	1.776
Average	**2219**	**1.215**	**1786**	**2.055**
Std Deviation	213	0.360	382	0.286

Table 4.13 – Summary of Grinded & Sandblasted

Steel-to-Composite Tests using M Adhesive

Figure 4.26 shows the observed failure modes of some of the adhesive M used for the grinded and sandblasted steel-to-composite lap shear specimens. Failure of the adhesive from the steel substrate is visible, but the majority of the failures were cohesive.

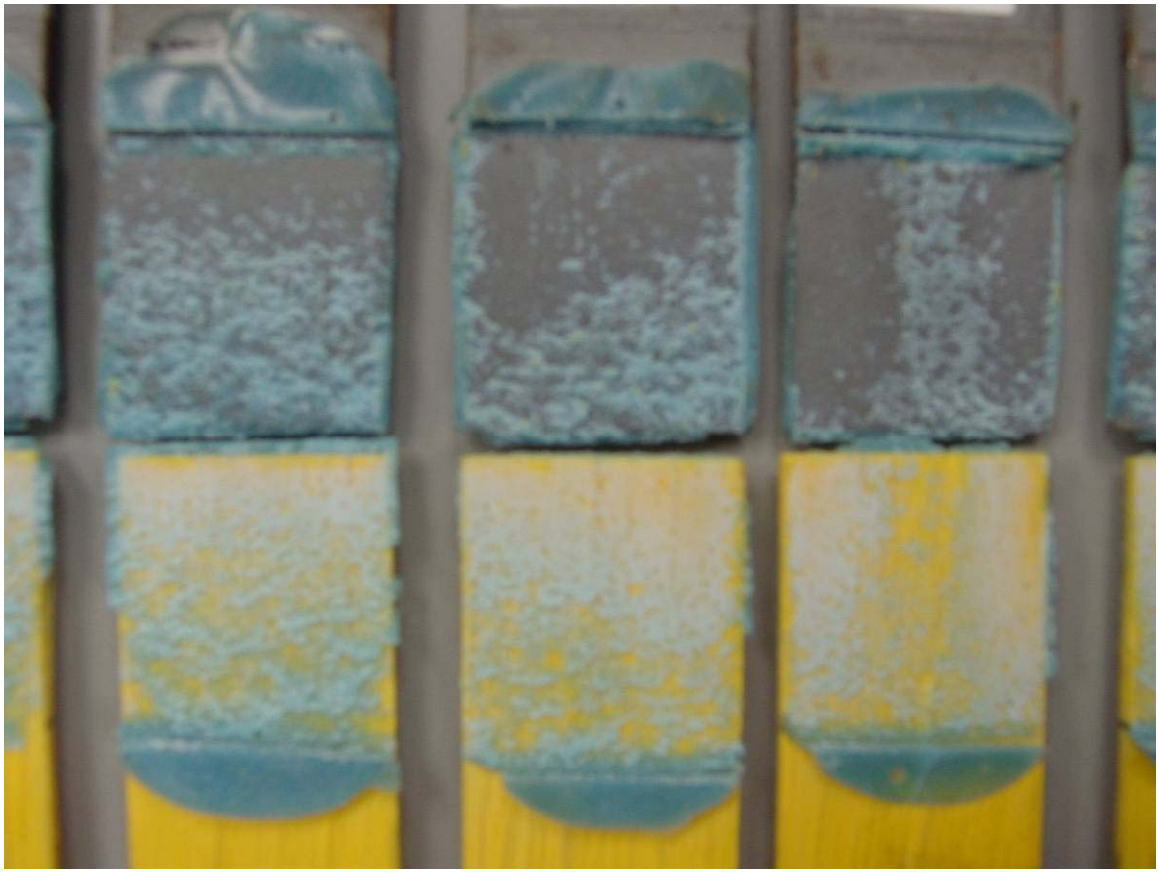

Figure 4.26 – Grinded & Sandblasted Steel-to-Composite Failure Modes using M Adhesive

Figure 4.27 and Table 4.14 show the results of the adhesive S used for grinded and sandblasted steel-to-composite lap shear tests. The shapes of these curves are very desirable because of the initial linear behavior with high shear modulus of 500 ksi, the significant strain before reaching the ultimate shear strength, and the continued deformation before failure. These shapes are very desirable and allow gradual failure. However, the large variation of the test results gave some concern on the consistency of the observed behavior. The standard deviation of the ultimate shear strength was 310 psi, which represent a deviation of 13 percent from the average. However, the average

ultimate shear strength was 44.0 percent higher than that of the hand-sanded steel-to-composite specimens. It should also be noted that the lowest strength of the grinded and sandblasted specimen is higher than the ultimate strength of the highest value measured for the hand-sanded specimen. It was also observed that the initial behavior of the hand-sanded and grinded and sandblasted specimens was linear and followed the same path until failure occurred abruptly for the hand-sanded specimens. This abrupt behavior could be contributed by the presence of mill scale. The behavior suggests that using the grinding and sandblasting method removes the mill scale prior to bonding, and therefore provides a failure mode that is quite ductile.

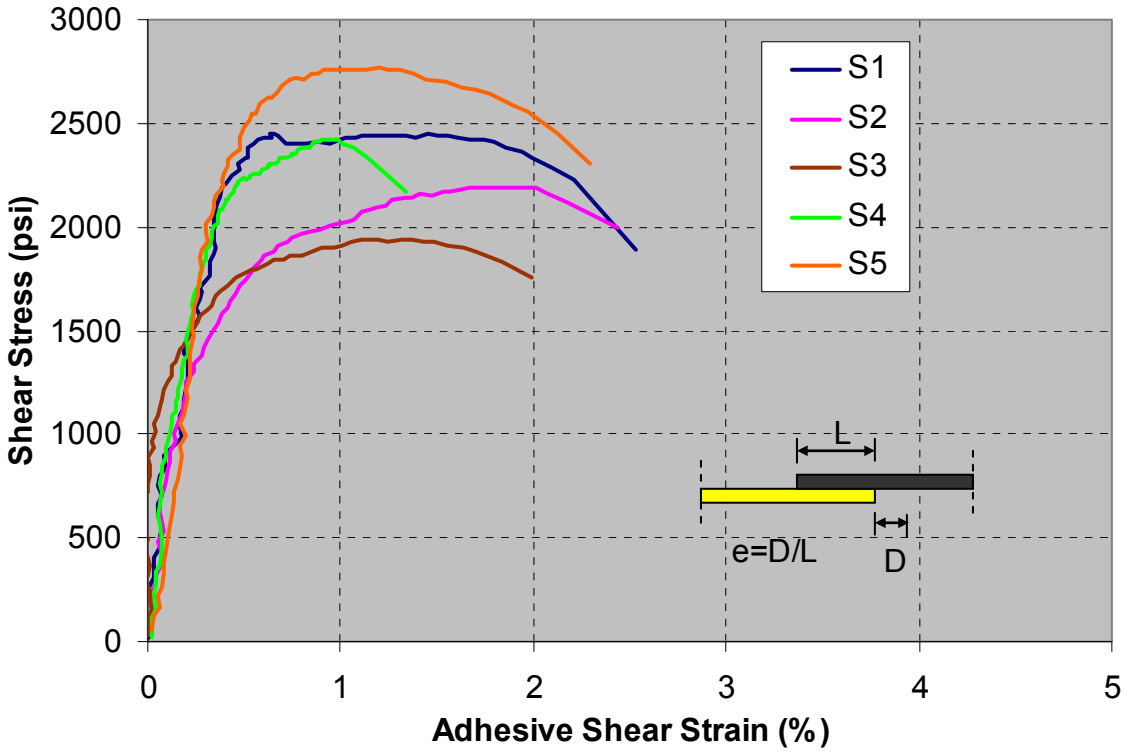

Figure 4.27 – Results of Grinded & Sandblasted Steel-to-Composite Tests using S Adhesive

Specimen	Ultimate Shear Strength (psi)	Adhesive Shear Strain at Ultimate Strength (%)	Shear Stress at Failure (psi)	Strain at Failure (%)
S1	2451	1.456	1894	2.528
S2	2194	1.769	1995	2.434
S3	1938	1.370	1756	1.989
S4	2421	0.983	2174	1.341
S5	2770	1.207	2310	2.292
Average	**2355**	**1.357**	**2026**	**2.117**
Std Deviation	310	0.292	220	0.479

Table 4.14 – Summary of Grinded & Sandblasted

Steel-to-Composite Tests using S Adhesive

Figure 4.28 shows the failure modes observed for the adhesive S used for the grinded and sandblasted steel-to-composite lap shear specimens. As was noted above, there is no mill scale on the failure surfaces. However, several large voids can be seen at the ends of the pictured specimens. These voids were most apparent on specimens S2 and S3, with smaller voids on S4 and S5. The photos of the three specimens from the left to right, S2, S3, and S4 were the specimens that produced the lowest results presented in figure 4.27. This finding explained the high variation of the measured failure strength. It is also important to note, however, that the shear strength of any adhesive bond is mostly related to the width of the bond, and not to the length. Therefore, the percentage of missing bond area is not directly proportional to the loss in shear strength, although it does have an effect. Of approximately 200 specimens tested in this project, these four were the only that displayed these large voids. The voids are likely caused by a combination of air bubbles forming in the adhesive and the high viscosity of adhesive S. The air bubbles

can be avoided with special attention when applying the adhesive and the exact viscosity of adhesive S is still being adjusted. However, it should be noted that variation of the test results obtained from these tests is very useful since it provides the range of shear strengths that may be present in field applications, considering the possibility of void formations. Apart from the voids, the failure mode was combined cohesive and adhesive.

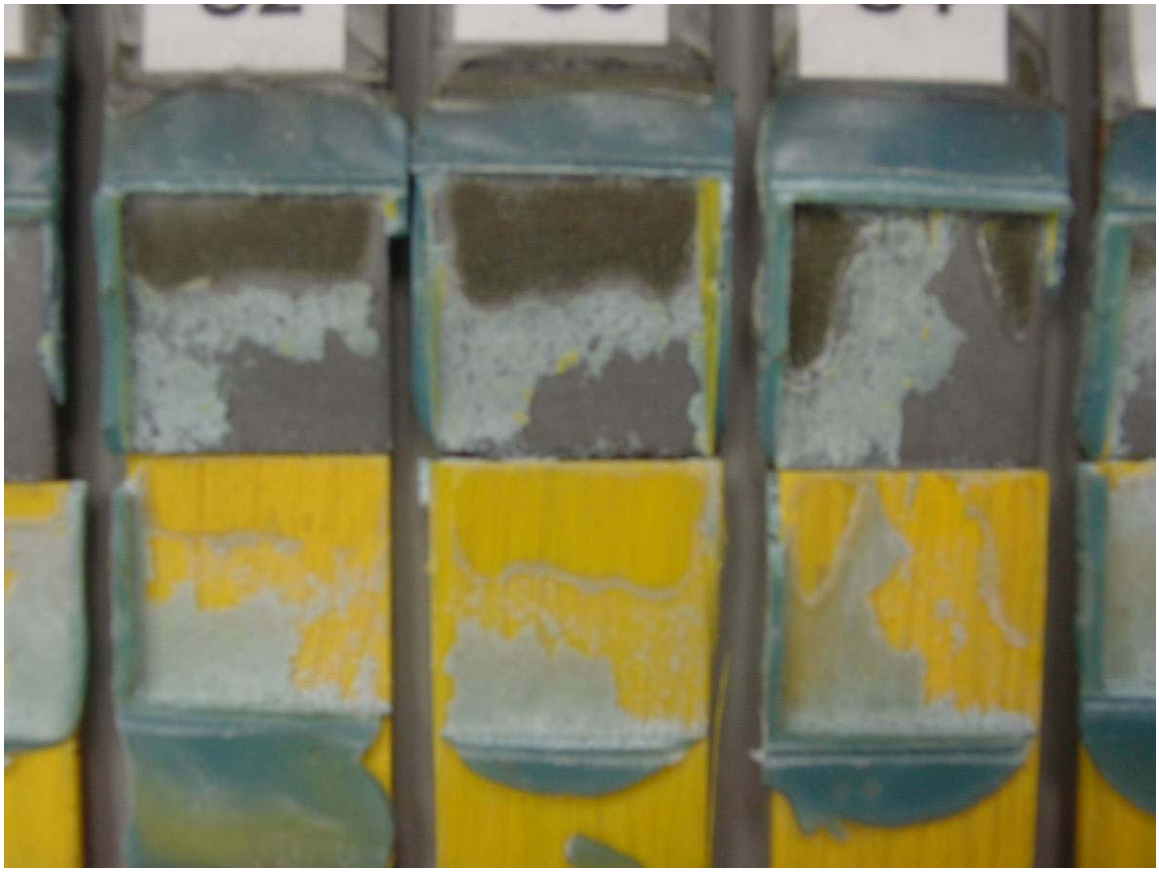

Figure 4.28 – Grinded & Sandblasted Steel-to-Composite Failure Modes using S Adhesive

Both the hand-sanded and grinded and sandblasted specimens were cured with weights to apply pressure to the bond area. The grinded and sandblasted preparation, along with the

presence of an appropriate amount of pressure during the bonding and curing process, has proven to be the most effective method for the steel-to-composite bond. To compare the behaviors of the two adhesives with steel-to-composite bonds, it is most appropriate to use the results obtained from this proven preparation method. The stress-strain relationship for adhesive S is much more desirable than that for adhesive M. Both adhesives were fairly inconsistent, with a standard deviation from the ultimate shear strength of 9.5 percent and 13.2 percent for adhesive M and S, respectively. The high deviation of adhesive S can be mostly explained by the formation of some voids. Additionally, the average ultimate shear strength of adhesive S is 6.1 percent higher than that of adhesive M.

4.3 Phase II: Environmental Exposure

Table 4.15 shows a summary of all of the environmental exposure tests performed and the conditions used in each case, as well as the number of specimens that were repeated for each test and the average time the load was sustained up-to-failure. Data for each individual specimen is located in Appendix B.

Adhesive	Material	Prep Conditions	Temp (F)	pH	Load (lb)	# Repeat	Avg Fail Time (hr)
S	Composite-to-Composite	Air Bonded & Cured	72	7	800	2	>1000
			120	7	200	3	>1000
					600	3	>1000
					800	3	92.97
			140	4	200	3	>1000
					600	3	8.27
				7	200	3	>1000
					600	3	78.15
					800	3	2.00
				9.5	200	3	>1000
					600	3	5.88
		Underwater Bonded & Cured	140	4	600	2	27.68
				7	600	2	74.93
				9.5	600	2	26.93
	Steel-to-Composite	Air Bonded & Cured	120	7	200	2	>1000
					600	2	16.54
			140	7	200	2	>1000
					800	2	0.52
M	Composite-to-Composite	Air Bonded & Cured	120	7	200	3	>1000
					600	3	2.64
					800	3	0.12
			140	4	200	3	>1000
					600	3	0.13
				7	200	3	>737.45
					600	3	0.15
					800	3	0.17
				9.5	200	3	>1000
					600	3	0.14
		Underwater Bonded & Cured	140	4	600	2	0.02
				7	600	2	0.01
				9.5	600	2	0.08
	Steel-to-Composite	Air Bonded & Cured	120	7	200	2	>1000
					600	2	3.84
			140	7	200	2	>1000
					800	2	0.03

Table 4.15 – Environmental Exposure Summary

Figure 4.29 is a graphical representation of the effect of the substrate on the time to failure. The label C following the type of adhesive, M or S, represents composite bonded to composite, while the label S represents composite bonded to steel. All specimens shown in Figure 4.29 were bonded and cured in air, and were tested in water with a pH value of 7. The specimens beginning with M represent specimens bonded with the M adhesive, and specimens beginning with S represent those bonded with the S adhesive. Figure 4.29 is split into 4 sections, each showing the behavior of the adhesive at different testing temperatures and loads, with different materials bonded. In the first section (A), in which the temperature is 120° Fahrenheit and the load is 200 pounds, none of the specimens failed, which is shown by the abbreviation NF (No Failure). Therefore, it is concluded that at such moderate environmental conditions and low load, no degradation in the bond characteristics for either adhesive is present with either substrate. In the second section (B), however, where the temperature is 120° Fahrenheit and the load is increased to 600 pounds, the effect of the load was significant enough to affect the bond of adhesive M for both the steel-to-composite and composite-to-composite specimens, as well as adhesive S for steel-to-composite specimens. The composite-to-composite specimens of adhesive S did not fail at temperature 120° Fahrenheit under loads of 600 pounds. The effect of the substrate is therefore seen clearly with the S adhesive, although the steel and composite substrates performed similarly with the M adhesive. It should be mentioned that both substrates performed significantly poorer than even the steel-to-composite specimen of S adhesive. The third section of the graph (C), with specimens at a temperature of 140° Fahrenheit and subjected to a load of 200 pounds, is similar to the

other section at 200 pounds, and shows little effect from the substrate at this low load level. It can be noted, however, that some, but not all, of the M adhesive specimens actually did fail with the composite-to-composite bond, but none failed with the steel-to-composite bond. The last section (D), at a temperature of 140° Fahrenheit and a load of 800 pounds, which was extremely high, all specimens performed poorly. However, it can still be observed that the composite-to-composite specimens using the S adhesive outperformed the steel-to-composite specimens using the S adhesive. Results indicate also that in general the adhesive S outperformed the adhesive M. Overall, this graph suggests that the S adhesive performs much better with composite-to-composite bonds than with steel-to-composite bonds when subjected to severe environmental conditions, but outperforms the M adhesive regardless of the substrate.

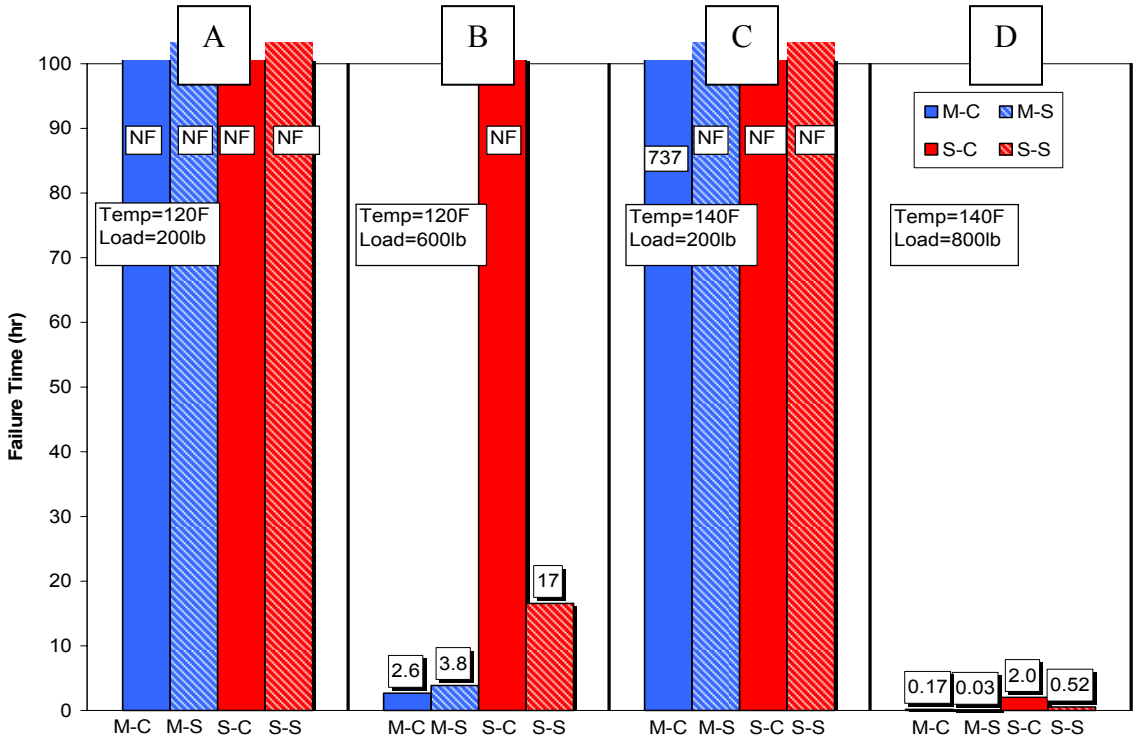

Figure 4.29 – Effect of Substrate on Adhesive Durability

Figure 4.30 shows the effect of the bonding and curing condition on the performance of the adhesive. Specimens marked "A" were bonded and cured in air, while specimens marked "UW" were bonded and cured under-water. All specimens in this graph are composite-to-composite, and were tested at a temperature of 140° Fahrenheit and loaded with 600 pounds. The three sections of the graph provide the results of three different pH values. Under these loading and environmental conditions, all of the specimens failed before reaching the 1000 hour limit that was set to mimic the environmental exposure tests for the original adhesive. However, there is little difference in the failure time between the specimens bonded and cured in air and those bonded and cured under-water with adhesive S. In fact, under non-neutral pH conditions, the specimens that were bonded and cured under-water actually performed somewhat better than those bonded and cured in air. This suggests that the bonding and curing conditions have little effect on the performance of adhesive S. Because of the short failure times of the adhesive M specimens, the results are inconclusive on whether the bonding and curing conditions affect the performance of adhesive M. It can also be noted that the S adhesive significantly outperformed the M adhesive in all cases.

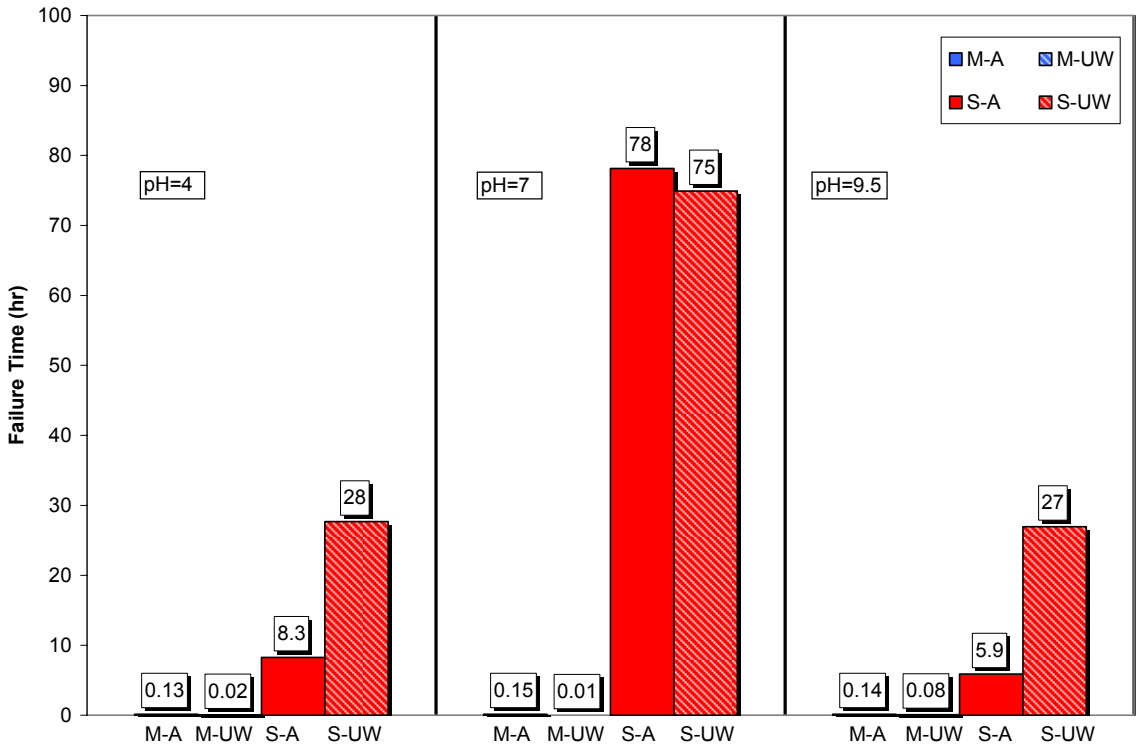

Figure 4.30 – Effect of Bonding and Curing Environment on Adhesive Durability

Figure 4.31 explores the effect of the temperature on the performance of the adhesives. The number denoted to the specimens tested at different temperatures reflects the degrees of temperature in Fahrenheit. All specimens on the graph are composite-to-composite, air cured and bonded, and tested in water with a pH of 7. The graph is split into three sections using three different load values. The effect of the temperature is most obvious at an applied load of 800 pounds to the S adhesive. The two raises in temperature greatly decrease the failure time of the specimen. At room temperature the specimen did not fail at all, while at 140° Fahrenheit, it failed after only 2 hours. The same pattern is seen with the S adhesive at a load of 600 pounds. The M adhesive performed poorly at these two loads, making the effect of temperature hard to conclude. At 200 pounds, however, it can

be seen that temperature also significantly affects the M adhesive, while it did not cause failure in the S adhesive.

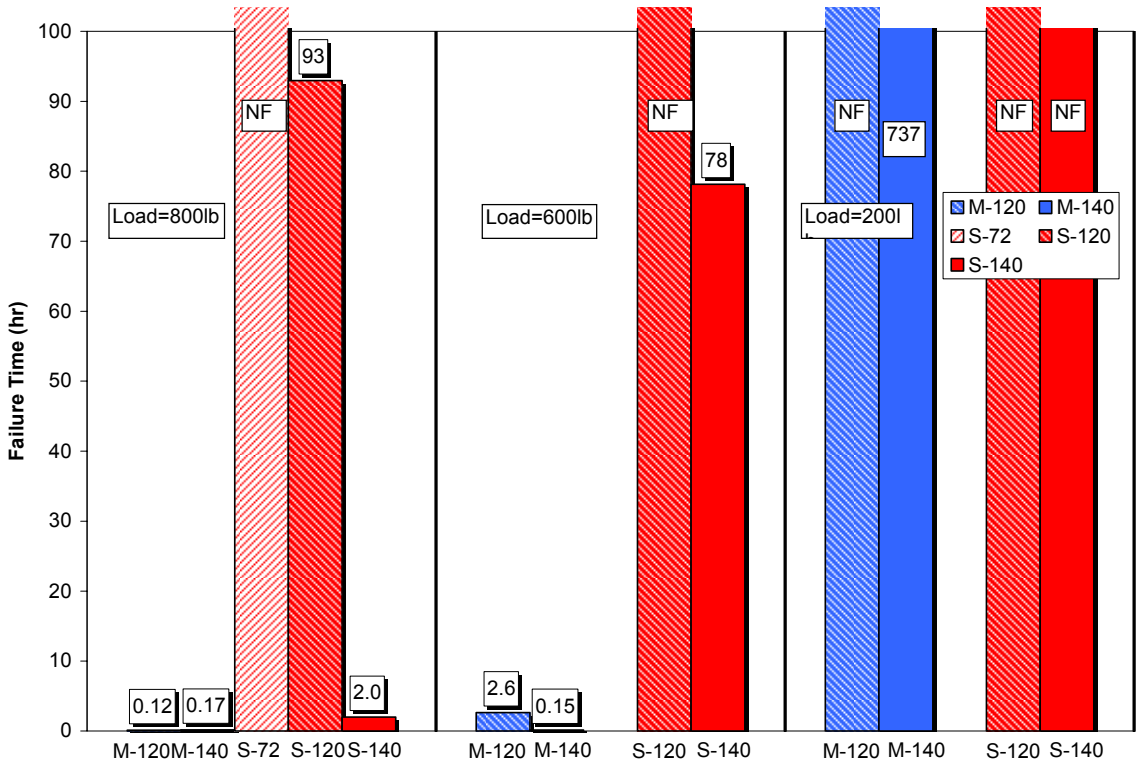

Figure 4.31 – Effect of Temperature on Adhesive Durability

Figure 4.32, shows the effect of the pH level on the bond behavior of the adhesives. The number denoted to the specimen indicates the pH level of its testing environment. All specimens tested were composite-to-composite and subjected to a temperature of 140° Fahrenheit. The graph is split into three sections of different load levels and bonding and curing conditions. The only air bonded and cured specimens that failed at 200 pounds were the adhesive M specimens at a pH of 7, suggesting that adhesive M performs slightly worse at a neutral pH. At 600 pounds, all of the specimens failed, and all of the

adhesive M specimens failed at such low values that the effect of pH cannot accurately be determined. However, it should be mentioned that the performance of the S adhesive at a pH level of 7 was better than at a pH of 4 or 9.5 at 600 pound loads. This concludes that extreme pH levels do have some effect on the performance of adhesive S.

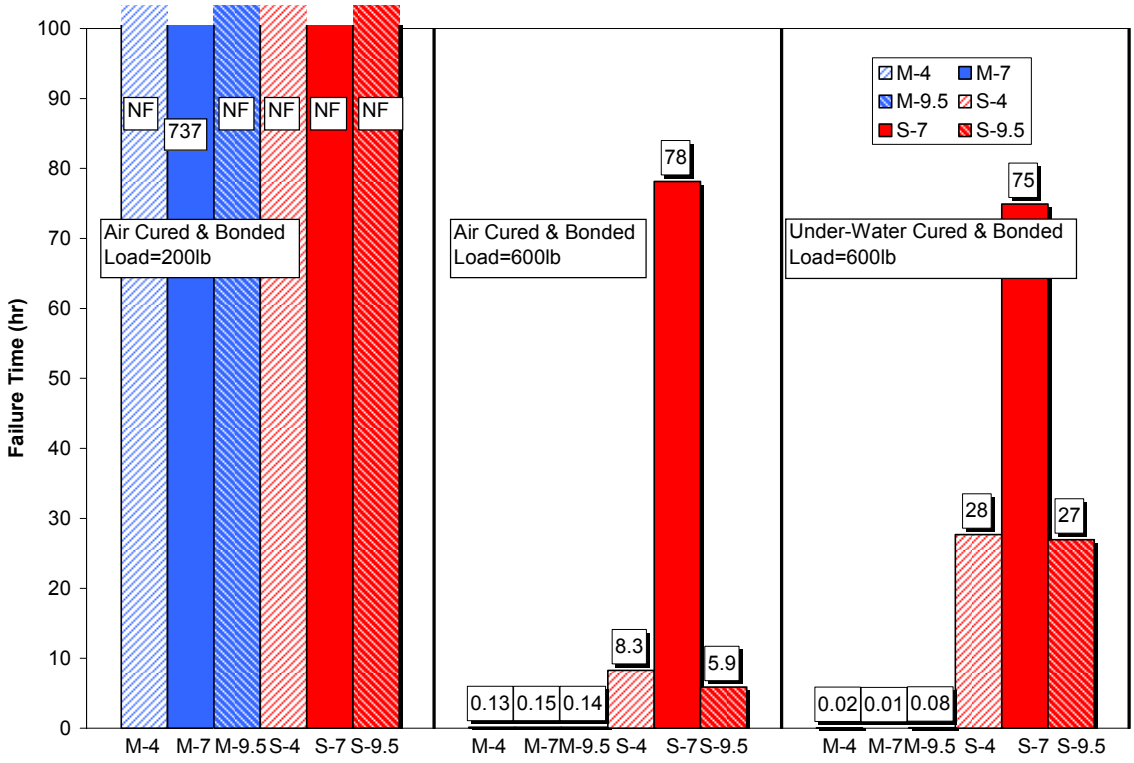

Figure 4.32 – Effect of pH Level on Adhesive Durability

Figures 4.33 and 4.34 show the failure modes of some of the adhesive M and adhesive S environmental exposure specimens, respectively. Both of the adhesives show failures that are mostly cohesive, with some significant adhesive failures at certain locations.

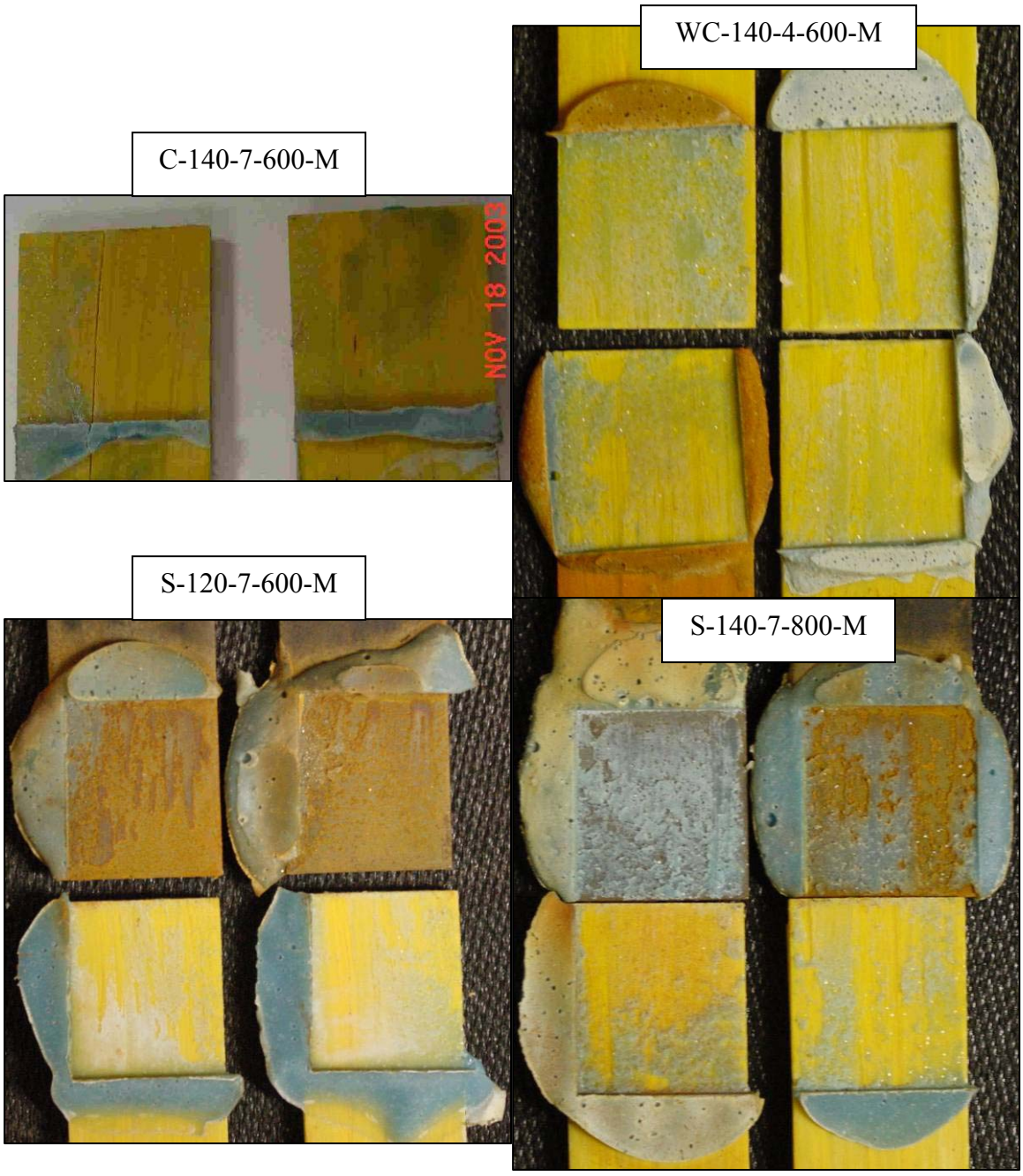

Figure 4.33 – Adhesive M Environmental Exposure Failure Modes

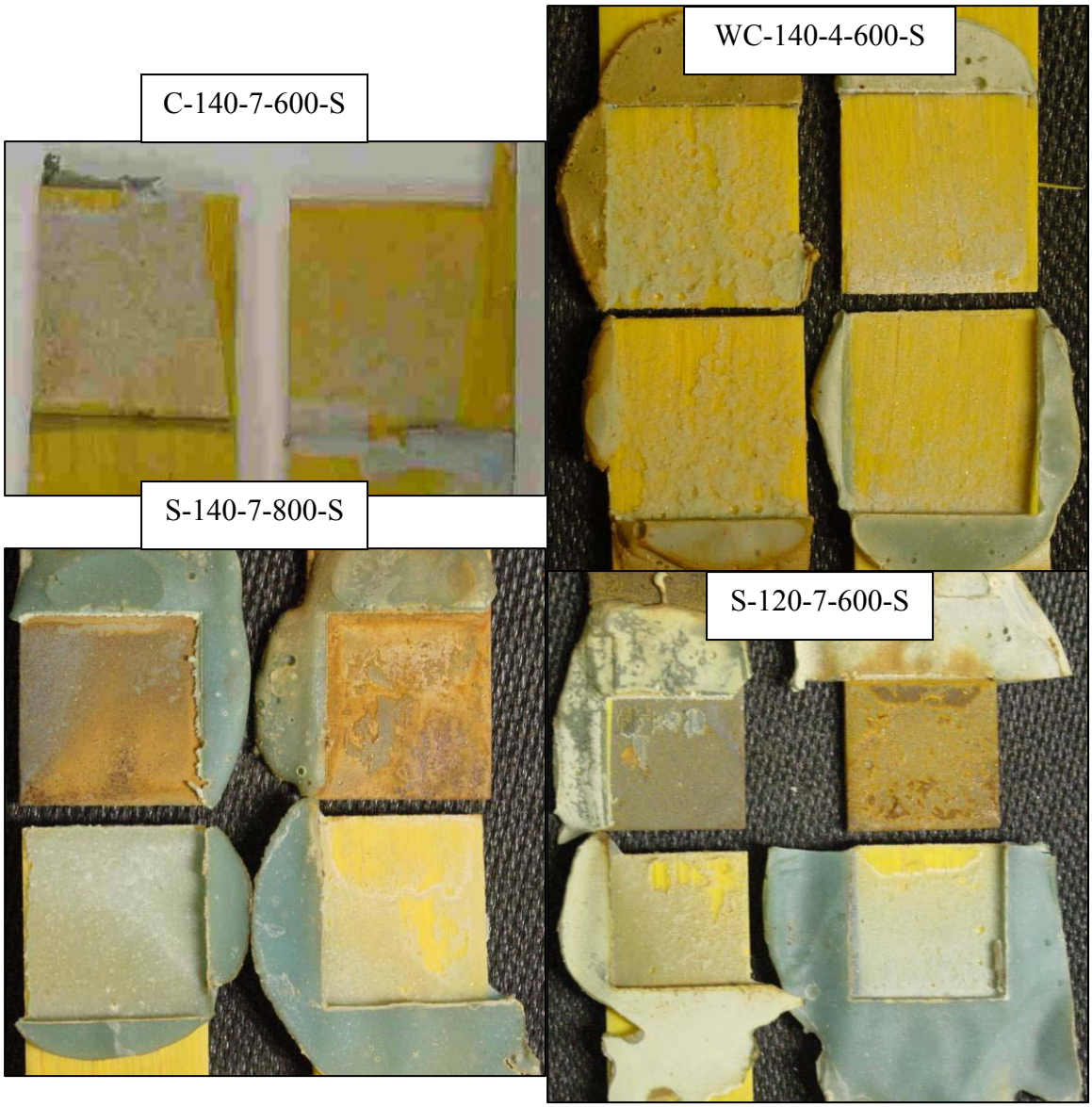

Figure 4.34 – Adhesive S Environmental Exposure Failure Modes

Figure 4.35 and Table 4.16 show the results of the lap shear tests that were performed on the adhesive M composite-to-composite specimens that did not fail after 1000 hours of environmental exposure testing. This graph shows the degradation that occurred within the bond due to the severe environmental conditions. All of the specimens maintained a modulus similar to the typical unconditioned specimen, but all failed fairly abruptly at a

low stress. One of the C-140-4-200 specimens experienced partial failure, then carried more load before reaching complete failure. The C-140-4-200 specimens were the most degraded specimens, showing a drop in average ultimate shear strength of 55.2 percent. The least degraded were the C-120-7-200 specimens, which showed only a 22.7 percent drop in average ultimate shear strength. These specimens also had the most desirable shaped stress versus strain curve. From these results, it seems that environmental temperature had the greatest effect on bond degradation, with non-neutral pH also contributing.

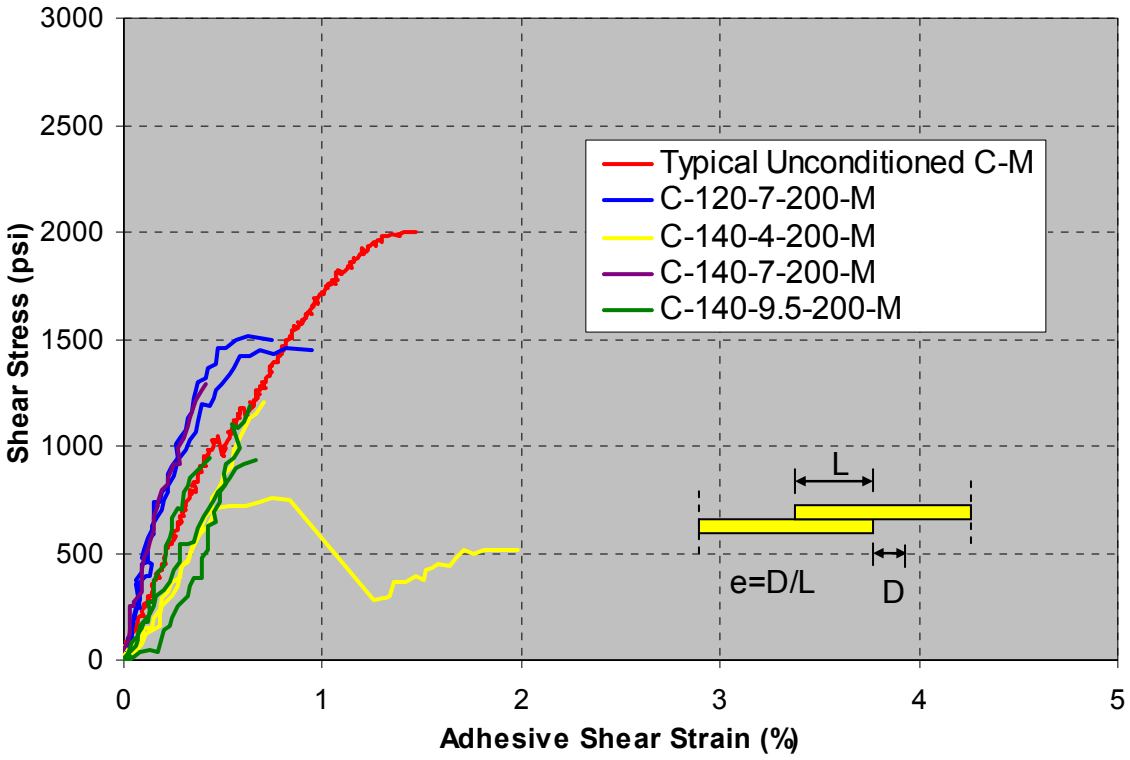

Figure 4.35 – Adhesive M Composite-to-Composite Lap-Shear Results After 1000 Hours of Environmental Testing

Specimen	Ultimate Shear Stress (psi)	Adhesive Shear Strain at Ultimate Stress (%)	Shear Stress at Failure (psi)	Strain at Failure (%)
C-M Average	**1924**	**1.285**	**1856**	**1.500**
Std Deviation	213	0.295	279	0.483
C-120-7-200-M1	1518	0.625	1494	0.744
C-120-7-200-M2	1456	0.818	1450	0.944
Average	**1487**	**0.721**	**1472**	**0.844**
Std Deviation	44	0.136	31	0.142
C-140-4-200-M1	517	1.812	510	1.985
C-140-4-200-M2	1207	0.707	1207	0.707
Average	**862**	**1.260**	**859**	**1.346**
Std Deviation	488	0.781	493	0.903
C-140-7-200-M4	**1288**	**0.408**	**1288**	**0.408**
C-140-9.5-200-M1	946	0.437	946	0.437
C-140-9.5-200-M2	1189	0.634	1189	0.634
C-140-9.5-200-M3	933	0.667	933	0.667
Average	**1023**	**0.579**	**1023**	**0.579**
Std Deviation	144	0.124	144	0.124

Table 4.16 – Adhesive M Composite-to-Composite Lap-Shear Summary After 1000 Hours of Environmental Testing

Figure 4.36 shows the failure modes of the adhesive M used for composite-to-composite environmental specimens tested to failure in lap shear. The failures are visually similar to those that failed during environmental testing and consist of mostly cohesive, but some adhesive, failure.

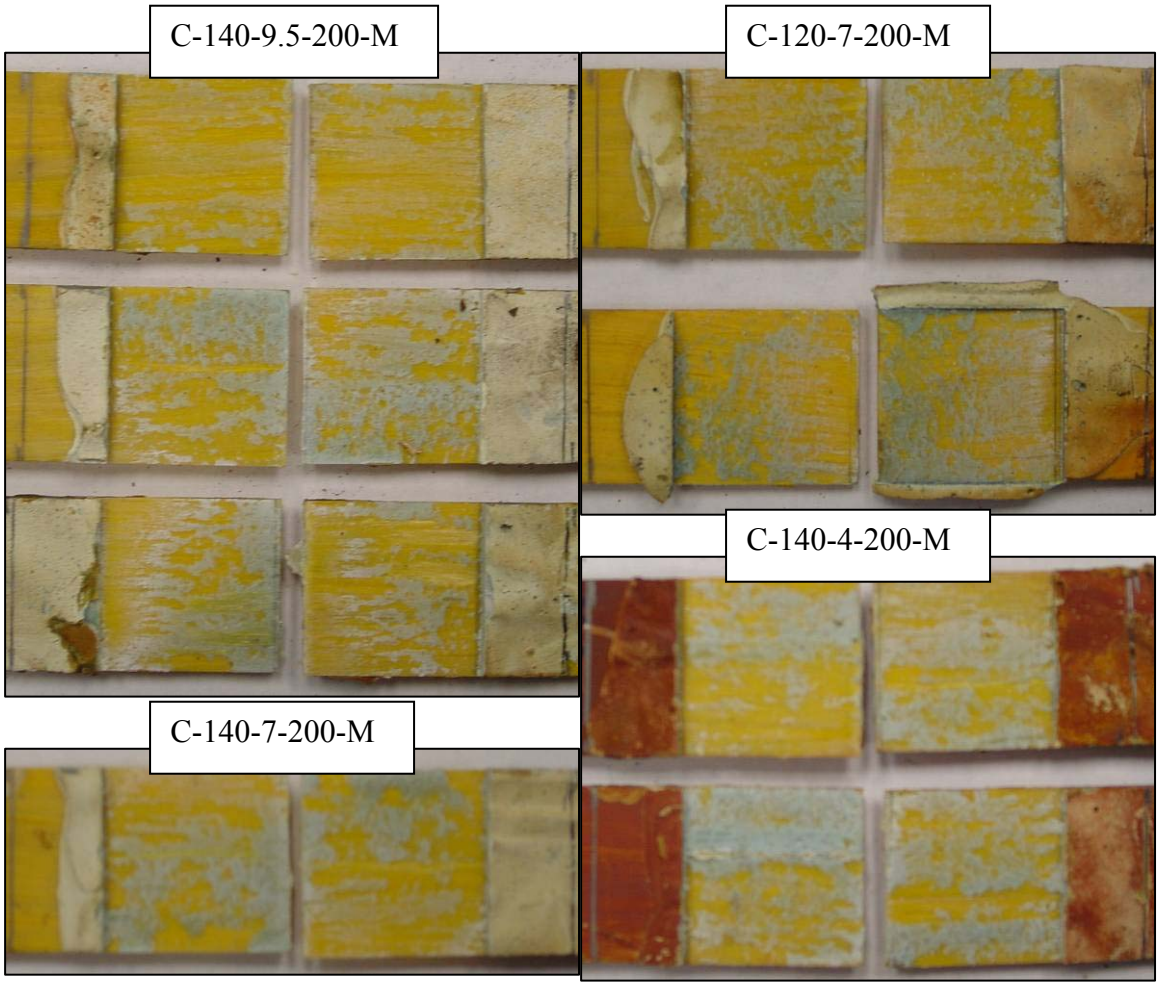

Figure 4.36 – Adhesive M Composite-to-Composite Failure Modes After 1000 Hours of Environmental Testing

Figure 4.37 and Table 4.17 show the results of the lap shear tests performed on adhesive S composite-to-composite specimens that did not fail after 1000 hours of environmental testing. All of the specimens retained a similar modulus to the typical unconditioned specimen in the linear region with the exception of the C-120-7-600 specimens. It seems that the stiffness of the adhesive was affected at this elevated temperature and load combination. The specimens with the most strength degradation were the C-140-4-200

specimens, with a loss in average ultimate shear strength of 33.0 percent. Similar to the adhesive M specimens, these specimens show a trend of degradation amount due to elevated temperature, but also affected by non-neutral pH levels. The specimens tested at room temperature in a neutral pH did not show any degradation, even with a sustained load of 800 pounds. It is also important to note that the C-140-4-200 specimens were the most degraded with both adhesives, but the average ultimate shear strength of the C-140-4-200 adhesive S specimens was 86.1 percent higher than that of the adhesive M specimens.

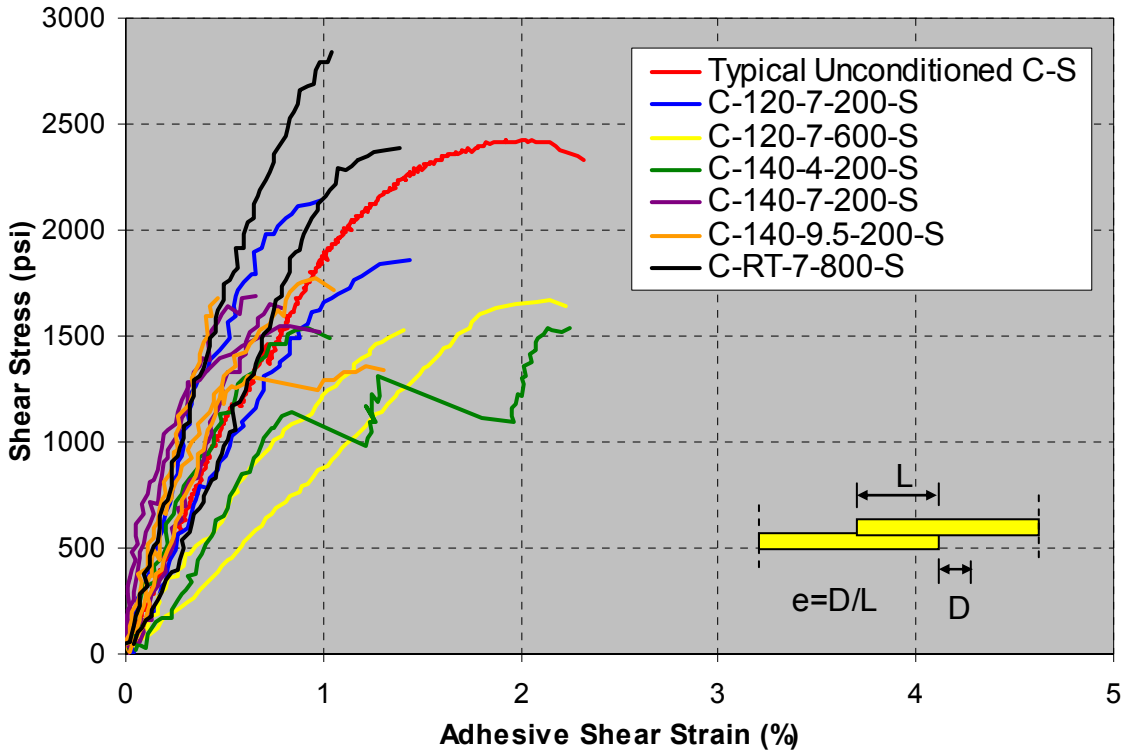

Figure 4.37 – Adhesive S Composite-to-Composite Lap-Shear Results After 1000 Hours of Environmental Testing

Specimen	Ultimate Shear Stress (psi)	Adhesive Shear Strain at Ultimate Stress (%)	Shear Stress at Failure (psi)	Strain at Failure (%)
C-S Average	**2259**	**1.835**	**2214**	**2.063**
Std Deviation	246	0.431	244	0.579
C-120-7-200-S1	2141	0.997	2141	0.997
C-120-7-200-S2	1855	1.436	1855	1.436
Average	**1998**	**1.217**	**1998**	**1.217**
Std Deviation	202	0.311	202	0.311
C-120-7-600-S2	1531	1.409	1531	1.409
C-120-7-600-S4	1669	2.146	1644	2.228
Average	**1600**	**1.777**	**1588**	**1.819**
Std Deviation	97	0.521	80	0.579
C-140-4-200-S1	1537	0.922	1487	1.035
C-140-4-200-S2	1537	2.244	1537	2.244
Average	**1537**	**1.583**	**1512**	**1.639**
Std Deviation	0	0.935	35	0.855
C-140-7-200-S1	1543	0.782	1518	0.986
C-140-7-200-S2	1687	0.662	1687	0.662
C-140-7-200-S3	1655	0.730	1637	0.788
Average	**1628**	**0.725**	**1614**	**0.812**
Std Deviation	75	0.060	86	0.163
C-140-9.5-200-S1	1680	0.467	1680	0.467
C-140-9.5-200-S2	1363	1.215	1344	1.306
C-140-9.5-200-S3	1774	0.960	1718	1.048
Average	**1606**	**0.880**	**1581**	**0.940**
Std Deviation	215	0.380	206	0.430
C-RT-7-800-S1	2844	1.042	2844	1.042
C-RT-7-800-S2	2384	1.390	2384	1.390
Average	**2614**	**1.216**	**2614**	**1.216**
Std Deviation	326	0.246	326	0.246

Table 4.17 – Adhesive S Composite-to-Composite Lap-Shear Summary After 1000 Hours of Environmental Testing

Figure 4.38 shows the failure modes of the adhesive S specimens tested to failure in lap shear after 1000 hours of environmental testing. The failure modes of these specimens are more like that of the unconditioned adhesive S lap shear specimens than that of the specimens that failed during environmental testing, in that they consist of cohesive, adhesive, and substrate failure modes. This suggests that when failure is not caused by

the environmental conditions, the degradation to the adhesive S bond is similar to the degradation of the composite substrate.

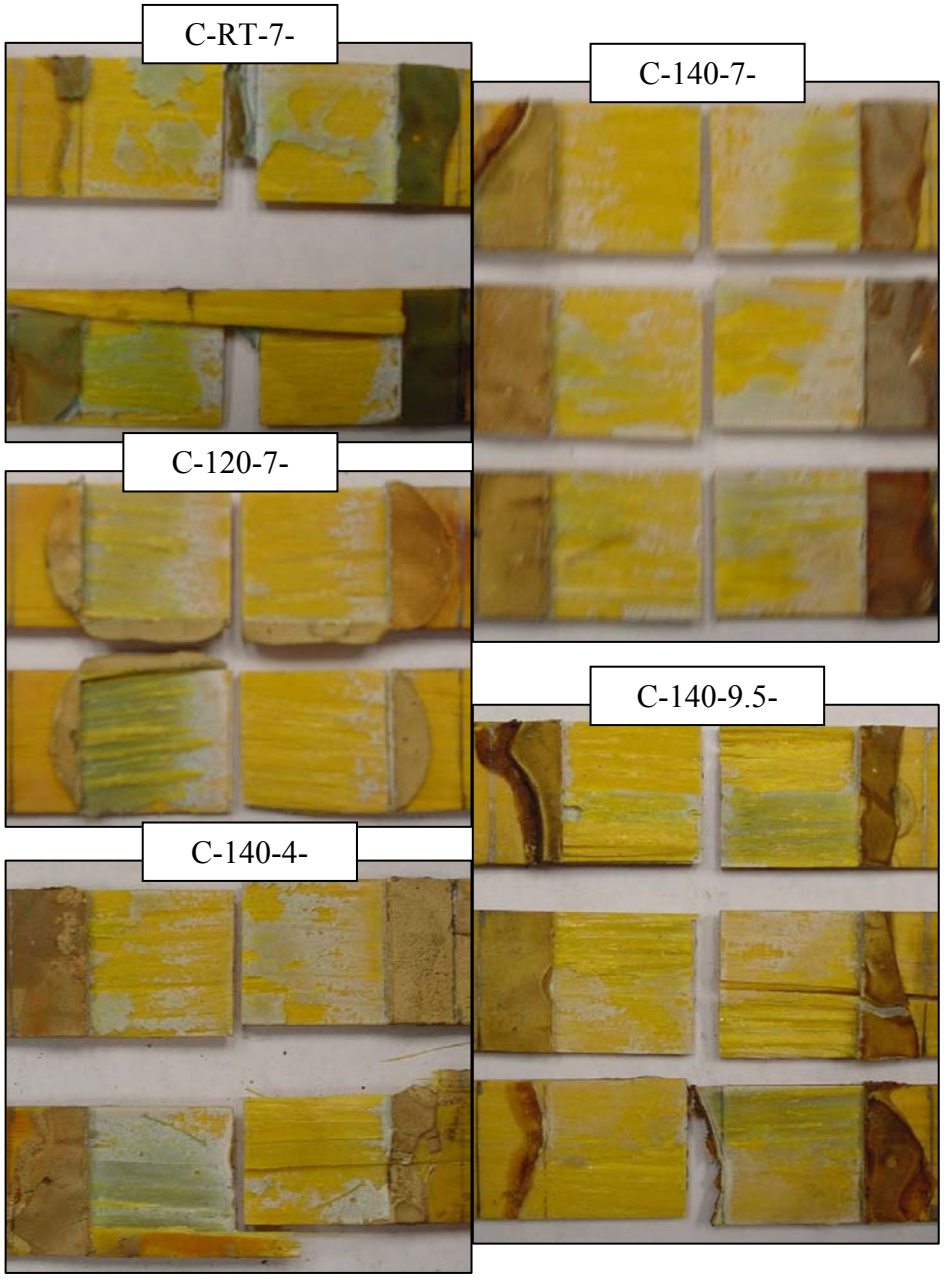

Figure 4.38 – Adhesive S Composite-to-Composite Failure Modes After 1000 Hours of Environmental Testing

Figure 4.39 and Table 4.18 show the results of adhesive M used for the steel-to-composite specimens tested to failure in lap shear after 1000 hours of environmental testing. As with the composite-to-composite specimens, the environmental exposure specimens followed a relationship similar to that of the unconditioned specimen, but failed at a much lower load. Also, the specimens that were subjected to a higher temperature environment showed a higher degradation than those subjected to the lower temperature environment, as can be seen by their decreases in average ultimate shear strength of 36.9 percent and 22.9 percent, respectively.

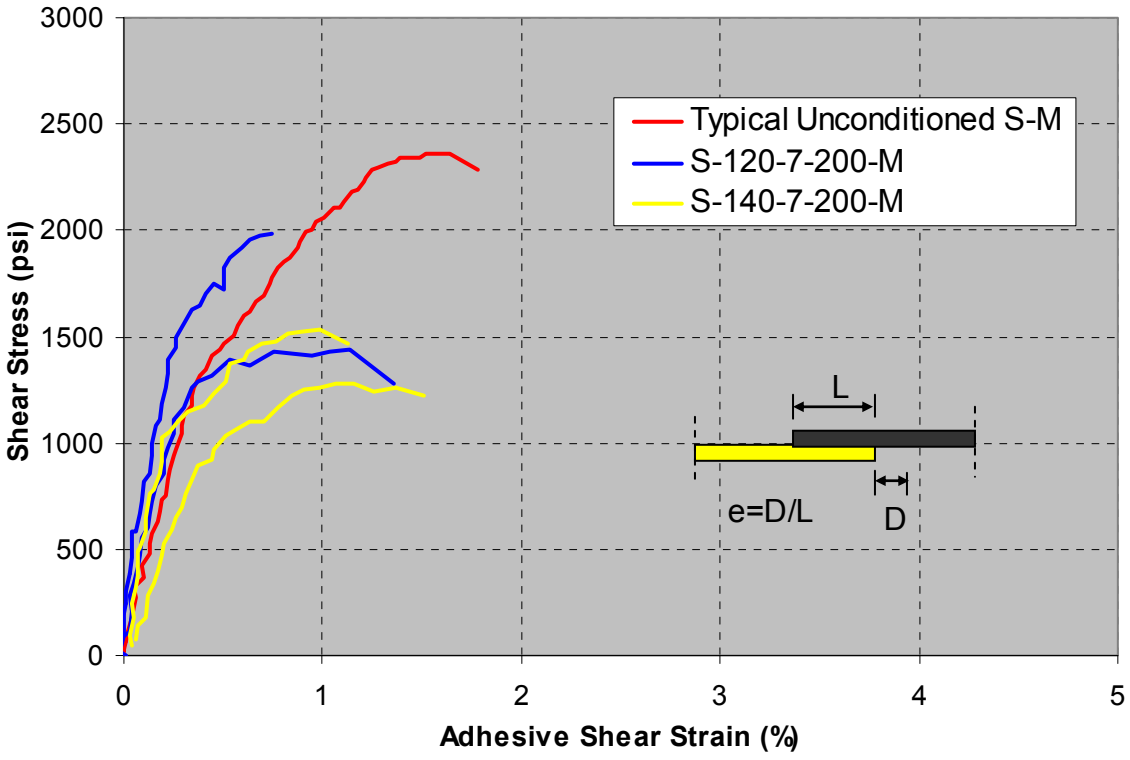

Figure 4.39 – Adhesive M Steel-to-Composite Lap-Shear Results After 1000 Hours of Environmental Testing

Specimen	Ultimate Shear Stress (psi)	Adhesive Shear Strain at Ultimate Stress (%)	Shear Stress at Failure (psi)	Strain at Failure (%)
S-M Average	**2219**	**1.215**	**1786**	**2.055**
Std Deviation	213	0.360	382	0.286
S-120-7-200-M1	1438	1.133	1282	1.359
S-120-7-200-M2	1985	0.744	1985	0.744
Average	**1711**	**0.939**	**1634**	**1.052**
Std Deviation	387	0.275	497	0.435
S-140-7-200-M1	1537	0.987	1469	1.122
S-140-7-200-M2	1263	1.369	1226	1.512
Average	**1400**	**1.178**	**1347**	**1.317**
Std Deviation	194	0.270	172	0.276

Table 4.18 – Adhesive M Steel-to-Composite Lap-Shear Summary

After 1000 Hours of Environmental Testing

Figure 4.40 shows the failure modes of the adhesive M used for the specimens tested to failure by lap shear after 1000 hours of environmental exposure testing. Again, the failure modes are similar to those seen from the environmental exposure tests, with cohesive failure most prevalent, but also some adhesive failure from the composite substrate present.

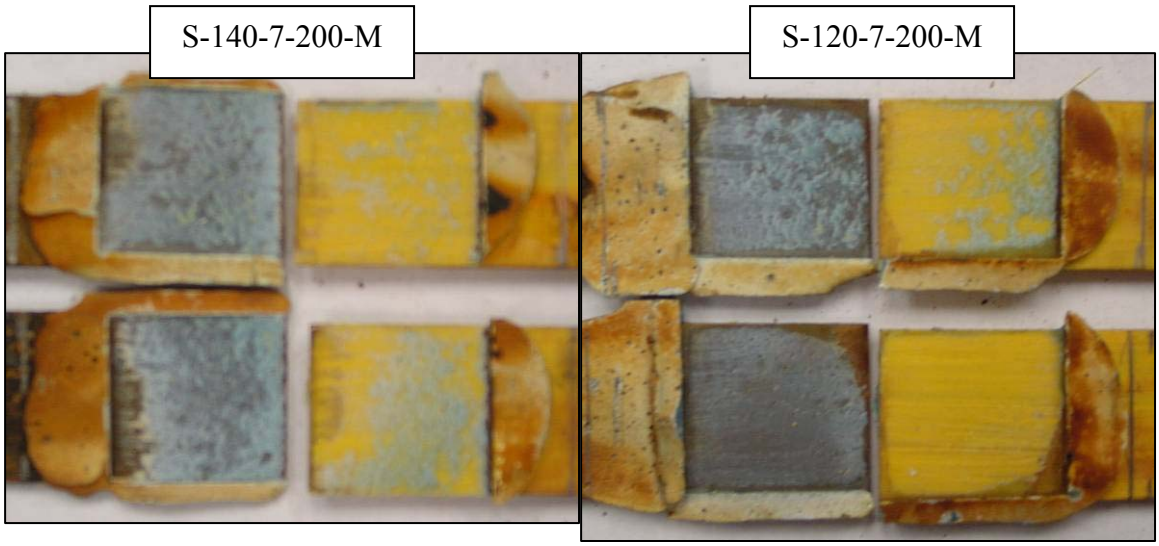

Figure 4.40 – Adhesive M Steel-to-Composite Failure Modes

After 1000 Hours of Environmental Testing

Figure 4.41 and Table 4.19 show the results of the adhesive S specimens tested to failure in lap shear after 1000 hours of environmental testing. These specimens follow the same trend as the environmentally tested composite-to-composite adhesive S specimens. The shape of the curve is similar to the typical unconditioned specimen, and the specimen subjected to the higher temperature environment showed the most degradation, with a loss of ultimate shear strength of 11.0 percent. The adhesive S steel-to-composite specimens, however, showed much less bond degradation than the adhesive S composite-to-composite specimens. Also, the most degraded S-140-7-200 adhesive S specimen had an ultimate shear strength 50 percent higher than that of the S-140-7-200 adhesive M specimens.

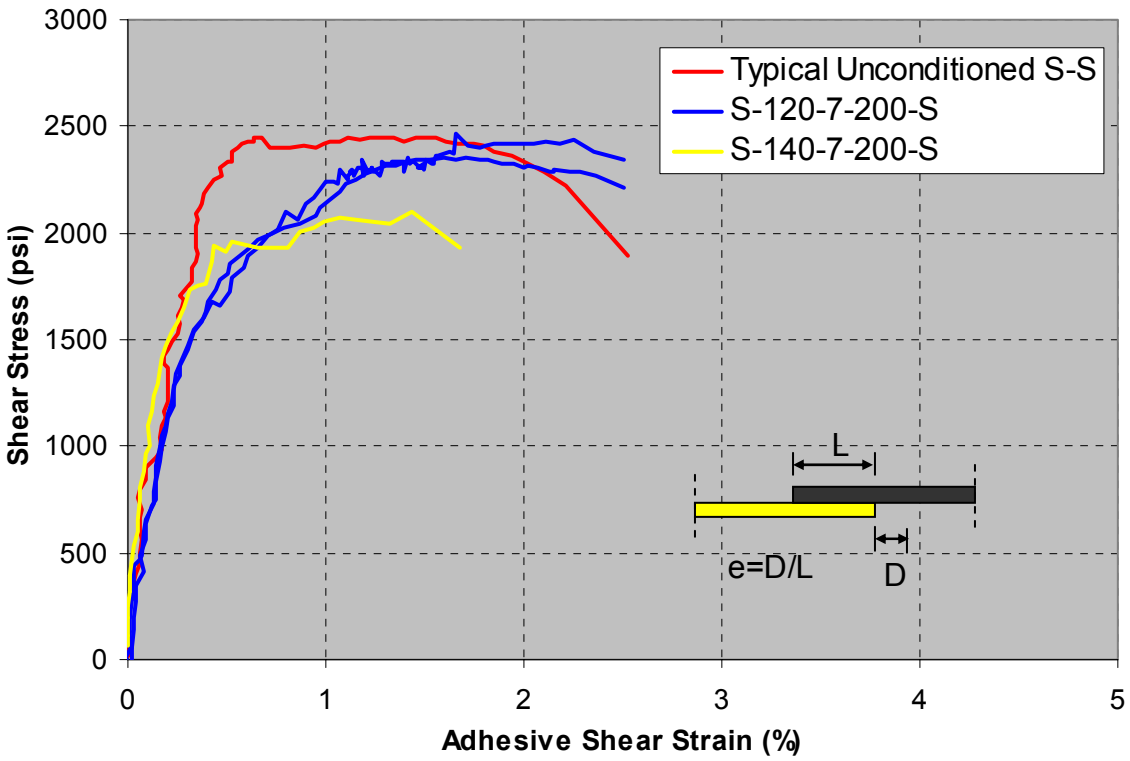

Figure 4.41 – Adhesive S Steel-to-Composite Lap-Shear Results

After 1000 Hours of Environmental Testing

Specimen	Ultimate Shear Stress (psi)	Adhesive Shear Strain at Ultimate Stress (%)	Shear Stress at Failure (psi)	Strain at Failure (%)
S-S Average	**2355**	**1.357**	**2026**	**2.117**
Std Deviation	310	0.292	220	0.479
S-120-7-200-S1	2352	1.592	2215	2.506
S-120-7-200-S2	2433	2.258	2346	2.500
Average	**2393**	**1.925**	**2281**	**2.503**
Std Deviation	57	0.471	92	0.004
S-140-7-200-S2	**2097**	**1.438**	**1935**	**1.672**

Table 4.19 – Adhesive S Steel-to-Composite Lap-Shear Summary

After 1000 Hours of Environmental Testing

Figure 4.42 shows the failure modes of the adhesive S steel-to-composite specimens tested to failure in lap shear after 1000 hours of environmental testing. The majority of the failure is adhesive at the steel surface, although two areas are adhesive at the composite surface. One of the most interesting observations is the condition of the steel surface, which appears to have experienced no corrosion or any degradation while adhered to adhesive S.

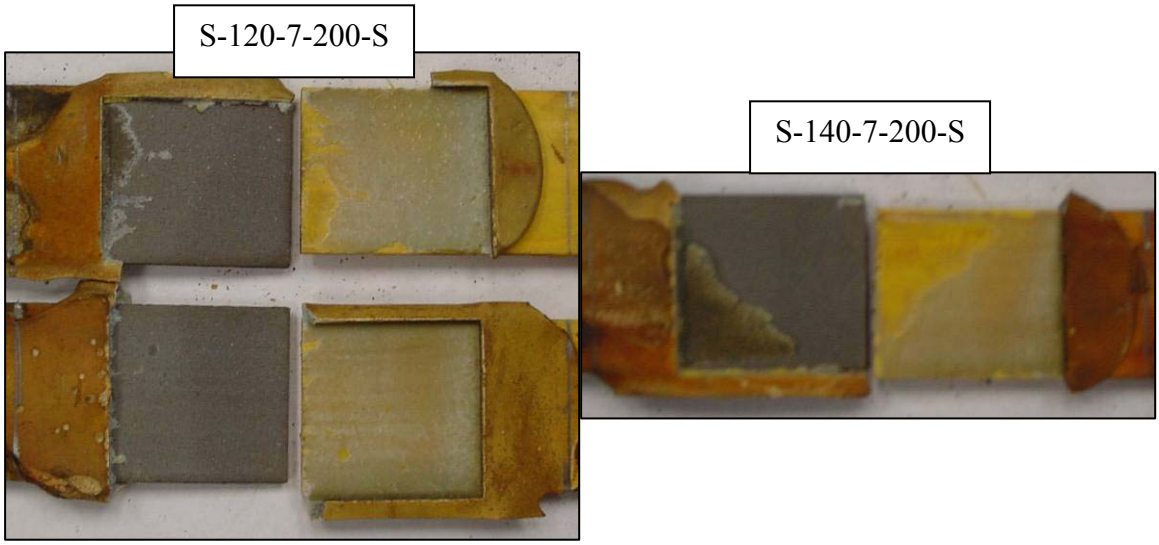

Figure 4.42 – Adhesive S Steel-to-Composite Failure Modes After 1000 Hours of Environmental Testing

4.4 Phase III: Cleavage Peel

The results of the cleavage peel tests are presented in terms of load versus displacement that occurred at the point of the applied load, as is designated by the ASTM D 380 – 98 specification. The ultimate load and distance peeled at that load are also tabulated, as well as the load and distance peeled just before failure. Since the bond width of all specimens was one inch, the cleavage peel strength of each adhesive is equal to the ultimate load. These values can be used only for comparison for specimens bonded and tested in identical manners. The load and distance peeled just before failure is useful in understanding the behavior of the bond after initial cracking.

Figure 4.43 shows the results of the adhesive M cleavage peel tests. The specimens all follow a similar linear path at a rate of approximately 5 pounds per inch until the initial crack forms. After the initial crack, the load decreases as the crack propagates, causing increase of the distance peeled until failure is reached.

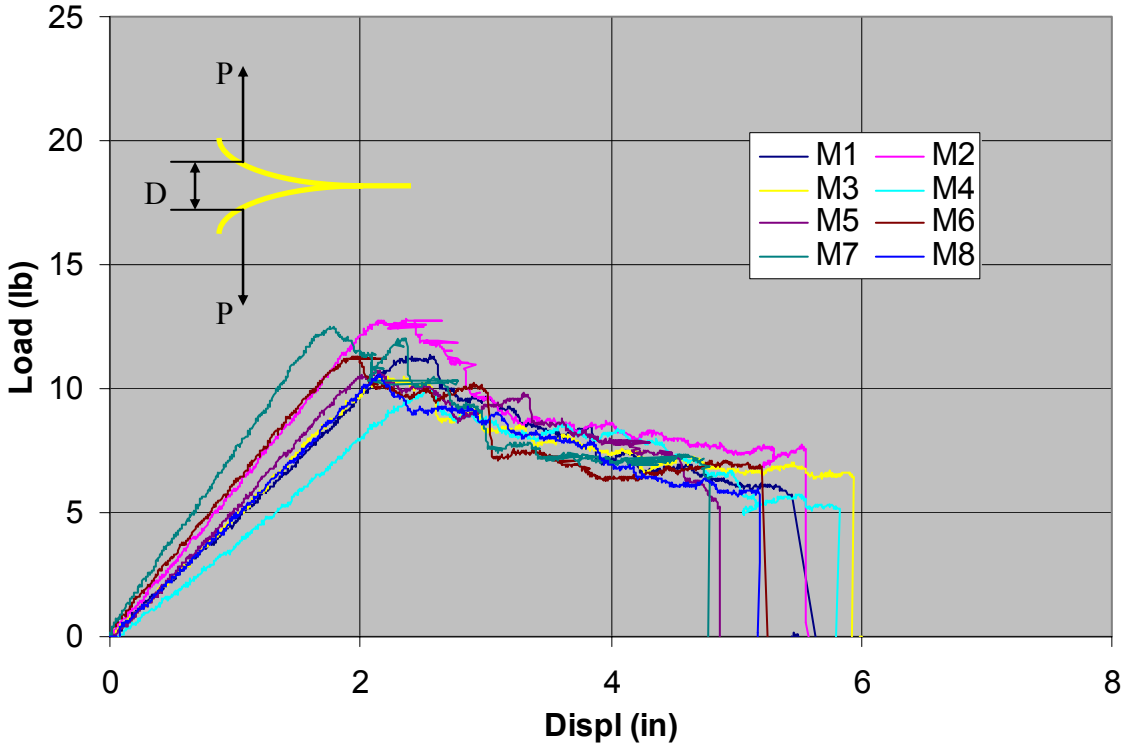

Figure 4.43 – Adhesive M Cleavage Peel Results

Figure 4.44 shows the results of the adhesive S cleavage peel tests. All of the load versus displacement relationships begin on a linear path at a rate of approximately 7 pounds per inch. After initial cracking is achieved the specimens behave in two distinctive ways. Four of the specimens behaved similar to adhesive M, while three specimens failed immediately. One specimen displays a combination of the two behaviors. These differences in behavior become clear after inspecting the failure modes.

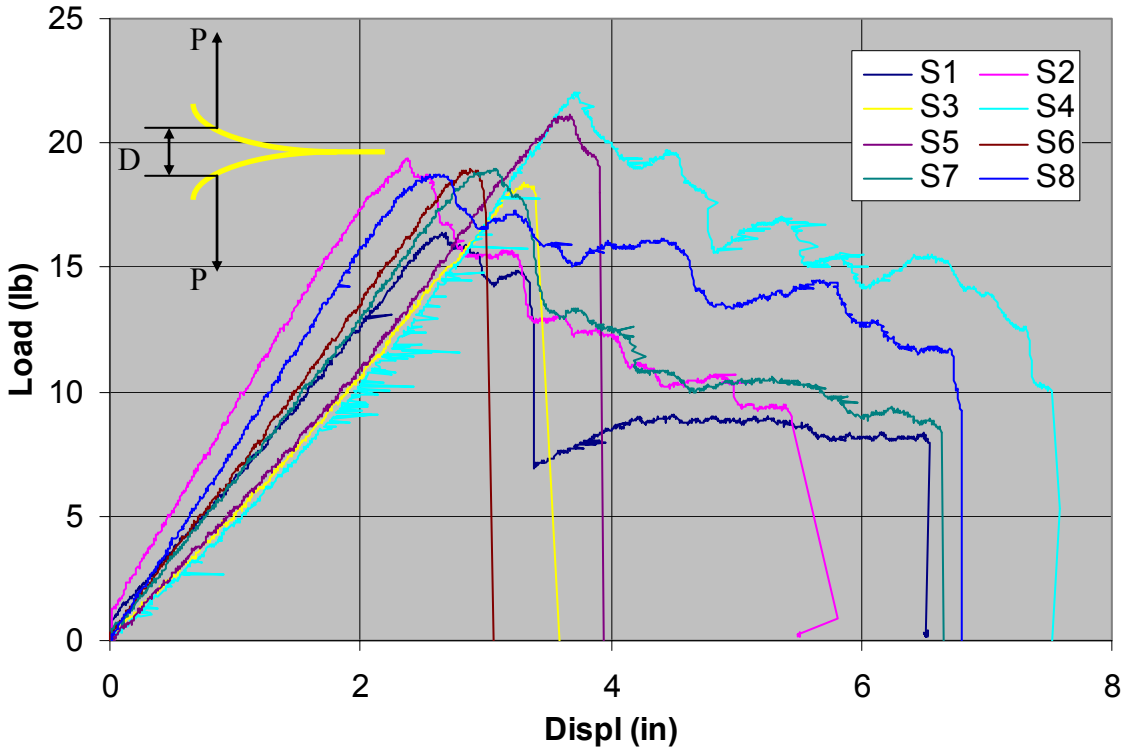

Figure 4.44 – Adhesive S Cleavage Peel Results

Table 4.20 summarizes the results of all of the cleavage peel tests. The two failure modes of the adhesive S specimens are averaged both as a whole and separately because of the dramatic differences in their behavior. The most important observation from the summary chart is that the average cleavage peel strength of adhesive S was 72 percent higher than that of adhesive M.

Cleavage Peel Summary Table				
	Initial Crack (max load)		Failure	
Specimen	Load (lb)	Displacement (in)	Load (lb)	Displacement(in)
M1	11.4	2.6	5.7	5.4
M2	12.8	2.4	7.5	5.6
M3	10.5	2.2	6.4	5.9
M4	10.0	2.5	5.0	5.8
M5	10.7	2.2	5.2	4.9
M6	11.3	1.9	6.9	5.2
M7	12.5	1.8	6.3	4.8
M8	10.6	2.1	5.7	5.2
Average	**11.2**	**2.2**	**6.1**	**5.4**
Std Dev	1.00	0.28	0.84	0.42
S1**	16.4	2.6	7.8	6.5
S2	19.4	2.4	8.7	5.5
S3*	18.4	3.3	17.5	3.4
S4	22.0	3.7	10.0	7.5
S5*	21.1	3.7	18.0	3.9
S6*	19.0	2.9	17.2	3.0
S7	19.0	3.1	8.4	6.6
S8	18.8	2.6	9.2	6.8
Total Avg	**19.3**	**3.0**	**12.1**	**5.4**
Total SD	1.71	0.50	4.57	1.74
Adh Fail Avg	19.8	2.9	9.1	6.6
Adh Fail SD	1.51	0.59	0.71	0.86
Mat Fail Avg	19.5	3.3	17.6	3.4
Mat Fail SD	1.42	0.40	0.43	0.46
% Difference of S Avg from M Avg	**71.7%**	**37.5%**	**99.0%**	**1.0%**
*Material Failure, **Combination Failure				

Table 4.20 – Cleavage Peel Summary

Figure 4.45 shows the failure modes of the adhesive M cleavage peel specimens. The failure mode is mainly cohesive, which is the desired failure mode in cleavage peel testing.

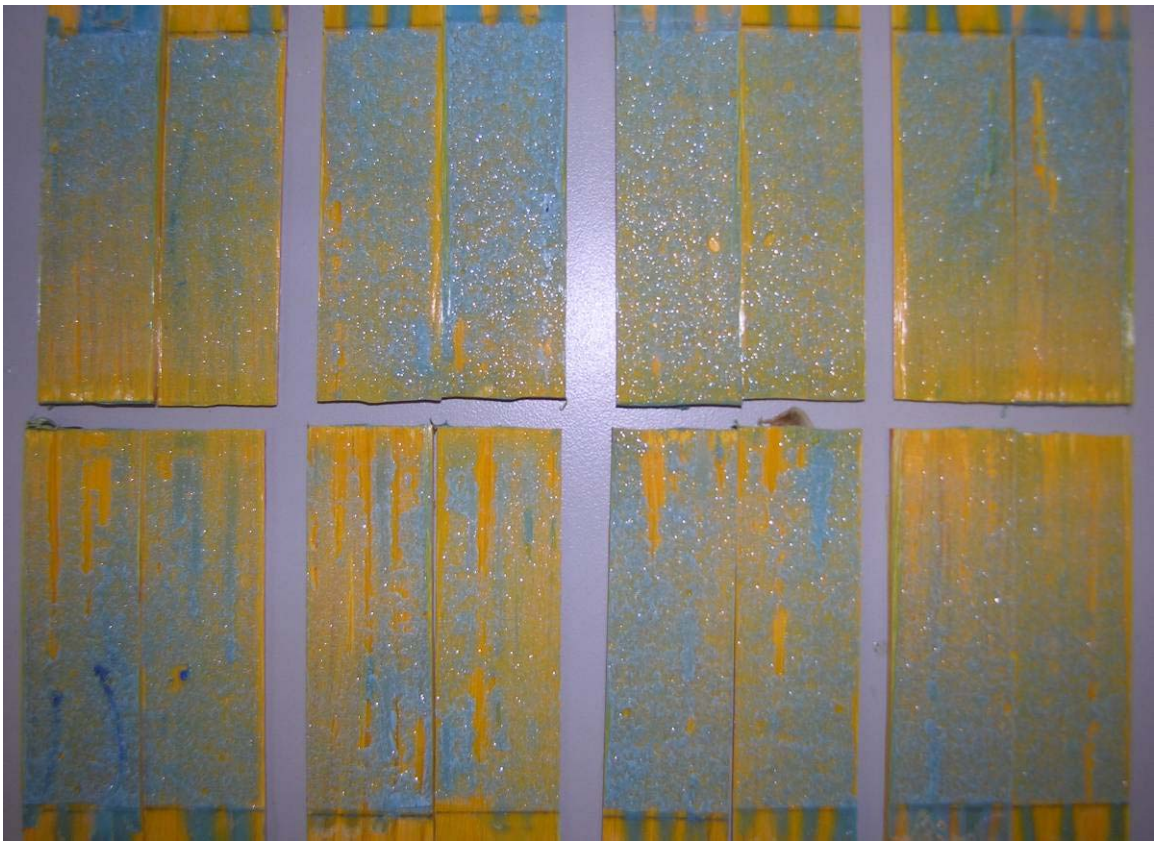

Figure 4.45 – Adhesive M Adhesive/Cohesive Failure Modes

Figure 4.46 shows the two failure modes for the adhesive S cleavage peel specimens. All of the specimens that failed abruptly after reaching the ultimate load failed within the composite substrate, as can be seen in the photographs labeled "Substrate." The other adhesive S specimens failed in a mostly cohesive mode, with some adhesive failure apparent. That fact that failure occurred within the adhesive and within the substrate suggests that the cleavage peel strength of the adhesive is similar to the peel strength of the composite substrate.

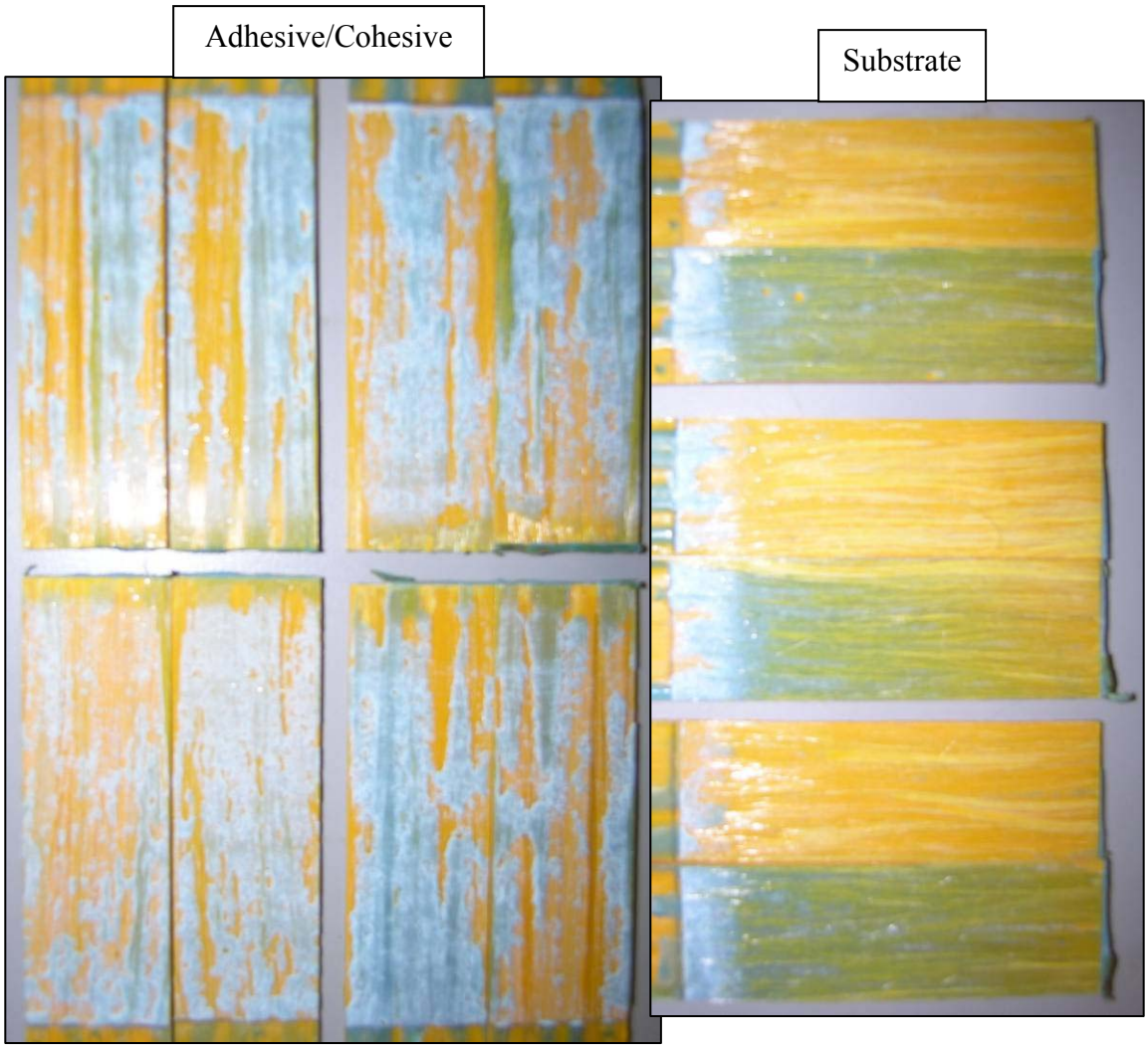

Figure 4.46 – Adhesive S Failure Modes

4.5 Phase IV: Creep

For the creep phase of testing, the relative displacement of the two substrates was recorded at a rate of 0.01 scans per second, which represent reading every 100 seconds or 1.67 minutes. Reading of the instrumentation was begun just before loading, and was continued for 48 hours. The instantaneous displacement was determined by examining the first 30 minutes of displacement data, and finding the point at which the displacements became nearly constant. The displacement at this stage, which took place at an average time of 6.67 minutes, was considered the initial displacement. This initial displacement was then detracted from the subsequent displacements to obtain the creep values. The results are displayed as the average creep values versus time. All of the raw displacement data from the creep testing is located in Appendix C.

Figures 4.47 and 4.48 show the results of the creep tests for adhesives M and S used for the composite-to-composite specimens and loaded to 400 and 600 pounds, respectively. Both adhesives behaved very similarly, with the majority of the creep taking place within the first ten hours. After which, the slope of the creep curve became very small, suggesting that the creep is fully developed and will not lead to failure at these low loads.

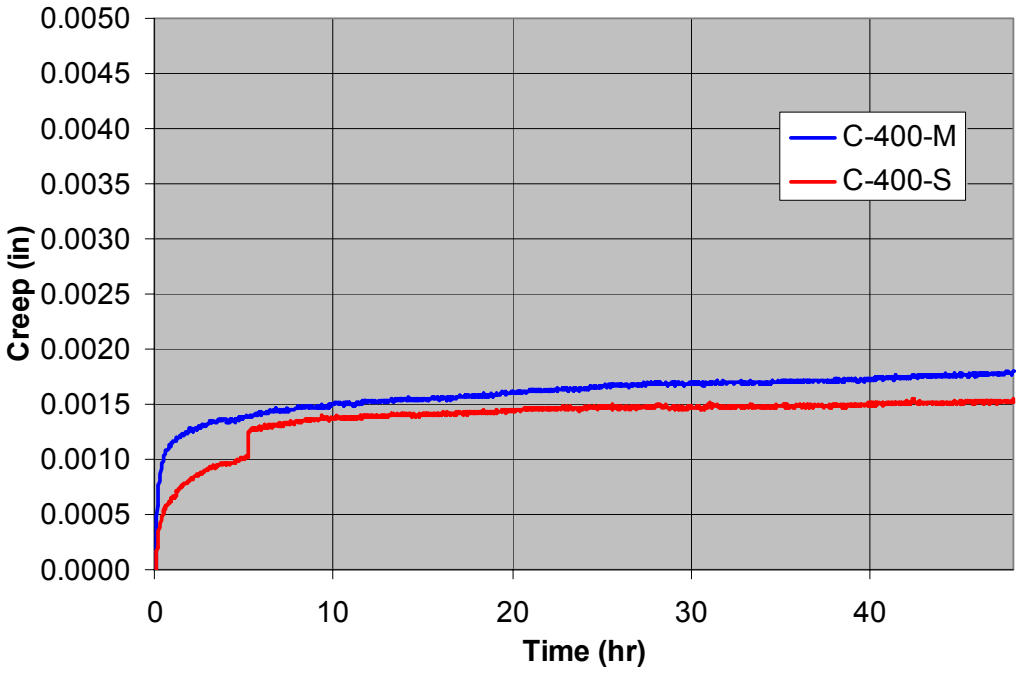

Figure 4.47 – Composite-to-Composite Creep with 400 Pound Load

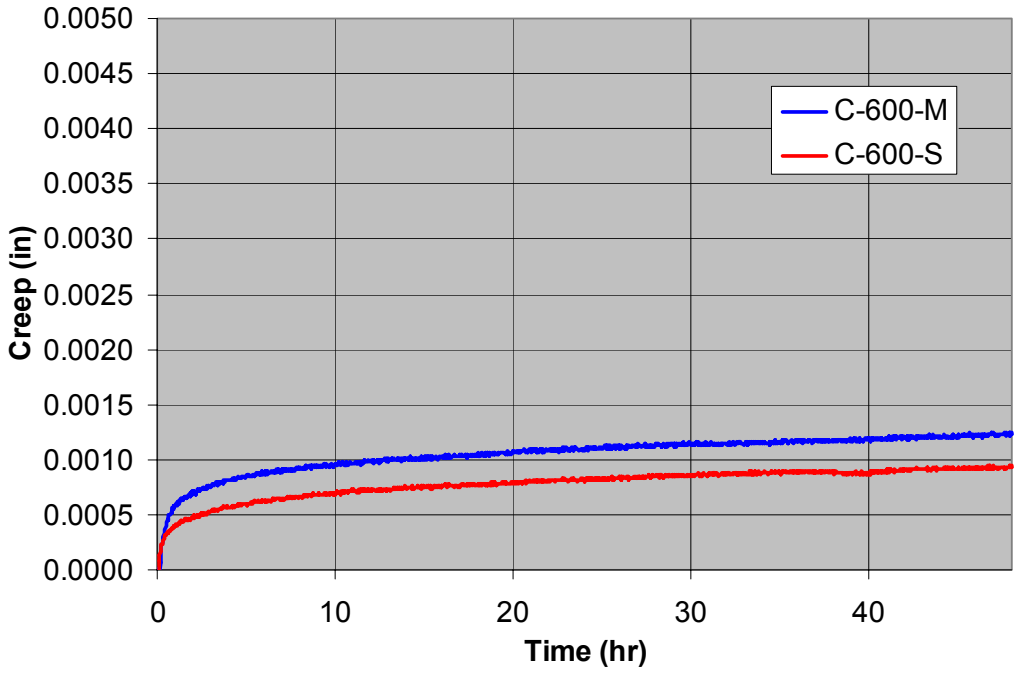

Figure 4.48 – Composite-to-Composite Creep with 600 Pound Load

Figure 4.49 shows the creep results for composite-to-composite specimens tested with a sustained load of 800 pounds. The difference in behavior of the two adhesives is more apparent under this level of higher load. The majority of the creep still takes place in the beginning, with adhesive M showing much more initial creep. More importantly, however, is that the curve of adhesive S begins to flatten much more than the curve of adhesive M after the first ten hours. At the rate that adhesive M is still creeping after 48 hours, it is possible that failure may eventually occur. It is much less likely that creep at a sustained load of 800 pounds would lead to failure in the adhesive S specimens.

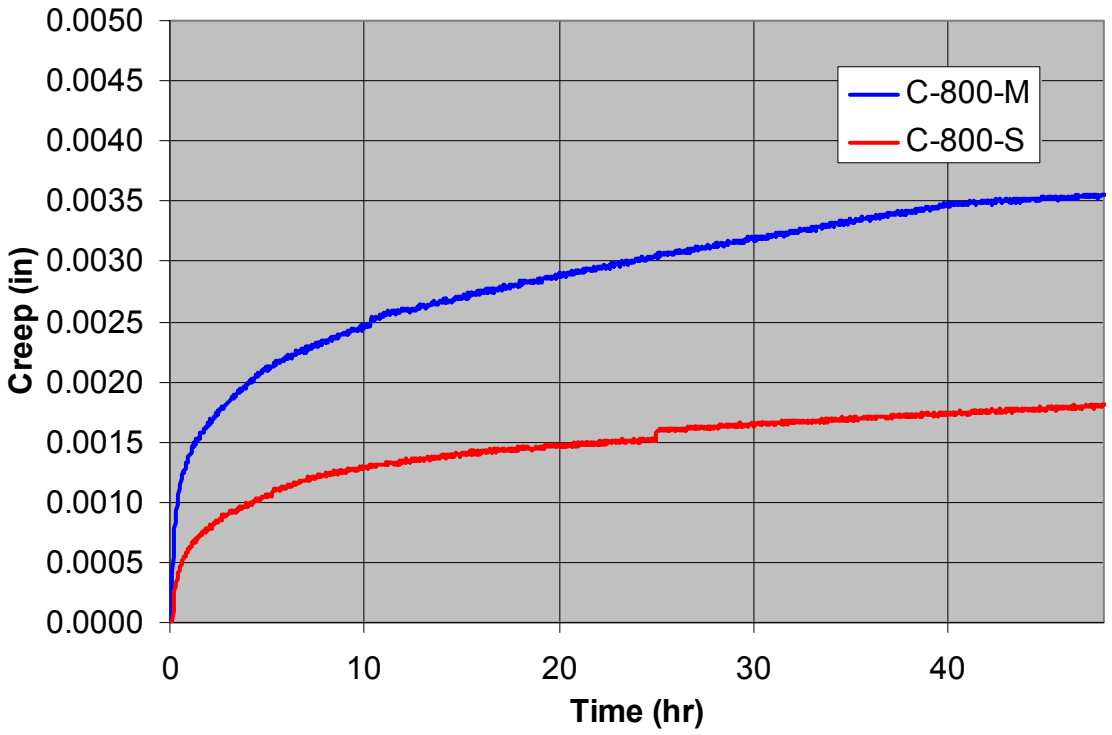

Figure 4.49 – Composite-to-Composite Creep with 800 Pound Load

Figure 4.50 shows the results of the composite-to-composite creep tests at a sustained load of 1000 pounds. All adhesive M specimens tested at this load failed before testing was complete, with an average time to failure of about 14 hours, as seen on the graph. None of the adhesive S specimens failed within the 48 hour monitoring time, but the curve of the data is far from acceptable at this level. Although failure did not occur in the 48 hours, extremely large amounts of relative displacement took place, and the slope at 48 hours is large enough to suggest that failure will eventually occur at a sustained load of 1000 pounds.

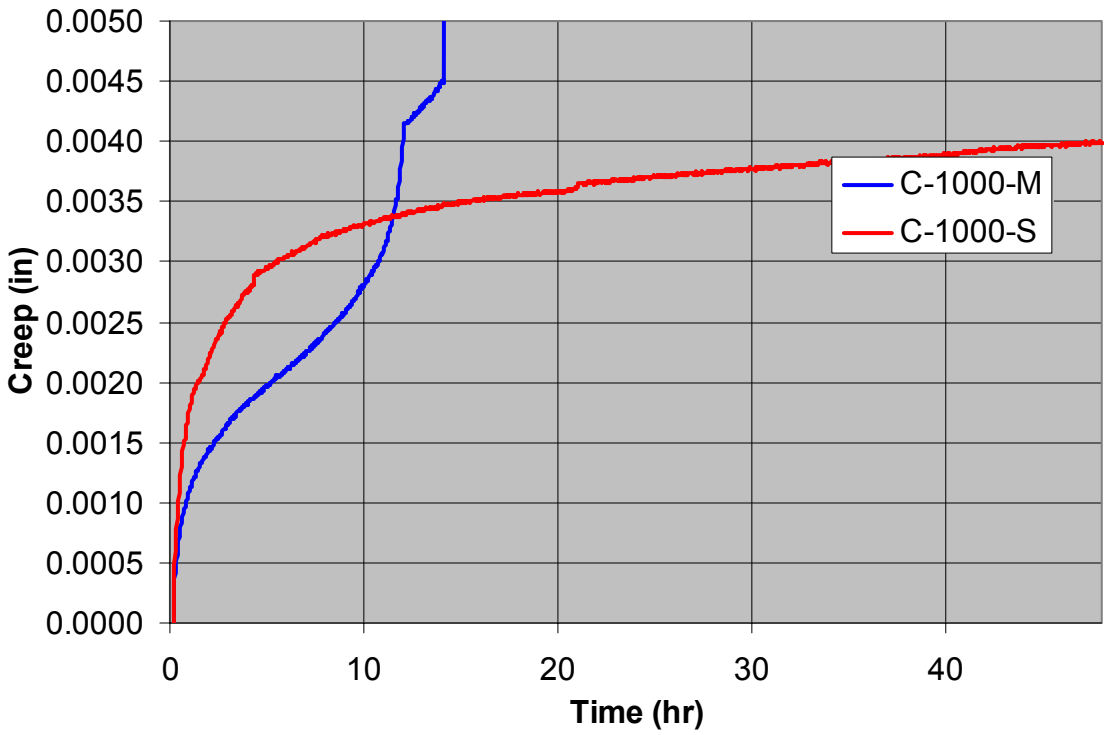

Figure 4.50 – Composite-to-Composite Creep with 1000 Pound Load

Figures 4.51 and 4.52 show the behavior of the steel-to-composite creep specimens loaded at 400 and 600 pounds, respectively. Similar to the composite-to-composite specimens at these loads, most of the creep takes place in the beginning, and both adhesives display acceptable performance at this level.

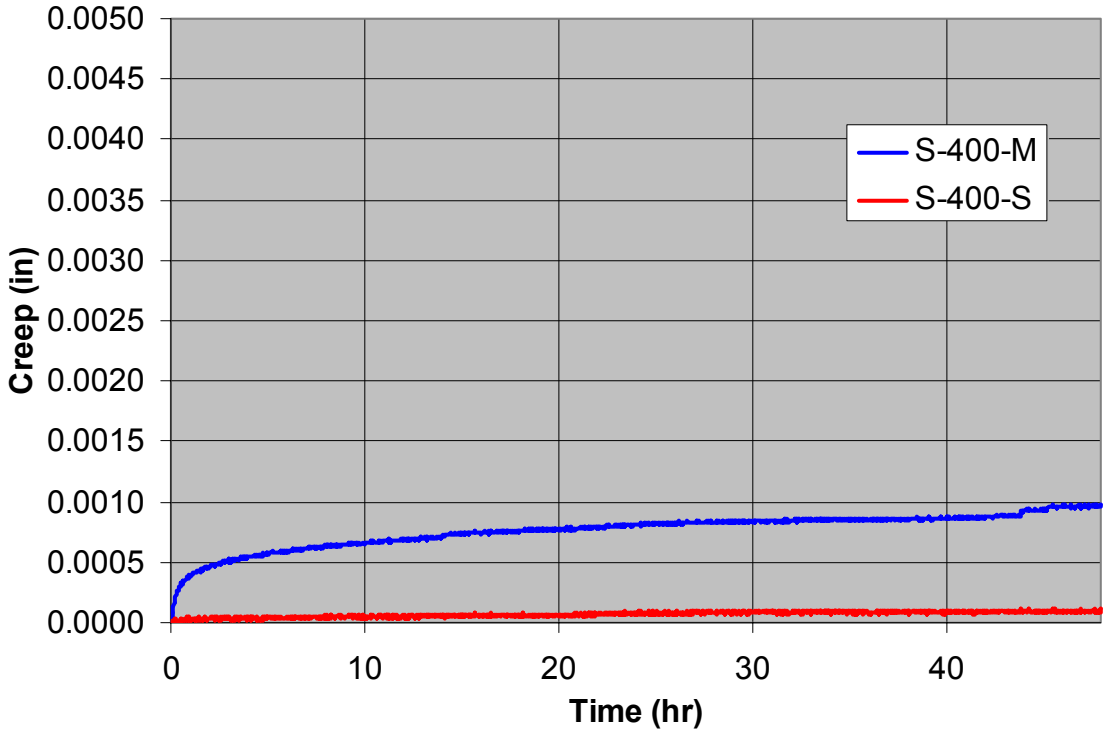

Figure 4.51 – Steel-to-Composite Creep with 400 Pound Load

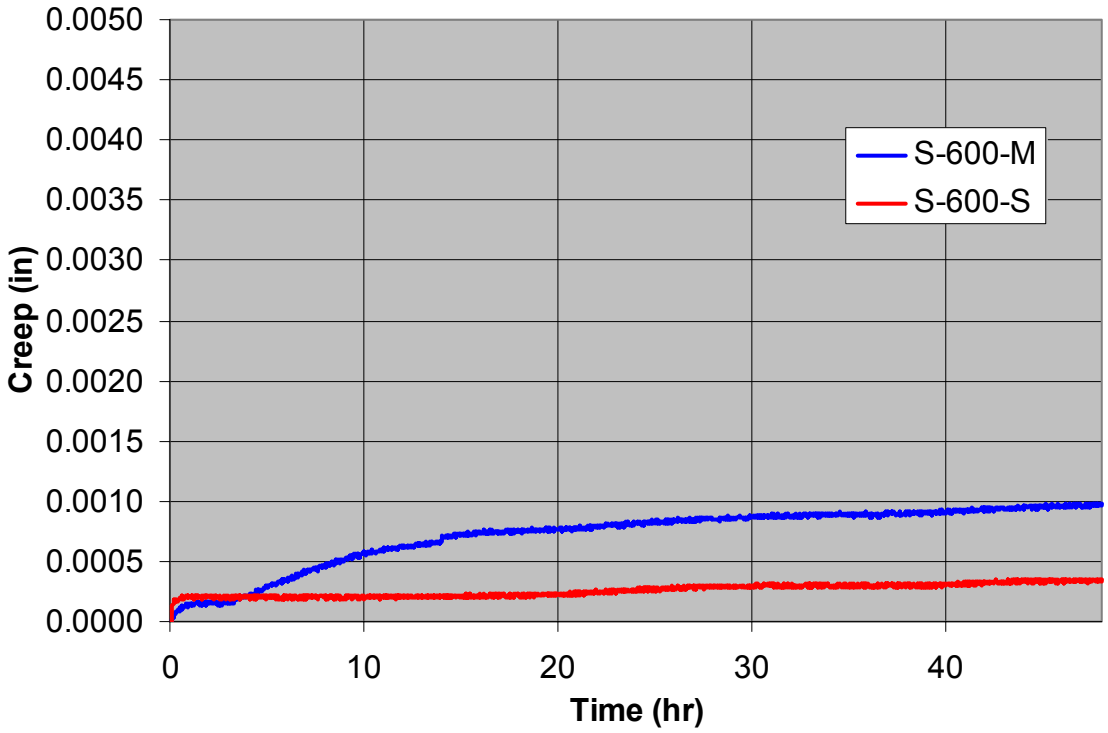

Figure 4.52 – Steel-to-Composite Creep with 600 Pound Load

Figure 4.53 shows the average results of the steel-to-composite creep tests performed under sustained loads of 800 pounds. Unlike the composite-to-composite specimens at this load level, the performances of both adhesives are acceptable. Some significant creep is apparent in the first several hours. However, later the displacements level off and show no signs that creep based failure may potentially occur.

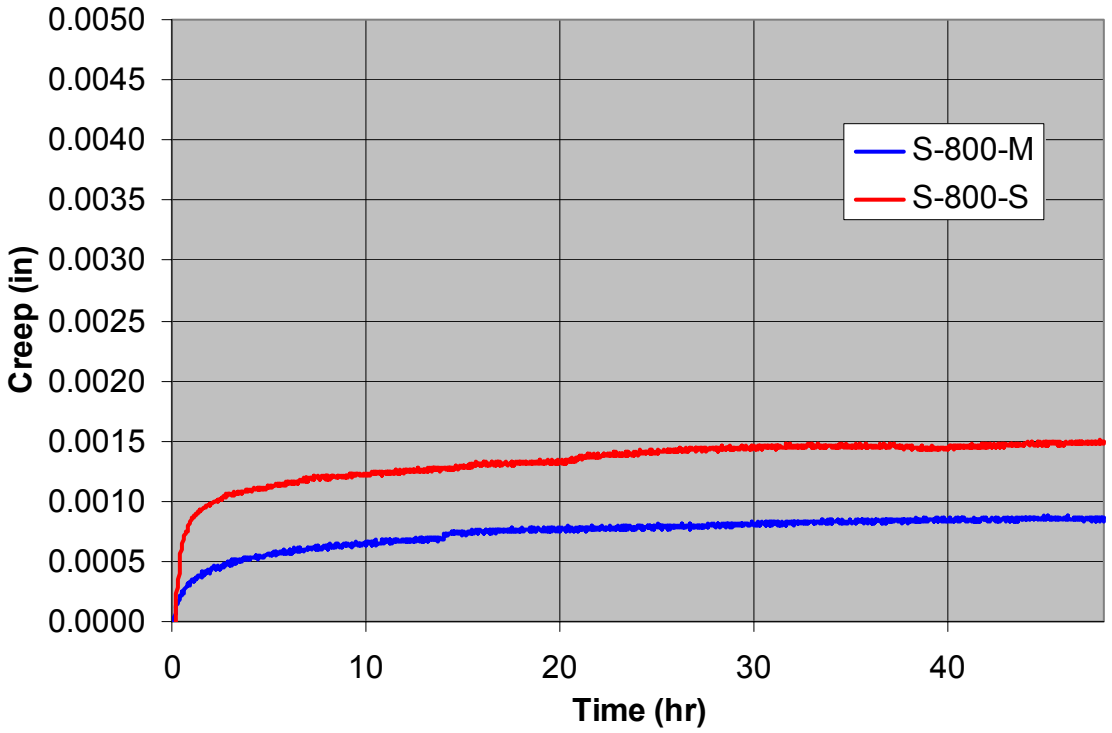

Figure 4.53 – Steel-to-Composite Creep with 800 Pound Load

The average results of the steel-to-composite creep tests performed with a sustained load of 1000 pounds shown in Figure 4.54 are similar to the composite-to-composite creep tests performed with a sustained load of 1000 pounds. None of the specimens using the S adhesive failed, while the specimens using the M adhesive failed after an average of 14 hours. Although none of the specimens using the S adhesive failed, there is a very large amount of creep, and the behavior within the 48 hours that was monitored suggests that failure will eventually occur from excessive creep.

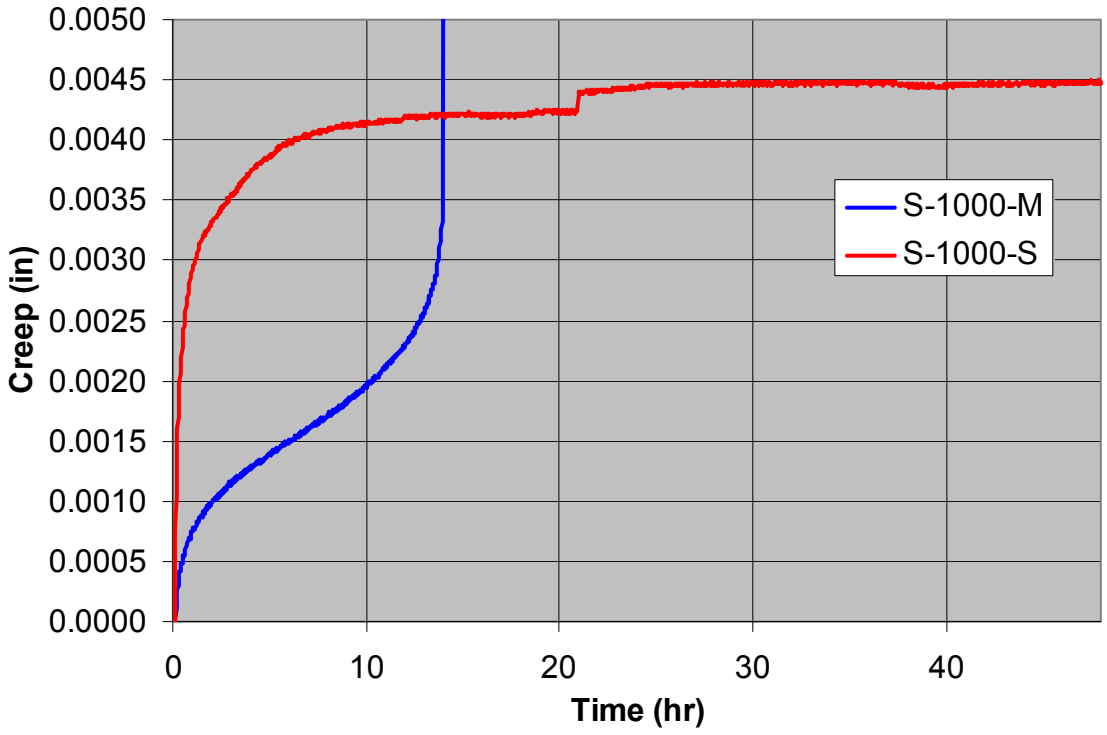

Figure 4.54 – Steel-to-Composite Creep with 1000 Pound Load

5.0 Summary and Conclusions

5.1 Summary

Structural adhesives are an important factor in the growing use of FRP composite materials for civil engineering and structural applications. As these adhesives continue to play a larger role in the design process, the need to study their performance and properties greatly increases. Specifically, more information is needed to determine the affect of the various environmental conditions on their structural behavior, especially for unique applications, such as marine structures and the repair of steel pipelines.

The research presented in this thesis considered the performance of two structural adhesives proposed for marine applications and the repair of steel pipes. The main focus of the research is their shear properties, the effect of environmental conditions on the adhesive behavior, the cleavage peel behavior, and the short-term creep properties. The effect of surface preparation techniques of the substrate and the effect of pressure during curing were also examined.

5.2 Conclusions

Results from the composite-to-composite lap shear tests show that amount of hand-sanding performed on the composite substrate surface significantly effects the behavior of the bond, regardless of the adhesive used. The data shows that thoroughly-sanding the composite substrate surface can increase the average shear strength of the bond by at least 20 percent, compared to lightly-sanding the surface. Application of appropriate pressure

to the joint during the curing process can cause an increase of average shear strengths of 60 percent compared to the shear strengths of bonded joints with too much pressure or without using pressure.

Grinding and sandblasting the steel substrate surface, instead of simply hand-sanding the surface, was found to increase the average shear strength by at least 40 percent. It can therefore be concluded that in order to achieve optimal performance from either adhesive, the composite substrate surface should be thoroughly hand-sanded, the steel substrate surface should be grinded and sandblasted, and the joint should be pressured by approximately 5 psi during the curing process.

Test results of the lap shear tests indicated that the behavior of the S adhesive is more desirable than adhesive M. Under optimal preparation conditions, the average shear strength of the S adhesive was at least 17 and 6 percent higher than that of the M adhesive for composite-to-composite and steel-to-composite specimens, respectively. It should be noted that the lower percentage increase of the average shear strength of the steel-to-composite specimens using the S adhesive was due the presence of some voids in the bond area. In addition to the higher average shear strengths, the S adhesive displayed also more ductile failure modes in comparison to the M adhesive.

The results from the environmental exposure tests allow several conclusions to be drawn. Temperature proved to have the most significant effect on the performance of both adhesives. Rises in temperature could cause shorter service of the joints. Of the

specimens tested to failure after surviving 1000 hours of severe environmental conditions, those that had been conditioned at 140° Fahrenheit exhibited the most degradation in shear performance.

The pH level of the environment also proved to have a negative effect on the performance of both adhesives, although its effect was less significant than that of temperature. The effect of bonding and curing underwater on the M adhesive was inconclusive because of the very short times measured before failure. Bonding and curing underwater for the adhesive S did not affect the performance of the S adhesive. Additionally, both adhesives performed better with composite-to-composite bonds than with steel-to-composite bonds when submitted to the severe environment. It should be mentioned in general that the specimens that used the S adhesive outperformed all similar specimens that used the M adhesive under the severe environmental conditions.

Results from the cleavage peel tests can be used only for comparison of the two adhesives subjected to the same conditions. The most notable discovery is that the average cleavage peel strength of adhesive S is at least 70 percent higher than that of adhesive M. In addition, the initial linear displacement of the S adhesive was stiffer than that of the M adhesive, and the S adhesive specimens that failed cohesively showed more ductile failure after initiation of cracks in comparison to those specimens that used the M adhesive. Failure of some of the specimens bonded with S adhesive was by failure within the composite substrate surface, which therefore caused the failure to be abrupt at the ultimate load.

The results of the short-term creep study suggest that both adhesives can sustain permanent stresses of 400 and 600 psi, whether bonding composite-to-composite or steel-to-composite. Both adhesives can sustain 800 psi of shear stress for bonding steel-to-composite, and adhesive S can sustain 800 psi of shear stress for bonding composite-to-composite. Failure of adhesive M did not occur within 48 hours for composite-to-composite joints subjected to a stress of 800 psi, but the creep behavior suggests that failure would eventually occur. Adhesive M failed within 48 hours for all tested specimens subjected to a stress of 1000 psi. Adhesive S did not fail within 48 hours for any tested specimens subjected to a stress of 1000 psi, but the creep behavior suggests that failure would eventually occur.

REFERENCES

ASTM D 3163 – 01, "Standard Test Method for Determining Strength of Adhesively Bonded Rigid Plastic Lap-Shear Joints in Shear by Tension Loading", West Conshohocken, PA, American Society for Testing and Materials, 2001.

ASTM D 3807 – 98 (Reapproved 2004), "Standard Test Method for Strength Properties of Adhesives in Cleavage Peel by Tension Loading (Engineering Plastics-to-Engineering Plastics)", West Conshohocken, PA, American Society for Testing and Materials, 2004.

ASTM D 5573 – 99, "Standard Practice for Classifying Failure Modes in Fiber-Reinforced-Plastic (FRP) Joints", West Conshohocken, PA, American Society for Testing and Materials, 1999.

ASTM D 5868 – 01, "Standard Test Method for Lap Shear Adhesion for Fiber Reinforced Plastic (FRP) Bonding", West Conshohocken, PA, American Society for Testing and Materials, 2001.

Banton, C., Patrick, A., Porter, P., "Underwater Repair Using Composite Split-Sleeves", Pipeline Rehabilitation and Maintenance Conference, Bahrain, January 2005.

Chavez, O., Porter, P., "Composite Repairs – Design, Properties and New Applications", Congreso Internacional de Ductos, Puebla, Puebla, 2003.

El Damatty, A.A., Abushagur, M., "Testing and Modeling of Shear and Peel Behavior for Bonded Steel/FRP Connections", *Thin-Walled Structures 41*, 2003: 987–1003.

Keller, T., Castro, J., Schollmayer, M., "Adhesively Bonded and Translucent Glass Fiber Reinforced Polymer Sandwich Girders", *Journal of Composites for Construction*, September/October 2004: 461-470.

Keller, T., Kunzle, O., Wyss, U., "Finding the Right Bond", *Civil Engineering*, March 1999, Volume 69 Issue 3: 64-67

Malvar, L.J., Joshi, N.R., Beran, J.A., "Environmental Effects on the Short-Term Bond of Carbon Fiber-Reinforced Polymer (CFRP) Composites", *Journal of Composites for Construction*, February 2003: 58-63

Porter, P.C., Meade, R., "An Effective Repair Alternative", 6th International Pipeline Exposition & Conference, Mexico, 2001.

Veer, F.A., Schönwälder, J., Zuidema, J., Kranenburg, C., "Failure Criteria for Transparent Acrylic Adhesive Joints Under Static, Fatigue and Creep Loading", The 15th European Conference of Fracture, Stockholm, Sweden, August 2004.

APPENDIX A

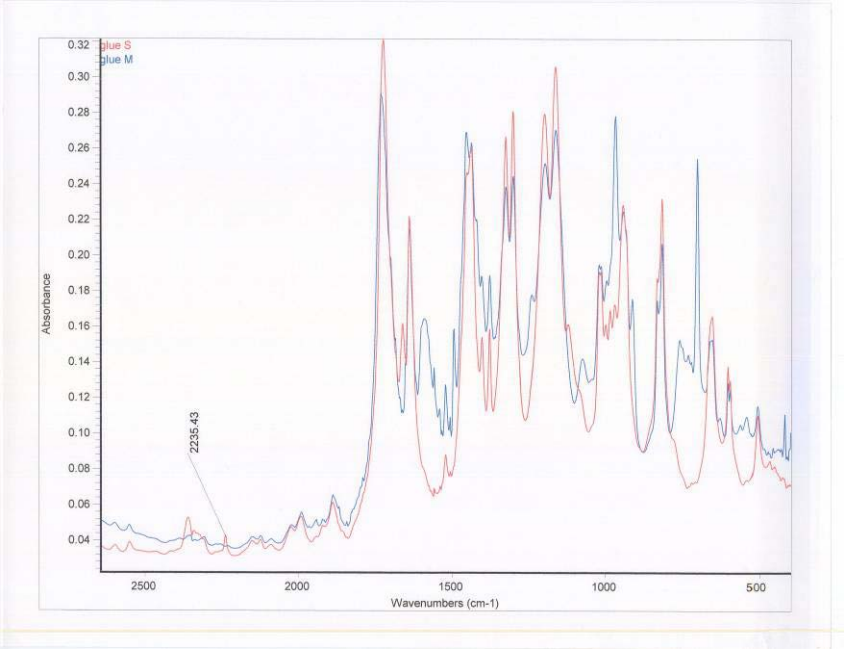

Figure A.1 – FTIR Spectra 1

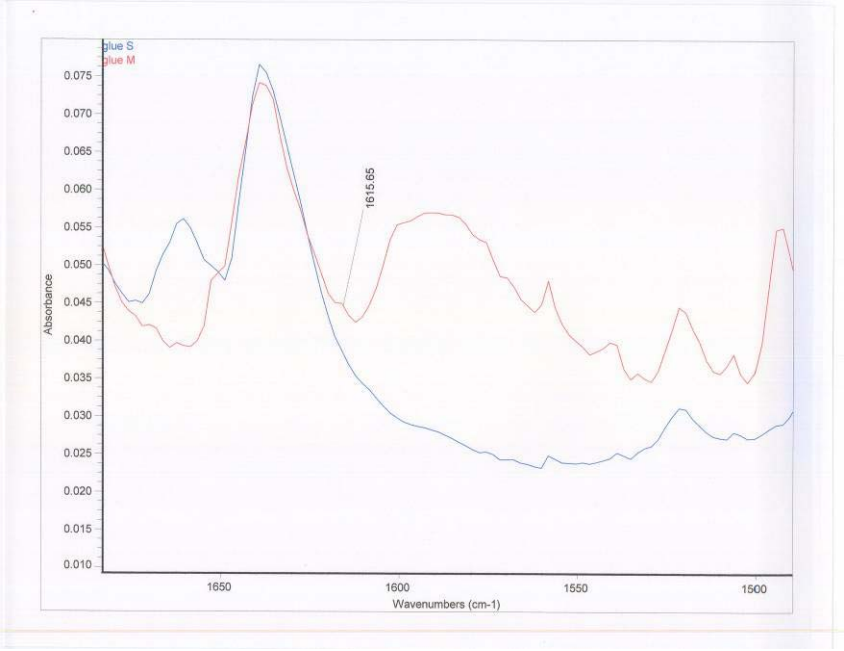

Figure A.2 – FTIR Spectra 2

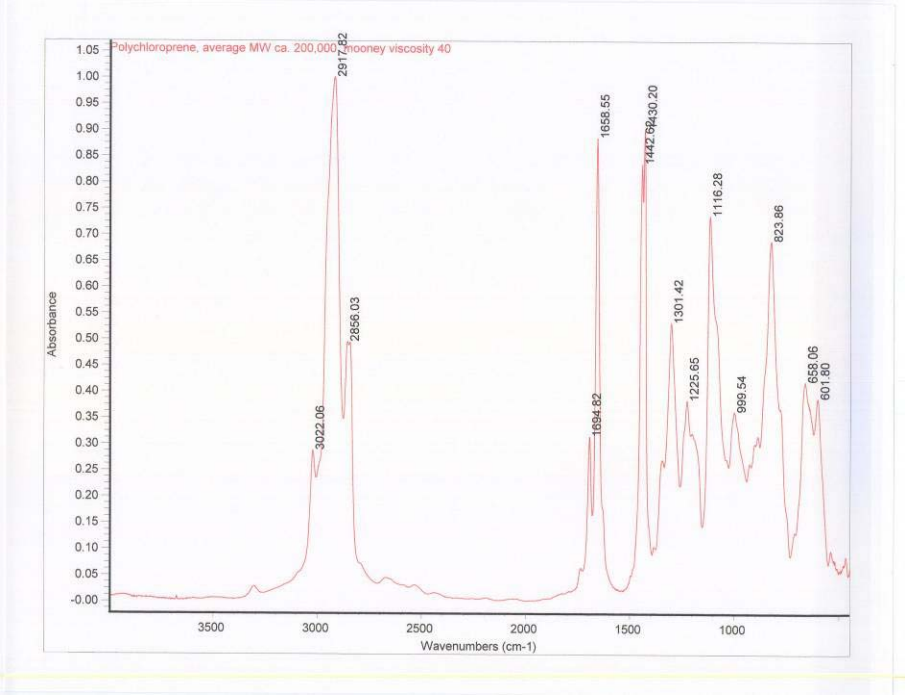

Figure A.3 – FTIR Spectra with Polychloroprene

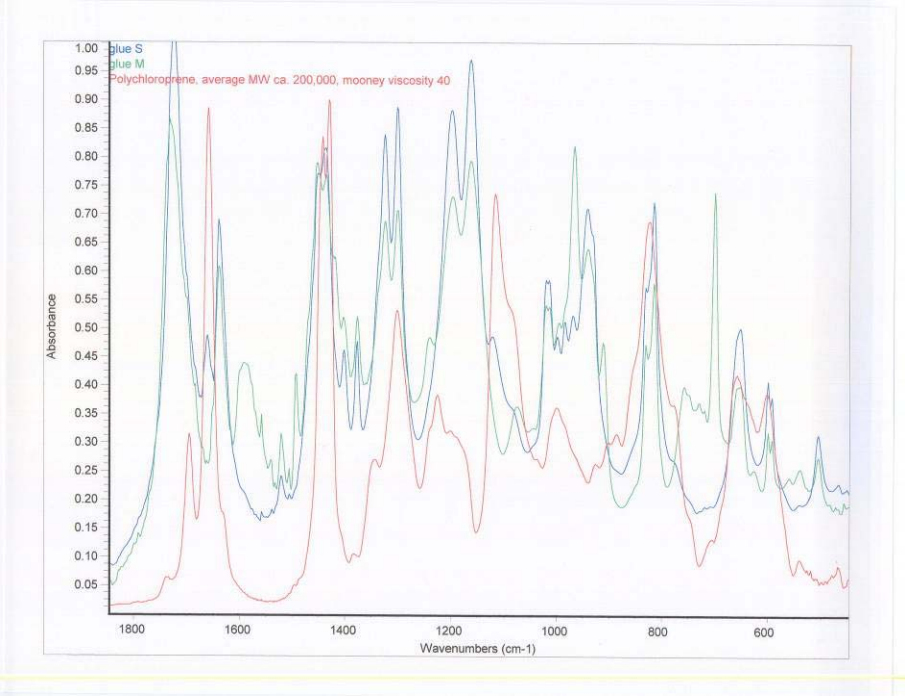

Figure A.4 – FTIR Spectra with Polychloroprene

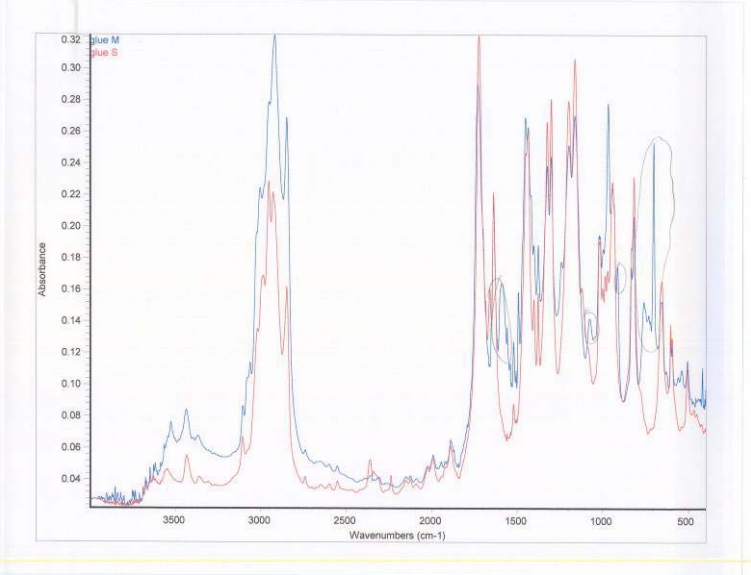

Figure A.5 – FTIR Spectra 3

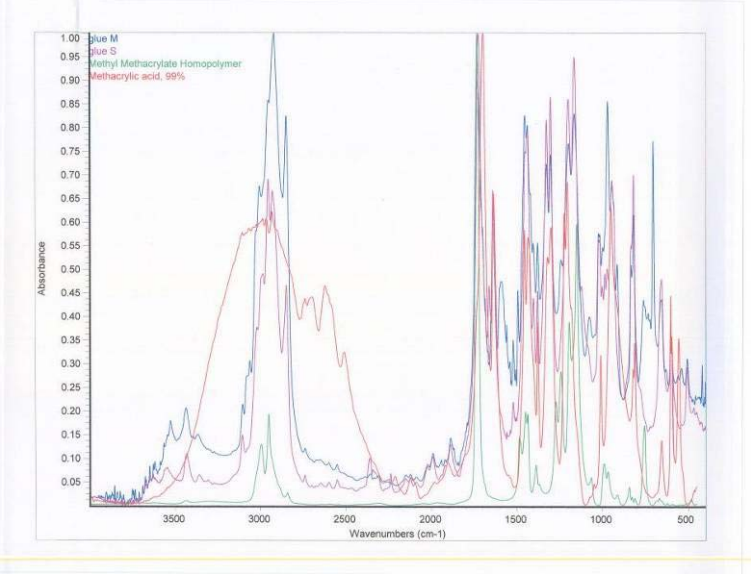

Figure A.6 – FTIR Spectra with Methyl Methacrylate Homopolymer and Methacrylic Acid

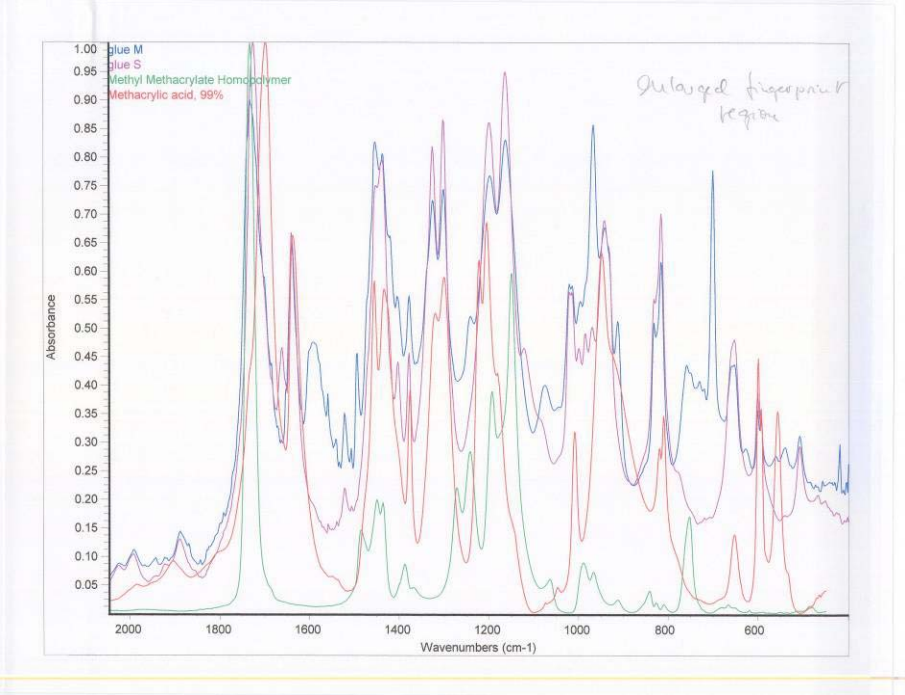

Figure A.7 – Enlarged Fingerprint Region of FTIR Spectra with Methyl Methacrylate Homopolymer and Methacrylic Acid

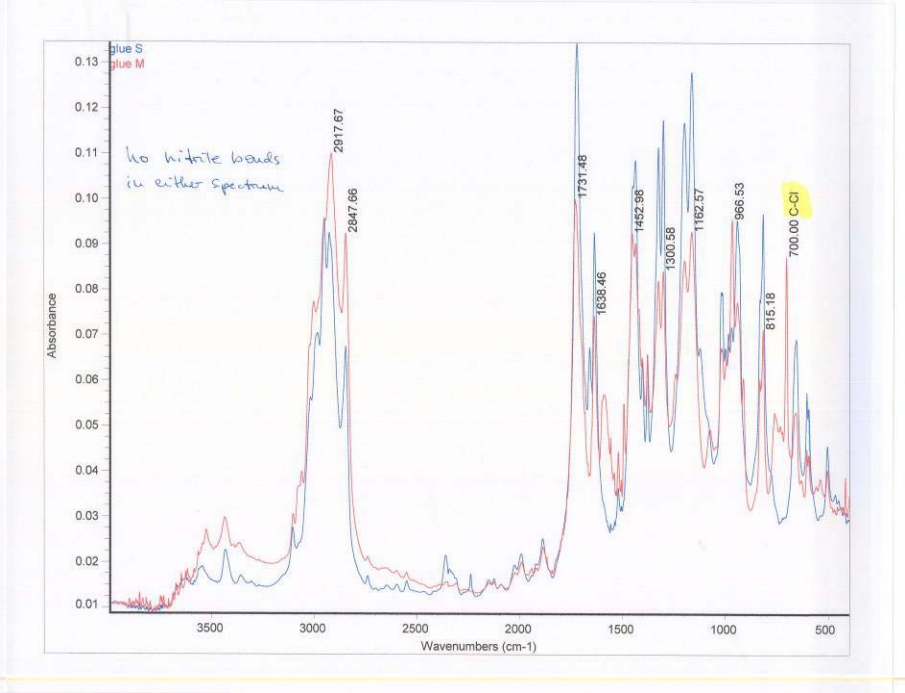

Figure A.8 – FTIR Spectra with No Nitrile Bonds

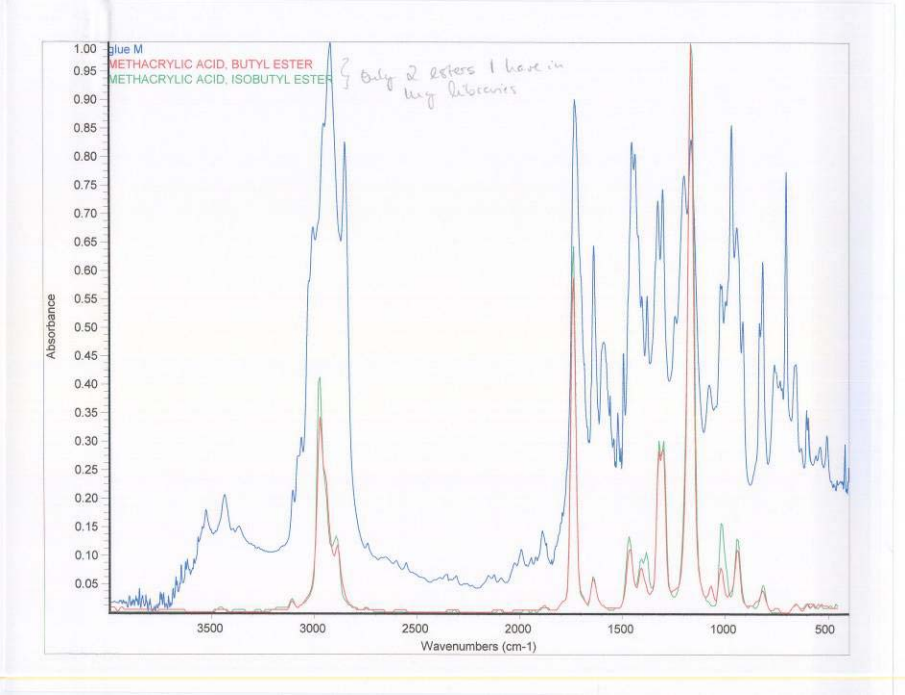

Figure A.9 – FTIR Spectra with Butyl Ester and Isobutyl Ester 1

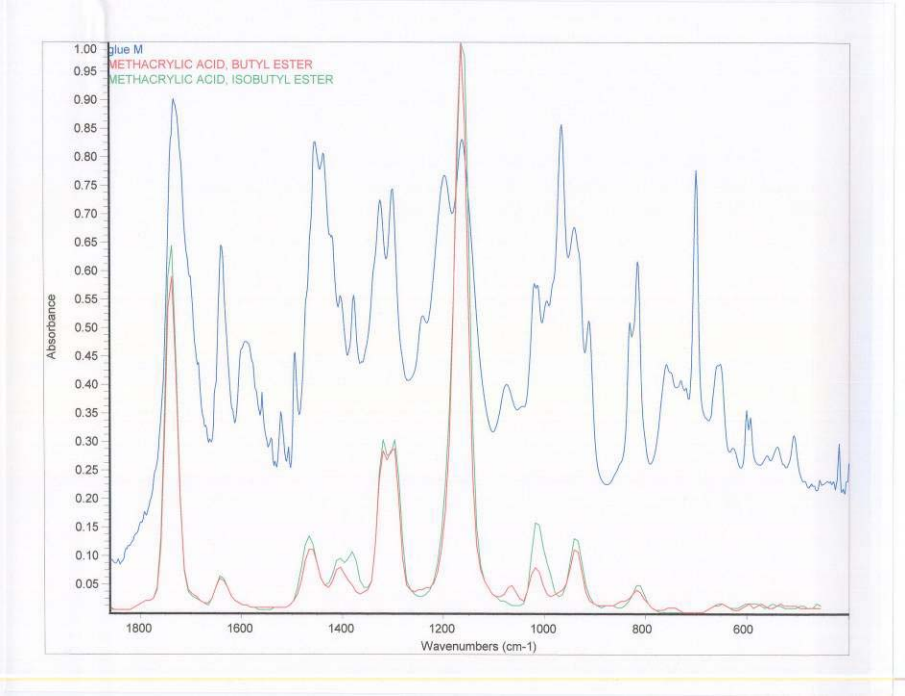

Figure A.10 – FTIR Spectra with Butyl Ester and Isobutyl Ester 2

Appendix B

Environmental Condition	Adhesive	#	Failure Time (hr)	Average Failure Time (hr)	Standard Deviation (hr)
C-72-7-800	S	1	>1000	>1000	0.000
		2	>1000		
C-120-7-200	S	1	NA	>1000	0.000
		2	>1000		
		3	>1000		
		4	>1000		
	M	1	>1000	>1000	0.000
		2	NA		
		3	>1000		
C-120-7-600	S	1	NA	>1000	0.000
		2	NA		
		3	854.65		
		4	>1000		
		5	NA		
		6	>1000		
	M	1	1.52	2.639	2.536
		2	0.25		
		3	6.15		
		4	2.73		
C-120-7-800	S	1	NA	92.967	67.602
		2	0.80		
		3	2.70		
		4	0.10		
		5	NA		
		6	8.75		
		7	165.05		
		8	82.87		
		9	30.98		
	M	1	0.20	0.117	0.029
		2	0.10		
		3	0.10		
		4	0.10		
		5	0.10		
		6	0.15		

Values in gray were not included in averages because of heater malfunction, grip failure, or similar problem.

Table B.1 – Environmental Exposure Raw Data 1

Type	Adhesive	#	Failure Time	Average Failure Time (hr)	Standard Deviation
C-140-4-200	S	1	>1000	>1000	0.000
		2	NA		
		3	>1000		
	M	1	>1000	>1000	0.000
		2	>1000		
		3	407.52		
C-140-4-600	S	1	10.90	8.267	3.134
		2	9.10		
		3	4.80		
	M	1	0.17	0.133	0.073
		2	0.18		
		3	0.05		
C-140-7-200	S	1	0.70	>1000	0.000
		2	>1000		
		3	>1000		
		4	>1000		
	M	1	NA	>737.45	269.161
		2	750.22		
		3	462.13		
		4	>1000		
C-140-7-600	S	1	0.00	78.150	72.196
		2	0.90		
		3	129.20		
		4	6.40		
		5	27.10		
	M	1	0.00	0.150	0.071
		2	0.00		
		3	0.10		
		4	0.20		
		5	0.00		
C-140-7-800	S	1	0.10	2.000	NA
		2	0.50		
		3	0.00		
		4	2.00		
		5	0.10		
	M	1	0.00	0.167	NA
		2	0.00		
		3	0.17		
		4	0.00		

Values in gray were not included in averages because of heater malfunction, grip failure, or similar problem.

Table B.2 – Environmental Exposure Raw Data 2

Type	Adhesive	#	Failure Time	Average Failure Time (hr)	Standard Deviation
C-140-9.5-200	S	1 2 3	>1000 >1000 >1000	>1000	0.000
	M	1 2 3	>1000 >1000 >1000	>1000	0.000
C-140-9.5-600	S	1 2 3	0.20 7.95 3.82	5.884	2.922
	M	1 2 3	0.13 0.23 0.07	0.144	0.084
UC-140-4-600	S	1 2	19.62 35.73	27.675	11.396
	M	1 2	0.02 0.02	0.017	0.000
UC-140-7-600	S	1 2	67.95 81.90	74.925	9.864
	M	1 2	0.00 0.02	0.008	0.012
UC-140-9.5-600	S	1 2	223.33 26.93	26.933	NA
	M	1 2	0.12 0.05	0.083	0.047
S-120-7-200	S	1 2	>1000 >1000	>1000	0.000
	M	1 2	>1000 >1000	>1000	0.000
S-120-7-600	S	1 2	24.97 8.12	16.542	11.915
	M	1 2	4.78 2.90	3.842	1.332
S-140-7-200	S	1 2	NA >1000	>1000	0.000
	M	1 2	>1000 >1000	>1000	0.000
S-140-7-800	S	1 2	0.42 0.62	0.517	0.141
	M	1 2	0.00 0.05	0.025	0.035

Values in gray were not included in averages because of heater malfunction, grip failure, or similar problem.

Table B.3 – Environmental Exposure Raw Data 3

Appendix C

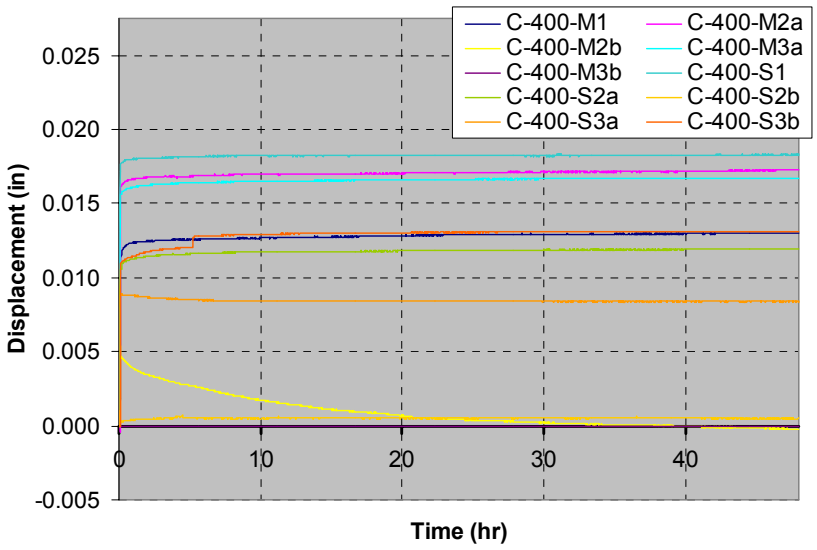

Figure C.1 – Raw Displacement Data from All

400 Pound Composite-to-Composite Creep Tests

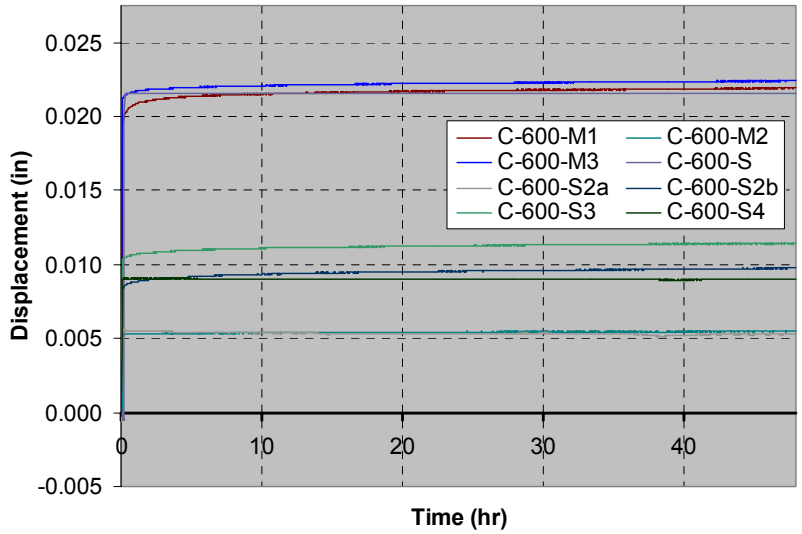

Figure C.2 – Raw Displacement Data from All

600 Pound Composite-to-Composite Creep Tests

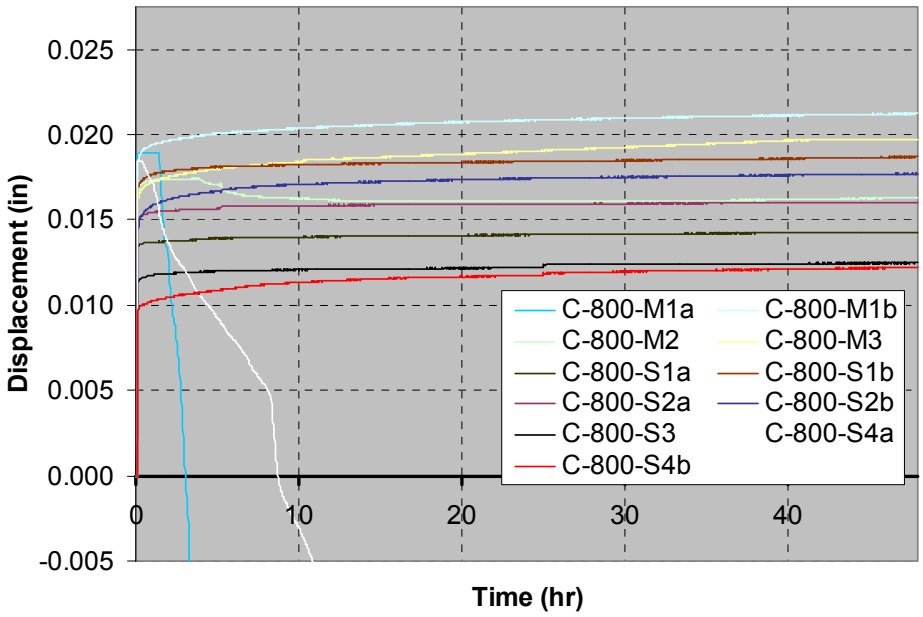

Figure C.3 – Raw Displacement Data from All

800 Pound Composite-to-Composite Creep Tests

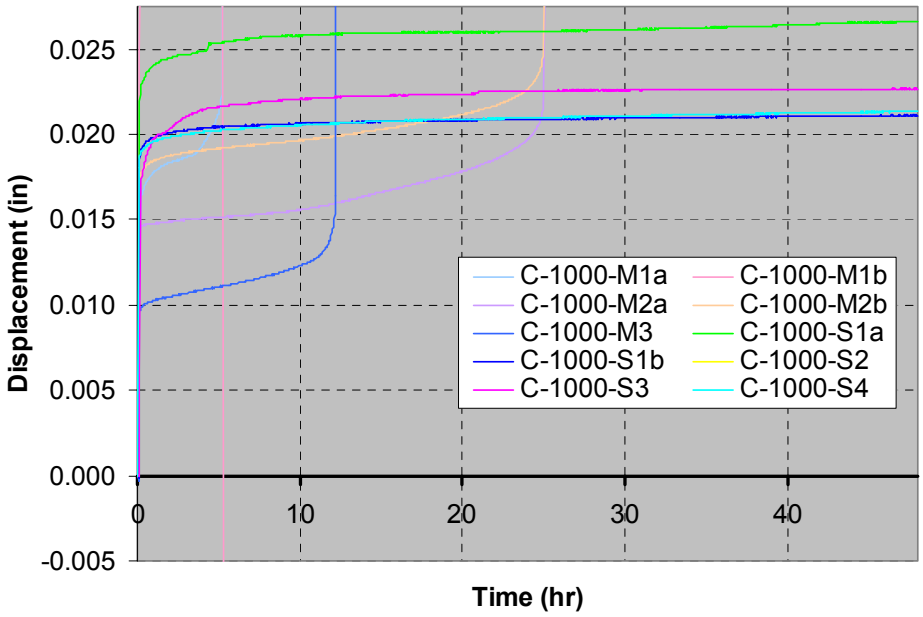

Figure C.4 – Raw Displacement Data from All

1000 Pound Composite-to-Composite Creep Tests

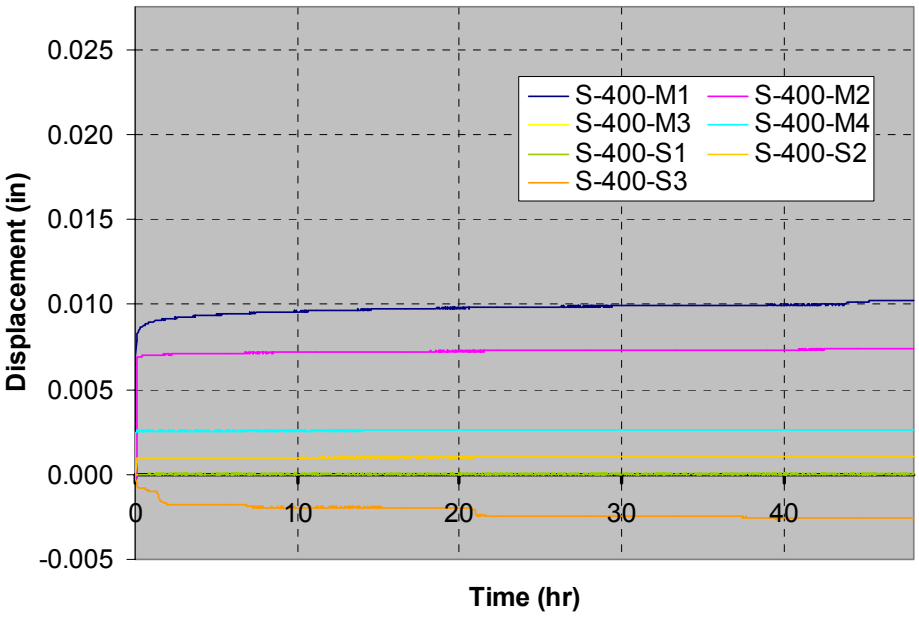

Figure C.5 – Raw Displacement Data from All

400 Pound Steel-to-Composite Creep Tests

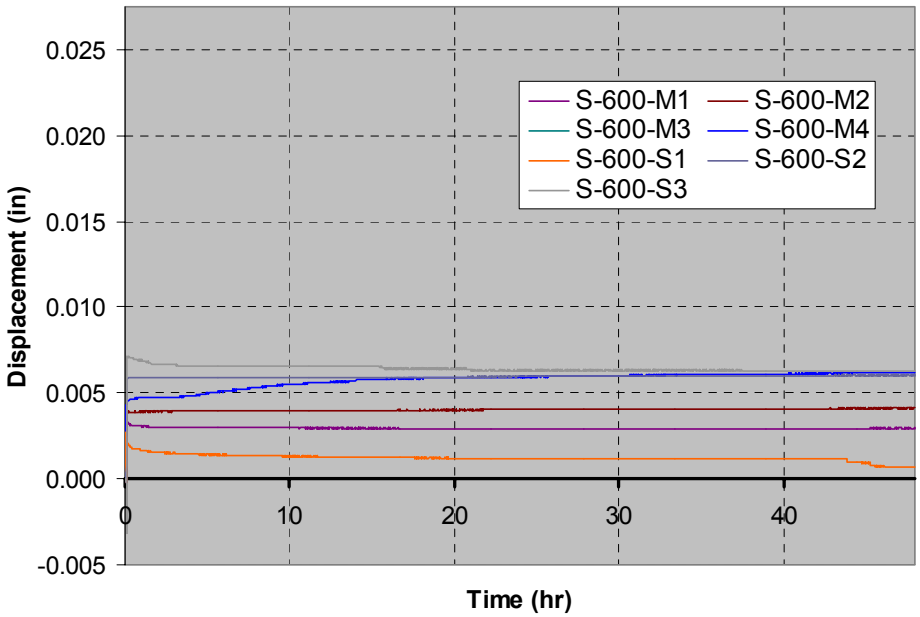

Figure C.6 – Raw Displacement Data from All

600 Pound Steel-to-Composite Creep Tests

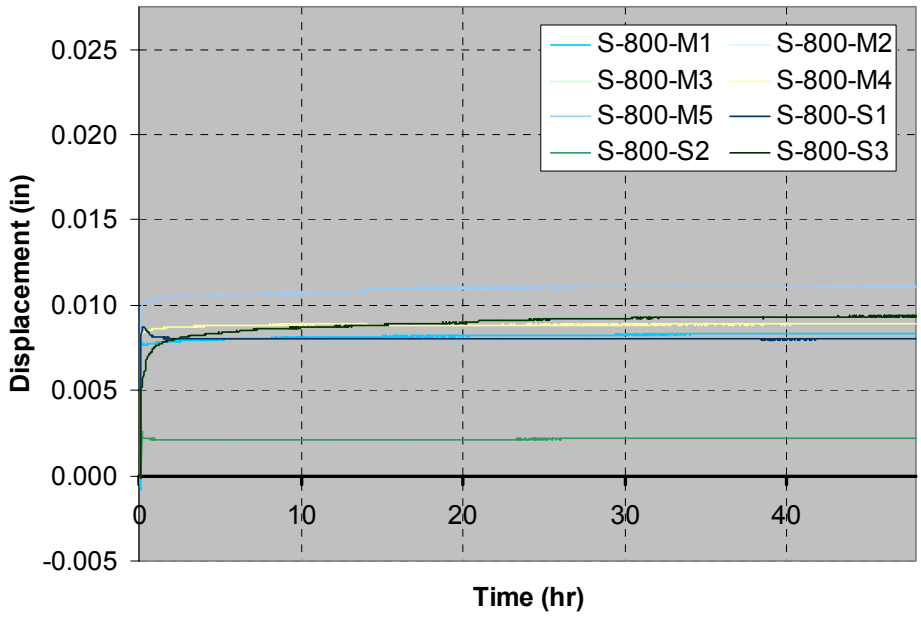

Figure C.7 – Raw Displacement Data from All

800 Pound Steel-to-Composite Creep Tests

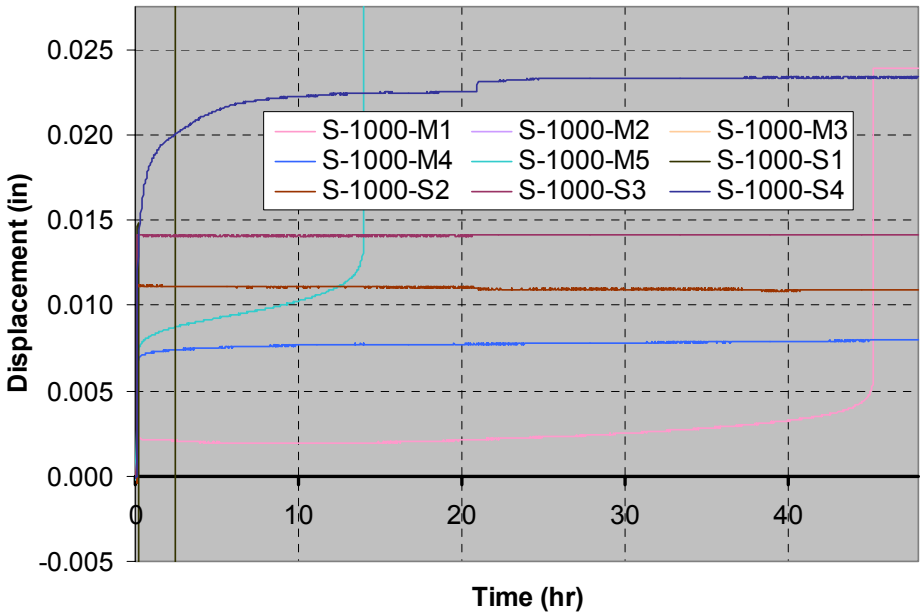

Figure C.8 – Raw Displacement Data from All

1000 Pound Steel-to-Composite Creep Tests